RIO

PUC

Dissertação de Mestrado

Reservoir-Wellhead Coupling in an Innovative Reservoir Simulator Based on a Plugin Architecture

Gustavo Henrique Gomes dos Santos

Pontifícia Universidade Católica do Rio de Janeiro
Centro Técnico Científico
Departamento de Engenharia Mecânica

Rio de Janeiro, 7 de outubro de 2025

Pontifícia
Universidade
Católica do
Rio de Janeiro

Dissertação de Mestrado

Reservoir-Wellhead Coupling in an Innovative Reservoir Simulator Based on a Plugin Architecture

Gustavo Henrique Gomes dos Santos

Orientação: Professor Ivan Fábio Mota de Menezes, D.Sc.
Coorientação: Daniel Nunes de Miranda Filho, Ph.D.

Dissertação apresentada como requisito parcial para a obtenção do grau de Mestre em Engenharia Mecânica pelo programa de Pós-Graduação em Engenharia Mecânica, no Departamento de Engenharia Mecânica.

Rio de Janeiro, 7 de outubro de 2025

Pontifícia
Universidade
Católica do
Rio de Janeiro

Reservoir-Wellhead Coupling in an Innovative Reservoir Simulator Based on a Plugin Architecture

Gustavo Henrique Gomes dos Santos

Dissertação apresentada como requisito parcial para a obtenção do grau de Mestre em Engenharia Mecânica. Aprovada pela Comissão examinadora abaixo:

Professor Ivan Fábio Mota de Menezes, D.Sc.
Orientador
Departamento de Engenharia Mecânica – PUC-Rio

Daniel Nunes de Miranda Filho, Ph.D.
Co-Orientador
Petróleo Brasileiro S.A. – Petrobras

Professor Marcos Vitor Barbosa Machado, D.Sc.
Petróleo Brasileiro S.A. – Petrobras

Vinícius Ramos Rosa, D.Sc.
Petróleo Brasileiro S.A. – Petrobras

Rio de Janeiro, 7 de outubro de 2025

Pontifícia
Universidade
Católica do
Rio de Janeiro

Gustavo Henrique Gomes dos Santos

Graduou-se em 2009 em Engenharia de Computação pelo Instituto Militar de Engenharia (Rio de Janeiro, Brasil). Trabalha na Petrobras desde 2010, onde se especializou em Engenharia de Petróleo. Possui experiência em garantia de escoamento, monitoramento da produção, gerenciamento e simulação de reservatórios, além de medição fiscal da produção de campos de petróleo offshore. Atualmente, trabalha com simulação de reservatórios em projetos de desenvolvimento da produção e na avaliação de novas áreas exploratórias.

Ficha Catalográfica

Santos, Gustavo Henrique Gomes dos

Reservoir-wellhead coupling in an innovative reservoir simulator based on a plugin architecture / Gustavo Henrique Gomes dos Santos ; orientador: Ivan Fábio Mota de Menezes ; co-orientador: Daniel Nunes de Miranda Filho. – 2025.

113 f. : il. color. ; 30 cm

Dissertação (mestrado)–Pontifícia Universidade Católica do Rio de Janeiro, Departamento de Engenharia Mecânica, 2025.

Inclui bibliografia

1. Engenharia Mecânica – Teses. 2. Simulação de reservatório. 3. Acoplamento de poço. 4. Simulador numérico. 5. Arquitetura de plugins. I. Menezes, Ivan Fábio Mota de. II. Miranda Filho, Daniel Nunes de. III. Pontifícia Universidade Católica do Rio de Janeiro. Departamento de Engenharia Mecânica. IV. Título.

CDD: 621

To my beloved parents, Carlos and Salette, for their support,
and to my fiancée, Fernanda, for her companionship
through the most challenging times.

Acknowledgments

I would like to first thank my advisors, professor Ivan Menezes and Daniel Miranda for guiding me throughout my research and for all the time they have provided me whenever I needed. I consider myself truly blessed for the opportunity to learn from them.

Then I wish to thank the entire GSIM team at Tecgraf Institute/PUC-Rio for making sure I always had a place to work and all the necessary tools. A special thanks to Eduardo Goichoechea for the countless meetings and fruitful discussions.

I also want to thank my friend and coworker, Pedro Henrique, for always being available for exchange of ideas and for helping me with the generation of inputs used in my research.

Finally, I thank Petrobras for allowing my academic development, and my manager, Rodrigo Pontes, for the support and the partial release from work so I could conduct my postgraduate studies.

This study was financed in part by the Coordenação de Aperfeiçoamento de Pessoal de Nível Superior - Brasil (CAPES) - Finance Code 001.

Abstract

Santos, Gustavo Henrique Gomes dos; Menezes, Ivan Fábio Mota de (Advisor); Miranda Filho, Daniel Nunes de (Co-Advisor). **Reservoir-wellhead coupling in an innovative reservoir simulator based on a plugin architecture** . Rio de Janeiro, 2025. 113p. Dissertação de Mestrado – Departamento de Engenharia Mecânica, Pontifícia Universidade Católica do Rio de Janeiro.

Effectively designing and managing today's complex oil and gas production systems, from the reservoir to the wellhead and surface facilities, require more than isolated simulations of each component. Traditional modeling approaches, treating the reservoir and surface network separately, often rely on assumed boundary conditions that fail to capture the real interactions between subsurface and surface flow. This separation can lead to inaccurate predictions and suboptimal operational strategies. A more unified simulation approach, where the entire system is modeled as a continuous flow network, enables a deeper understanding of system behavior, supports more accurate performance forecasts, and allows for better-informed decisions in field development and production optimization. This study introduces an implicit reservoir-wellhead coupling methodology within the GSIM numerical simulator, developed through a collaboration between Petrobras and PUC-Rio. The proposed approach addresses key pressure losses along the production system, which are major factors in maximizing hydrocarbon recovery. As a foundational step toward full integration of reservoir and surface simulations, the method leverages GSIM's plugin architecture and focuses on the residual and Jacobian matrix terms in Newton iterations. It uses vertical lift performance (VLP) tables in conjunction with nodal analysis to achieve effective coupling between surface and reservoir models. Bilinear and multidimensional linear interpolation of the hydraulics tables were implemented, tested, and validated against results from the commercial IMEX simulator, showing excellent agreement. Additional test cases were designed to compare the proposed coupling methodology with IMEX. Single-layer wells exhibited strong correspondence, while multilayer configurations revealed minor transient differences that resolved over time, demonstrating both the robustness of the method and GSIM's newly developed capability to simulate coupled systems. This implementation allows for precise specification of wellhead pressure without compromising the flexibility of GSIM's modular framework. The result is a reliable platform for integrated

reservoir-to-surface modeling, offering enhanced simulation accuracy and improved support for field development decisions by explicitly accounting for pipes and tubing pressure losses.

Keywords

Reservoir Simulation; Well Coupling; Numerical Simulator; Plugin Architecture.

Resumo

Santos, Gustavo Henrique Gomes dos; Menezes, Ivan Fábio Mota de; Miranda Filho, Daniel Nunes de. **Acoplamento reservatório-superfície em um simulador de reservatórios inovativo baseado em uma arquitetura de plugins**. Rio de Janeiro, 2025. 113p. Dissertação de Mestrado – Departamento de Engenharia Mecânica, Pontifícia Universidade Católica do Rio de Janeiro.

Efetivamente projetar e gerenciar os complexos sistemas de produção de petróleo da atualidade, desde o reservatório até a cabeça do poço e as instalações de superfície, exige mais do que simulações isoladas de cada componente. Abordagens tradicionais de modelagem, que tratam separadamente o reservatório e a rede de superfície, frequentemente dependem de condições de contorno estimadas, as quais não capturam adequadamente as interações entre o escoamento no meio poroso, nos poços e na superfície. Essa separação pode resultar em previsões imprecisas e estratégias operacionais subótimas. Uma abordagem de simulação mais unificada, na qual todo o sistema é modelado como uma rede de escoamento contínua, permite uma compreensão mais aprofundada do comportamento do sistema, proporciona previsões mais precisas e apoia decisões mais bem fundamentadas no desenvolvimento e na otimização da produção. Este estudo apresenta uma metodologia de acoplamento implícito entre reservatório e cabeça do poço no simulador numérico GSIM, desenvolvido por meio de uma parceria entre a Petrobras e a PUC-Rio. A abordagem considera as perdas de pressão ao longo do sistema de produção, um fator crítico para a maximização da recuperação de hidrocarbonetos. Como um passo inicial para a integração completa entre as simulações de reservatório e superfície, o método se apoia na arquitetura de plugins do GSIM, com foco nos termos residuais e da matriz Jacobiana nas iterações de Newton, utilizando tabelas de fluxo vertical multifásico (FVM), em conjunto com a análise nodal, para o acoplamento entre superfície e reservatório. Foram implementadas interpolação bilinear e linear multidimensional das tabelas hidráulicas, testadas e validadas com base nos resultados do simulador comercial IMEX, apresentando excelente correspondência. Casos de teste também foram desenvolvidos para comparar a metodologia de acoplamento proposta com o IMEX. Poços monocompletados apresentaram concordância notável, enquanto configurações multicompletadas mostraram pequenas diferenças transientes, que se dissiparam com o tempo, demonstrando a robustez do método e a nova capacidade do GSIM de replicar sistemas acoplados. Essa implementação permite especificações precisas de pressão na cabeça do poço, sem comprometer a flexibilidade do framework modular do GSIM. O resultado é uma plataforma confiável para

modelagem integrada do reservatório à superfície, oferecendo maior precisão nas simulações e melhor suporte à tomada de decisões no desenvolvimento de campos, ao considerar explicitamente as perdas de pressão nos dutos e nas colunas de produção.

Palavras-chave

Simulação de Reservatório; Acoplamento de Poço; Simulador Numérico; Arquitetura de Plugins.

Table of contents

List of figures

List of tables

List of Abreviations

WHP – Wellhead Pressure

BHP – Bottomhole Pressure

IPSM – Integrated Production System Modeling

PVT – Pressure-Volume-Temperature

FVF – Formation Volume Factor

GOC – Gas-oil Contact

WOC – Water-oil Contact

IPR – Inflow Performance Relationship

FIM – Fully Implicit Method

IMPES – Implicit Pressure, Explicit Saturation

AIM – Adaptive-Implicit Method

OPR – Outflow Performance Relationship

TPR – Tubing Performance Relationship

VLP – Vertical Lift Performance

GOR – Gas-oil Ratio

WCUT – Water Cut

LGR – Lift Gas rate

EOR – Enhanced Oil Recovery

API – Application Programming Interface

If a man knows not which port he sails, no wind is favorable

Lucius Annaeus Seneca.

1
Introduction

1.1
Theme presentation

The accurate forecasting and effective management of complex modern petroleum production systems, extending from the reservoir rock through wellbores to surface facilities, require an integrated simulation approach. Traditionally, the reservoir and the surface production network models were simulated separately, relying on estimated boundary conditions between the domains, simplifying the computational problem but often failing to capture the important interactions between the reservoir and the production system (Wang, 2019). The primary aim of reservoir simulation is to forecast a reservoir's future behavior and devise strategies to enhance hydrocarbon extraction under different operational scenarios (Chen, 2007). By integrating the domains, which form one interconnected flow system in reality (Boogaart, 2016; Bik Deli, 2021), a deeper comprehension of the system's behavior is achieved, supporting better field management decisions (Al-Mutairi et al., 2010).

Coupling reservoir, wellbore and surface facilities models provides a simulation that more accurately predicts reservoir deliverability (Breaux et al., 1985), which comes from the proper modeling of the interdependence between the parts, allowing different production strategies and yielding more reliable forecasts. An integrated system allows to simulate subsurface and surface pressure and multiphase flow behavior throughout the entire system, leading to the possibility of optimizing the entire reservoir development. Depending on the coupling scheme employed, benefits can include leveraging the rigor of third-party software for surface facilities modeling, and rigorous treatment of compositional fluid (Dobbs et al., 2011). An integrated simulation environment also fosters collaboration among experts from different disciplines, improving efficiency and the accuracy of predictions (Hiebert et al., 2011).

Despite the clear advantages, the integration is not without challenges and potential disadvantages. Accurately representing the flow within the wellbore and surface facilities along with their reservoir interactions is very complex

which can lead, depending on the case, to the preference for a separated well model approach (Williamson & Chappelear, 1981; Chappelear & Williamson, 1981). Dependent on pre-calculated tables, *ad hoc* coupling can lead to inaccuracies arising from interpolation and extrapolation, and often requires iteration and table updating. Despite being more automated, weak coupling can still result in inconsistencies across simulators and suffers from computational inefficiencies due to the sequential nature of iterative calculations (Hiebert et al., 2011). Reservoir simulations make use of a simplified fluid representation, like the black oil model, or a lumped compositional representation, making it hard to restore detailed compositional information usually required by processing plant simulations (Barroux et al., 2000). Using conventional techniques for full-field integrated models can also be very computationally intensive (Schiozer, 1994).

1.2 Motivation

Failing to account for the intrinsic interactions between the reservoir and the surface facilities, the traditional approach of simulating both as standalone systems has proven inadequate for providing reliable long-term production prediction and optimization. Therefore, a significant motivation for pursuing integrated simulation is the need to establish dynamic surface controls within a modern simulation, allowing the specification of operational constraints, such as wellhead pressure (WHP) or flow rate, which directly influence the performance of both production and injector wells. Controlling wells from surface rather than solely at the bottomhole provides a more realistic representation of actual field operations and management strategies (Schiozer, 1994; Barroux et al., 2000).

Integrated simulation encompassing factors like gravitational and frictional losses and multiphase flow effects is not only paramount for effective field operations but is intimately related to flow assurance issues (Jiang, 2008). When coupling realistic surface restrictions to the reservoir simulation, it is possible to assess if the wells may require some kind of artificial lift technology to optimize production or if they will operate within safe ranges of pressure, rates, and temperature, satisfying equipment limitations. It is also possible to gain insight into whether the wells can potentially present hydrate formation or paraffin deposition.

As a preliminary step towards achieving integrated simulation, the reservoir and surface facilities *ad hoc* coupling using pre-calculated hydraulic (or pressure drop) tables has been widely adopted in reservoir simulators (Trick,

1998; Rossi et al., 2015; Bik Deli, 2021). These tables, often generated by standalone well simulators, allow to consider pressure drop in the wellbores and pipes throughout the production system into the reservoir simulator. While having some limitations regarding accuracy due to data interpolation and extrapolation, the use of table lookup remains a fundamental component in many coupling strategies, offering computational advantages (Barroux et al., 2000; Rossi et al., 2015), paving the way for more sophisticated integrated production modeling approaches.

The GSIM Simulator, a collaborative effort by Petrobras and PUC-Rio, is a versatile and constantly evolving reservoir simulator, driven by an innovative and flexible plugin-based architecture that allows the incorporation of different models, numerical methods, and geometric treatments. Validations performed against commercial simulators attest to its ability to provide accurate results for different reservoir simulation scenarios, considering only bottomhole pressure and flow rate well specifications.

1.3 General objective

The general objective of this work is the implementation of a reservoir and surface coupled representation in a black oil reservoir simulator with a plugin architecture.

1.4 Specific objectives

The specific objectives of this work are listed as follows:

- Use the numerical reservoir simulator GSIM as a developing platform;
- Add pressure drop tables reading capabilities;
- Establish wellhead pressure specifications for controlling both production and injection wells using table lookup;
- Implement both single-completion and multi-completion well formulations;
- Compare results with the commercial simulator IMEX (CMG, 2022), from the Computer Modelling Group.

1.5 Main assumptions

The main assumptions used in this work are listed as follows:

- The formulation used for the black oil model considers a slight compressible fluid;
- A single porosity, single permeability model is adopted;
- Vertical Lift Performance (VLP) tables are used within proper input ranges, without extrapolation;
- Capillary effects are not considered in source and sink terms;
- IMEX is largely used in the industry and a validated reference simulator (Islam & Sepehrnoori, 2013).

1.6 Thesis outline

After this introduction, the thesis presents fundamental concepts describing the modeling of flow through porous media, the wellbore representation as part of the source and sink constraints, and the representation of pressure drop along production systems. Next, a literature review is presented starting with the description of the modern plugin-based GSIM, and a summary of previous work related to surface coupling. The following chapter presents the details of the implementation of the reservoir-wellhead coupling. Next the results are presented and discussed. Finally, conclusions and recommendations are laid out.

2
Fundamental concepts

2.1
Numerical reservoir simulation

The black oil numerical simulation of fluid flow within porous media constitutes a vital instrument for understanding reservoir behavior and enhancing hydrocarbon recovery. It starts with the mathematical description of multiphase flow phenomena, which are governed by mass conservation principles and Darcy's law, accounting for fluid accumulation, flux exchanges between grid blocks and source and sink terms. These governing equations are then discretized across structured or unstructured grid systems, transforming partial differential equations into algebraic forms suitable for computational solution.

The nonlinear characteristics of multiphase flow equations require the application of numerical techniques, such as the Newton's method, to effectively address the complex interactions among pressure and saturation variables. Initial conditions set the reservoir's starting parameters, including pressure distribution, fluid saturations, and phase interfaces. Wells boundary conditions are specified through either Neumann-type (flow rate) or Dirichlet-type (pressure) constraints.

Within the numerical model, wells are represented as internal boundaries that serve as localized sources or sinks. The modeling of these wells considers whether they are single or multi-completion, based on their intersection with particular grid blocks. Well control can include bottomhole pressure (BHP), wellhead pressure (WHP), or flow rate constraints for individual phases, with advanced control schemes incorporating fluid ratios like water cut and gas-oil ratio.

Extending this framework, the Integrated Production System Modeling (IPSM) approach couples reservoir behavior dynamically with surface facilities hydraulics. This coupling requires iterative updates of pressure constraints using various methodologies, such as implicit, explicit, or *ad hoc*.

2.2
Structure of an integrated reservoir and wellbore simulator

2.2.1 Fluid and rock characterization

From exploration and appraisal to development of a petroleum reservoir, the characterization of its fluids and rocks is crucial for the understanding required to properly design, manage and optimize the production of hydrocarbons.

There is a need to characterize the fluids in the reservoir by determining their composition and phase behavior under different pressure and temperature conditions, the Pressure-Volume-Temperature (PVT) properties, by analyzing collected fluid samples. For a black oil representation (Aziz & Settari, 1979; Craft et al., 1991; Ertekin et al., 2001), the following PVT parameters are important to define:

- Solution gas-oil ratio (R_s): The amount of gas dissolved in an oil at a given pressure and temperature referenced at standard conditions;
- Oil formation volume factor (Oil FVF or B_o): The ratio of oil volume, with the solution gas, at reservoir pressure and temperature conditions to its volume at standard conditions;
- Gas formation volume factor (Gas FVF or B_g): The ratio of gas volume at reservoir pressure and temperature conditions to its volume at standard conditions;
- Water formation volume factor (Water FVF or B_w): The ratio of water volume at reservoir pressure and temperature conditions to its volume at standard conditions;
- Bubble point pressure (p_b): The pressure at which the first bubble of gas appears in an oil reservoir;
- Dew point pressure (p_d): The pressure at which condensate begins to form from gas (relevant for gas reservoirs).

Rock characterization revolves around the physical and chemical aspects of the reservoir rocks and relies on core samples, well logs and seismic data. Information like lithology, which represents the rock type (e.g. sandstone and carbonate), porosity (ϕ), which represents the void space capable of storing fluids, absolute permeability (k), representing the capacity of the porous rock to transmit a single fluid, rock compressibility (c_f), mineralogy and mechanical strength are examples of key properties to be investigated.

Identifying the initial fluids saturations and fluid interfaces like gas-oil contact (GOC) and water-oil contact (WOC) along with the fluid and rock characterization result in the estimated initial hydrocarbon volumes.

As the flow in the porous medium involves the simultaneous flow of immiscible fluids (oil, water and gas), the concepts of effective permeability (k_e) and relative permeability (k_r) need also to be introduced. While the absolute permeability accounts for a single phase flowing through the reservoir, the effective permeability represents the ability of a specific phase to flow when other phases are present. Relative permeability of a phase is the ratio of the effective permeability of that phase to the absolute permeability ($k_r = k_e/k$), quantifying the impairment to flow of one phase on another (Chen, 2007). It is saturation dependent and influenced by wettability, i.e. which fluid preferentially adheres to the rock surface (Craig, 1971). Reservoir simulation usually makes use of two sets of relative permeability tables. One represents the relation between water saturation and the relative permeability of oil and water (k_{row} and k_{rw}, respectively). The other represents the relation between gas, or liquid, saturation and the relative permeability of oil and gas (k_{rog} and k_{rg}, respectively). The simulator also requires a three-phase model to compute the three phase k_{ro}, k_{rg} and k_{rw} (Corey et al., 1956; Stone, 1970, 1973; Aziz & Settari, 1979) based on the interpolated values from the two-phase tables for each iteration.

Due to the presence of multiple phases, pore size and rock wettability, all intrinsic to flow in porous medium of a hydrocarbon reservoir, capillary pressure becomes important to reservoir flow. The phenomenon involved, which is expressed by the pressure of the non-wetting phase minus the pressure of the wetting phase, leads to different pressure for each phase. For example, for a water-wet rock, $p_{cow} = p_o - p_w$ and $p_{cgo} = p_g - p_o$. These relationships are inputted in separate tables, saturation dependent, for the reservoir simulator.

2.2.2 Mathematical model

The mathematical model (Aziz & Settari, 1979; Ertekin et al., 2001) representing flow in porous medium is based on the diffusivity equation. For the black oil representation, it can be derived from conservation of mass and momentum, along with assuming a slightly compressive fluid and neglecting the energy equation by making the isotherm assumption for the reservoir.

The continuity equations in cartesian coordinates (3D) are

$$V_b \frac{\partial}{\partial t}\left(\frac{\phi S_o}{B_o}\right) = -\frac{\partial}{\partial x}\left(\frac{A_x}{B_o}u_{ox}\right)\Delta x - \frac{\partial}{\partial y}\left(\frac{A_y}{B_o}u_{oy}\right)\Delta y - \frac{\partial}{\partial z}\left(\frac{A_z}{B_o}u_{oz}\right)\Delta z + q_o \tag{2-1}$$

for the oil phase,

$$V_b \frac{\partial}{\partial t}\left(\frac{\phi S_w}{B_w}\right) = -\frac{\partial}{\partial x}\left(\frac{A_x}{B_w}u_{wx}\right)\Delta x - \frac{\partial}{\partial y}\left(\frac{A_y}{B_w}u_{wy}\right)\Delta y - \frac{\partial}{\partial z}\left(\frac{A_z}{B_w}u_{wz}\right)\Delta z + q_w \tag{2-2}$$

for the water phase, and

$$V_b \frac{\partial}{\partial t}\left(\frac{\phi S_g}{B_g} + \phi\frac{R_s}{B_o}S_o\right) = -\frac{\partial}{\partial x}\left(\frac{A_x}{B_g}u_{fgx} + A_x\frac{R_s}{B_o}u_{ox}\right)\Delta x - \frac{\partial}{\partial y}\left(\frac{A_y}{B_g}u_{fgy} + A_y\frac{R_s}{B_o}u_{oy}\right)\Delta y - \frac{\partial}{\partial z}\left(\frac{A_z}{B_g}u_{fgz} + A_z\frac{R_s}{B_o}u_{oz}\right)\Delta z + q_g \tag{2-3}$$

for the gas phase, where V_b is the bulk volume of the control volume, S_o, S_w and S_g are the oil, water and gas saturations, B_o, B_w and B_g are the oil, water and gas formation volume factors, R_s is the solution gas-oil ratio, A_x, A_y and A_z are the areas orthogonal to flow in each direction, u_{ox}, u_{oy} and u_{oz} are the oil velocities in each direction, u_{wx}, u_{wy} and u_{wz} are the water velocities in each direction, u_{fgx}, u_{fgy} and u_{fgz} are the free gas velocities in each direction, t is the time, Δx, Δy and Δz are dimensions of the control volume, and q_o, q_w and q_g are the volumetric flow rates of each phase at standard conditions.

For the momentum equation, Darcy's law (Hubbert, 1956) is employed with an extension considering relative permeabilities to account for multiphase flow in the reservoir

$$\mathbf{u}_\beta = -\frac{\mathbf{k}k_{r\beta}}{\mu_\beta}\left[\nabla p_\beta - \nabla(\gamma_\beta Z)\right], \tag{2-4}$$

where β is the fluid phase (which can be oil, water or gas), $\mathbf{u}_\beta$ is the velocity vector for phase β, $\mathbf{k}$ is the absolute permeability tensor, $k_{r\beta}$ is the relative permeability of phase β, μ_β is the viscosity of phase β, p_β is the pressure of phase β, γ_β is the fluid's phase gradient, and Z is the depth from an arbitrary point.

Combining Eq. (2-4) with Eqs. (2-1) through (2-3), results in the diffusivity equation

$$V_b \frac{\partial}{\partial t}\left(\frac{\phi S_o}{B_o}\right) = -\frac{\partial}{\partial x}\left[\frac{k_x A_x k_{ro}}{\mu_o B_o}\left(\frac{\partial p_o}{\partial x} - \gamma_o \frac{\partial Z}{\partial x}\right)\right]\Delta x - \frac{\partial}{\partial y}\left[\frac{k_y A_y k_{ro}}{\mu_o B_o}\left(\frac{\partial p_o}{\partial y} - \gamma_o \frac{\partial Z}{\partial y}\right)\right]\Delta y - \frac{\partial}{\partial z}\left[\frac{k_z A_z k_{ro}}{\mu_o B_o}\left(\frac{\partial p_o}{\partial z} - \gamma_o \frac{\partial Z}{\partial z}\right)\right]\Delta z + q_o \tag{2-5}$$

for the oil component,

$$V_b \frac{\partial}{\partial t}\left(\frac{\phi S_w}{B_w}\right) = -\frac{\partial}{\partial x}\left[\frac{k_x A_x k_{rw}}{\mu_w B_w}\left(\frac{\partial p_w}{\partial x} - \gamma_w \frac{\partial Z}{\partial x}\right)\right]\Delta x - \frac{\partial}{\partial y}\left[\frac{k_y A_y k_{rw}}{\mu_w B_w}\left(\frac{\partial p_w}{\partial y} - \gamma_w \frac{\partial Z}{\partial y}\right)\right]\Delta y - \frac{\partial}{\partial z}\left[\frac{k_z A_z k_{rw}}{\mu_w B_w}\left(\frac{\partial p_w}{\partial z} - \gamma_w \frac{\partial Z}{\partial z}\right)\right]\Delta z + q_w \tag{2-6}$$

for the water component, and

$$\begin{aligned} V_b \frac{\partial}{\partial t}&\left(\frac{\phi S_g}{B_g} + \phi \frac{R_s}{B_o} S_o\right) \\ &= -\frac{\partial}{\partial x}\left[\frac{k_x A_x k_{rg}}{\mu_g B_g}\left(\frac{\partial p_g}{\partial x} - \gamma_g \frac{\partial Z}{\partial x}\right) + \frac{k_x A_x k_{ro} R_s}{\mu_o B_o}\left(\frac{\partial p_o}{\partial x} - \gamma_o \frac{\partial Z}{\partial x}\right)\right]\Delta x - \\ &\quad \frac{\partial}{\partial y}\left[\frac{k_y A_y k_{rg}}{\mu_g B_g}\left(\frac{\partial p_g}{\partial y} - \gamma_g \frac{\partial Z}{\partial y}\right) + \frac{k_y A_y k_{ro} R_s}{\mu_o B_o}\left(\frac{\partial p_o}{\partial y} - \gamma_o \frac{\partial Z}{\partial y}\right)\right]\Delta y - \\ &\quad \frac{\partial}{\partial z}\left[\frac{k_z A_z k_{rg}}{\mu_g B_g}\left(\frac{\partial p_g}{\partial z} - \gamma_g \frac{\partial Z}{\partial z}\right) + \frac{k_z A_z k_{ro} R_s}{\mu_o B_o}\left(\frac{\partial p_o}{\partial z} - \gamma_o \frac{\partial Z}{\partial z}\right)\right]\Delta z + q_g \end{aligned} \tag{2-7}$$

for the gas component.

The terms containing the time derivatives are the accumulation terms, those containing the spatial derivatives are flux terms and the volumetric rates are the source and sink terms.

2.2.3 Numerical model

The diffusivity equation in the mathematical model is a nonlinear partial differential equation with analytical solution available only for rather simple cases. The nonlinearities arise from the dependence of the properties of fluid and rock, such as relative permeability, viscosity and density, on saturation, pressure and composition. Therefore, a numerical solution (Ertekin et al., 2001) is required and the finite difference method is employed to approximate the time and spatial derivatives, resulting in a reservoir discretized in grid blocks usually represented by i, j, k coordinates. Defining $\Phi_\beta = p_\beta - \gamma_\beta Z$, ψ_n as the set containing all neighboring blocks of a given grid block n, $T_{\beta x_i} = (k_{x_i x_i} A_{x_i} k_{r\beta})/(\Delta x_i \mu_\beta B_\beta)$, $\Delta\Phi_{\beta_{ln}} = \Phi_{\beta_l} - \Phi_{\beta_n}$, with l being a neighbor of n, Eqs. (2-5) through (2-7) can be rewritten as

$$\frac{V_b}{\Delta t}\left[\left(\frac{\phi S_o}{B_o}\right)^{n+1} - \left(\frac{\phi S_o}{B_o}\right)^{n}\right]_{i,j,k} = -\sum_{l\in\psi_n} T^m_{o_{ln}} \Delta\Phi^{n+1}_{o_{ln}} + q^{n+1}_{o_{i,j,k}} \tag{2-8}$$

for oil,

$$\frac{V_b}{\Delta t}\left[\left(\frac{\phi S_w}{B_w}\right)^{n+1} - \left(\frac{\phi S_w}{B_w}\right)^{n}\right]_{i,j,k} = -\sum_{l\in\psi_n} T^m_{w_{ln}} \Delta\Phi^{n+1}_{w_{ln}} + q^{n+1}_{w_{i,j,k}} \tag{2-9}$$

for water, and

$$\frac{V_b}{\Delta t}\left[\left(\frac{\phi S_g}{B_g} + \phi\frac{R_s S_o}{B_o}\right)^{n+1} - \left(\frac{\phi S_g}{B_g} + \frac{R_s S_o}{B_o}\right)^{n}\right]_{i,j,k} = -\sum_{l\in\psi_n}\left(T^m_{g_{ln}} \Delta\Phi^{n+1}_{g_{ln}} + R_{s_{ln}} T^m_{o_{ln}} \Delta\Phi^{n+1}_{o_{ln}}\right) + q^{n+1}_{g_{i,j,k}} \tag{2-10}$$

for gas, where superscripts n and $n+1$ represent consecutive time steps, with the superscript m assuming either the value n or $n+1$, depending on the implicitness of the solution for the specific block (Bastos, 2021).

2.2.4 Reservoir-wellbore coupling

The wells are represented as source and sink terms in the numerical reservoir simulation. These internal boundaries are frontiers between the reservoir and the external system, requiring specification for a well-posed problem. Two largely used specifications in reservoir simulators are the Neumann-type and Dirichlet-type boundary conditions. The former represents a condition where

the well produces or injects at a constant pressure gradient, which leads to a constant rate, and the latter represents a condition where the well operates with a constant bottomhole pressure (BHP). The BHP, alternatively represented as p_{wf}, is an additional variable that needs treatment.

Considering that a wellbore radius is much smaller than the block dimensions obtained from the spatial discretization used in the numerical solutions, the pressure values for those grid blocks cannot be used as a proxy for the p_{wf}. For comparison, while the radius of a well is in the order of a few decimeters, the dimension of a grid block may be of hundreds of meters. Therefore, a relationship between p_{wf}, the grid block pressure and rate is required.

Darcy's law (Dake, 1983) , in its radial form, assuming pseudosteady-state flow, and accounting for skin (Van Everdingen, 1953), gives the inflow performance relationship (IPR) which can be expressed, for the oil phase as

$$q_{o_{sc}} = -\frac{2\pi k_{ro} k_H h}{\mu_o B_o \left[\ln\left(\frac{r_e}{r_w}\right) - \frac{1}{2} + s\right]} \left(p_e - p_{wf}\right), \tag{2-11}$$

where k_{ro} is the oil relative permeability, k_H is the horizontal absolute permeability, h is the thickness of the reservoir, p_e is the external oil pressure, r_e is the external radius, r_w is the well radius and s is the skin.

Working with p_e, the pressure at the outer boundary is not practical because, in numerical simulation, the oil pressure in each grid block (p_o) is represented by the average pressure of its volume. Thus, an alternative (Dake, 1983) to Eq. (2-11) is

$$q_{osc} = -\frac{2\pi k_{ro} k_H h}{\mu_o B_o \left[\ln\left(\frac{r_e}{r_w}\right) - \frac{3}{4} + s\right]} \left(p_o - p_{wf}\right), \tag{2-12}$$

which can be simplified to

$$q_{o_{sc}} = -\frac{2\pi k_{ro} k_H h}{\mu_o B_o \left[\ln\left(0.472\frac{r_e}{r_w}\right) + s\right]} \left(p_o - p_{wf}\right). \tag{2-13}$$

Peaceman's model (Peaceman, 1978, 1983), compared this analytical solution to numerical solutions and concluded, for a numerical simulation, that the pressure of a block containing a well is the flowing pressure at an equivalent radius (r_{eq}) from the well, where

$$r_{eq} = 0.28 \frac{\left[\left(\frac{k_y}{k_x}\right)^{\frac{1}{2}} (\Delta x)^2 + \left(\frac{k_x}{k_y}\right)^{\frac{1}{2}} (\Delta y)^2\right]^{\frac{1}{2}}}{\left(\frac{k_y}{k_x}\right)^{\frac{1}{4}} + \left(\frac{k_x}{k_y}\right)^{\frac{1}{4}}}, \tag{2-14}$$

with Δx, Δy and Δz being the grid block dimensions and k_x, k_y and k_z its permeabilities.

Thus, the equation representing a multi-completed well producing oil flow rate in the simulation can be written as

$$q_{osc} = -\sum_{\sigma=1}^{M_w} \left\{ \frac{2\pi k_{ro} h \sqrt{k_x k_y}}{\mu_o B_o \left[\ln\left(\frac{r_{eq}}{r_w}\right) + s\right]} (p_o - p_{wf}) \right\}_\sigma , \tag{2-15}$$

with σ representing a well completion, and M_w the total number of completions. Defining a completion oil productivity index as

$$J_{o\sigma} = \left\{ \frac{2\pi k_{ro} h \sqrt{k_x k_y}}{\mu_o B_o \left[\ln\left(\frac{r_{eq}}{r_w}\right) + s\right]} \right\}_\sigma , \tag{2-16}$$

Eq. (2-15) can be rewritten as

$$q_{osc} = -\sum_{\sigma=1}^{M_w} \left[J_o \left(p_o - p_{wf}\right)\right]_\sigma . \tag{2-17}$$

Similar equations can be derived for water and gas phases. For an injector well, the main difference lies in the phase mobility term $k_{r\beta}/\mu_\beta$, by using the total mobility $(k_{ro}/\mu_o + k_{rw}/\mu_w + k_{rg}/\mu_g)$, leading to an injectivity index.

2.2.5 Solution of nonlinear equations

The resulting system of discretized nonlinear algebraic equations must be solved and, to that end, an iterative procedure is usually employed. One of the most common and useful techniques in reservoir simulation for that purpose is

the Newton-Raphson method, also known as Newton's method (Bastos, 2021; Wang, 2024).

Until a predefined convergence criteria is reached, at each iteration of the method the system of equations is linearized, in the form $\mathbf{J}\delta\mathbf{X} = -\mathbf{R}$, and passed down to a linear solver with the goal to obtain an update for the unknown variables. $\mathbf{R}$ is the vector of residuals, directly related to the equations discussed so far, $\delta\mathbf{X}$ is the vector of increments to the primary variables and $\mathbf{J}$ is the Jacobian matrix consisting of the derivatives of the residuals with respect to the primary variables.

For a black oil formulation, the reservoir primary variables are usually the grid block oil pressure (p_o), the water saturation (S_w) and one of the remaining phases saturation (S_o or S_g). When only two phases are present in a given block, meaning its pressure is above the bubble point, for oil reservoirs, the solution-gas/oil ratio (R_s) or bubble pressure p_b is used as primary variable instead of S_o or S_g (Ertekin et al., 2001).

For coupled simulators, well and surface facilities variables can add to this set of primary variables, increasing the complexity of the Jacobian matrix and requiring extra equations. Equation (2-18), adapted from Coats et al. (2004), exemplifies how the coupling between reservoir, well and surface facilities is approached by Newton's method. The Jacobian matrix ($\mathbf{J}$) is subdivided in a way that the derivatives of the residuals for each component can be assembled in smaller matrices, i.e.

$$\begin{bmatrix} \mathbf{J}_{rr} & \mathbf{J}_{rw} & \\ \mathbf{J}_{wr} & \mathbf{J}_{ww} & \mathbf{J}_{wf} \\ & \mathbf{J}_{fw} & \mathbf{J}_{ff} \end{bmatrix} \begin{bmatrix} \delta\mathbf{x}_r \\ \delta\mathbf{x}_w \\ \delta\mathbf{x}_f \end{bmatrix} = - \begin{bmatrix} \mathbf{R}_r \\ \mathbf{R}_w \\ \mathbf{R}_f \end{bmatrix}, \tag{2-18}$$

where

$\mathbf{J}_{rr}$ contains the derivatives of the reservoir residuals with respect to the reservoir variables;

$\mathbf{J}_{rw}$ contains the derivatives of the reservoir residuals with respect to the well variables;

$\mathbf{J}_{wr}$ contains the derivatives of the well residuals with respect to the reservoir variables;

$\mathbf{J}_{ww}$ contains the derivatives of the well residuals with respect to the well variables;

$\mathbf{J}_{wf}$ contains the derivatives of the well residuals with respect to the surface facilities variables;

$\mathbf{J}_{fw}$ contains the derivatives of the surface facilities residuals with respect to the well variables;

$\mathbf{J}_{ff}$ contains the derivatives of the surface facilities residuals with respect to the surface facilities variables;

$\delta\mathbf{x}_r$ contains the increments of reservoir variables;

$\delta\mathbf{x}_w$ contains the increments of well variables;

$\delta\mathbf{x}_f$ contains the increment of surface facilities variables;

$\mathbf{R}_r$ contains the reservoir residuals;

$\mathbf{R}_w$ contains the well residuals;

$\mathbf{R}_f$ contains the surface facilities residuals.

It is important to note that this representation allows for easy adaptation if only well and reservoir are coupled or if other subsystems were to be coupled.

Regarding the implicitness of the discrete equations within each Newton iteration, different solution schemes are available. The Fully Implicit Method (FIM) solves all primary variables simultaneously at each time step and iteration, which means the three reservoir variables are unknowns for each grid block (Chen, 2007), and is recognized for leading to a stable solution. On the other hand, the Implicit Pressure, Explicit Saturation (IMPES) method solves the pressure implicitly while treating saturation explicitly, which means only pressure increments are part of the vector of increments in the Newton's method, resulting in a more computational efficient but less stable solution. A combination of grid blocks using FIM and IMPES is possible and they can switch during the simulation considering some predefined criteria and computational cost. This is called Adaptive-Implicit Method (AIM) (Thomas & Thurnau, 1983; Forsyth Jr & Sammon, 1986; Collins et al., 1992).

2.3 Production systems

Describing flow in the subsurface is only the first step in an oil and gas development project. Ultimately, the objective is to bring the produced hydrocarbons to the market, ensuring economic viability. For that purpose, properly designing the production system is necessary and crucial in petroleum engineering.

2.3.1 Types of systems

Production systems comprise the flow from the bottom of the well, through the well tubing, pipes, pumps, manifolds to the process plant. In special cases, some process equipment, like separators, can be designed to operate before the topside facilities. Wells can have different geometries, ranging from vertical to deviated and horizontal wells, but can also have multiple branches radiating from the main wellbore. In summary, engineers may have at their disposal different options when approaching the development of a reservoir or multiple reservoirs at the same time. Hence, it is important to account for the impact of each option in the numerical simulation to substantiate a correct choice of production system.

These systems are usually categorized by their environment: mainly onshore and offshore projects. Although each presents its own peculiarities and unique challenges, the general idea is that each production system or combination of equipment impacts hydrocarbon recovery, due to different pressure losses in the whole production system.

Onshore projects usually lead to simple logistics by having wells drilled on solid ground and connected by flowlines to nearby process facilities. On the other hand, offshore projects are more complex since wells must be drilled offshore and must be connected to a fixed platform, to a floating platform or directly to a production treatment facility onshore (subsea-to-shore concept). Risers, which are vertical or inclined pipes, are needed for offshore platform connection and add to the complexity of this type of system.

2.3.2 Pressure drop in pipes

The fundamental equation governing fluid flow in pipes is derived from the application of the principles of conservation of mass and linear momentum. Assuming steady-state (Brill & Mukherjee, 1999), multiphase flow and a homogeneous mixture, it can be written as

$$\frac{dp}{dL} = -\frac{f\rho\nu^2}{2d} - \rho g sin\theta - \rho\nu\frac{d\nu}{dL}\,, \tag{2-19}$$

where :

p is the pressure,

L is the length of the pipe,

f is the Moody friction factor,

ρ is the fluid density,

ν is the fluid superficial velocity,

d is the internal diameter of the pipe,

g is the acceleration of gravity,

θ is the inclination of the pipe ($\theta = 0^o$ for a horizontal pipe).

The first term on the right-hand side of Eq. (2-19) is called the friction term, the second is called the elevation term and the last one is called the acceleration term.

The application of Eq. (2-19) for pressure drop prediction for a petroleum production system is a rather complex task due to several important factors. Some of these factors are discussed below.

Although the temperature is usually considered constant in the reservoir, the same is not true for flow along the pipes. Temperature changes because of heat exchange between the pipes and wellbore with the surroundings (rocks, air or water) present on the way from the bottom of the well to the process plant. Pressure and temperature variations cause phase changes within the fluid mixture. Therefore fluid properties for each phase vary significantly along the flow path.

Depending on pipe inclination, fluid properties and the flow rate of each phase, the multiphase flow can assume different patterns, also known as flow regimes. Each of them impacts the pressure drop differently. They are usually categorized by four patterns: bubble flow, slug flow, churn flow and annular flow (Brill & Mukherjee, 1999). It is important to remark that a well can present different flow regimes in different pipe sections.

2.3.3 Multiphase flow correlations

Given the complexity, petroleum engineers make broad use of multiphase flow correlations to estimate pressure drop in pipes and wellbores. In the literature there are many correlations, usually classified as empirical and mechanistic correlations, each with its specificity. They are developed based on experiments, field data, theoretical models and simplifying assumptions.

Empirical correlations are derived primarily from experimental data and mathematical relations and statistics to fit these data, resulting in correlations with limited theoretical basis but that can reasonably predict within the conditions they were developed. Mechanistic models do not depend only on experimental data but make different assumptions relating to physical

principles in order to predict flow regimes and their equations (Yahaya & Al Gahtani, 2010).

As previously discussed, depending on the production system, the flow from the bottomhole of the well to the process plant can have a combination of horizontal, inclined and vertical flow. Since some correlations were developed only for vertical flow, while others for horizontal or inclined flow, it is not unusual to consider different correlations for different pipe segments of a well. This is also true when we consider the existence of phase slip and different flow patterns in each segment, also demanding different correlations. When a production system is operating and well data can be obtained through regular well tests, the fitting of pressure drop can take place leading to the proper selection of correlations. While in the project phase, engineers must rely on broader correlations to predict the pressure drop.

The focus of this work is to use the prediction of pressure drop along the production systems in the numerical reservoir simulation. Although the correlations details are out of scope, Table 2.1 presents correlations largely used in the oil and gas industry.

Table 2.1: Classification of correlations. Adapted from Fevang et al. (2012).

Year	Correlation	Category	Slip	Flow regime
1963	Duns & Ros	Empirical	Yes	Yes
1963	Fancher & Brown	Empirical	No	No
1965	Hagedorn & Brown	Empirical	Yes	No
1967	Orkiszewski	Empirical	Yes	Yes
1973	Beggs & Brill	Empirical	Yes	Yes
1974	Gray	Empirical	Yes	No
1983	Mukerjee & Brill	Empirical	Yes	Yes
1983	OLGA-S	Mechanistic	Yes	Yes
2010	Petroleum Experts (1, 2, 3)	Empirical	Yes	Yes
2010	Petroleum Experts (4, 5)	Mechanistic	Yes	Yes

2.3.4 Nodal analysis

Nodal analysis is a foundational technique to analyze the performance of integrated systems, such as the flow from the reservoir through the wellbore and surface facilities (Brill & Mukherjee, 1999; Beggs, 2003). The main idea consists of dividing the production system at a specific point, also called node, into an upstream section, or inflow, and a downstream section, or outflow.

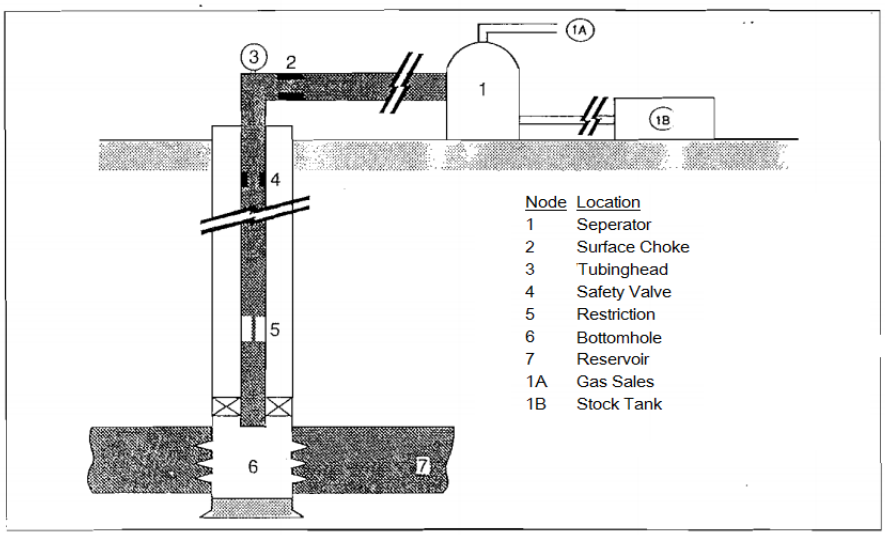

Figure 2.1: Location of various nodes. (Beggs, 2003).

Considering a producer well, the upstream section encompasses the flow from the reservoir to the chosen node and is characterized by the Inflow Performance Relationship (IPR), which describes the reservoir's ability to deliver production to that specific node by relating the flow rate to the pressure at that node. If the chosen node is the well's bottomhole, the IPR depends only on the flow through the porous medium, but if the node lies between the bottomhole and the surface, the pressure drop between the bottomhole and the node must be taken into account.

The IPR can present a nonlinear behavior due to multiphase flow in the porous medium. Simplified representations of this behavior have been proposed by Vogel (1968) and Fetkovich (1973). However, in some instances, a linear representation may be acceptable for nodal analysis.

The downstream section comprehends the flow from the node to the surface, which can encompass the wellbore, pipes and other equipments, depending on the chosen node. Usually the surface pressure is considered a defined boundary condition, representing, for example, the process plant's separator pressure or the topmost pressure of the well before gathering with the production of the other wells. This section is characterized by the Outflow Performance Relationship (OPR) also relating the flow rate to the pressure at the node, depending only on the pressure drop through pipes. It must be computed starting from the fixed surface pressure, for each flow rate, and adding all the pressure losses through the system until the node is reached. When the chosen node is the bottomhole, the OPR is also called Tubing Performance Relationship (TPR).

Boogaart (2016) illustrates in Figure 2.2 and Eq. (2-20) and Eq. (2-21)

the procedure of calculating the IPR and OPR for the tubing head as the chosen node in a simple production system.

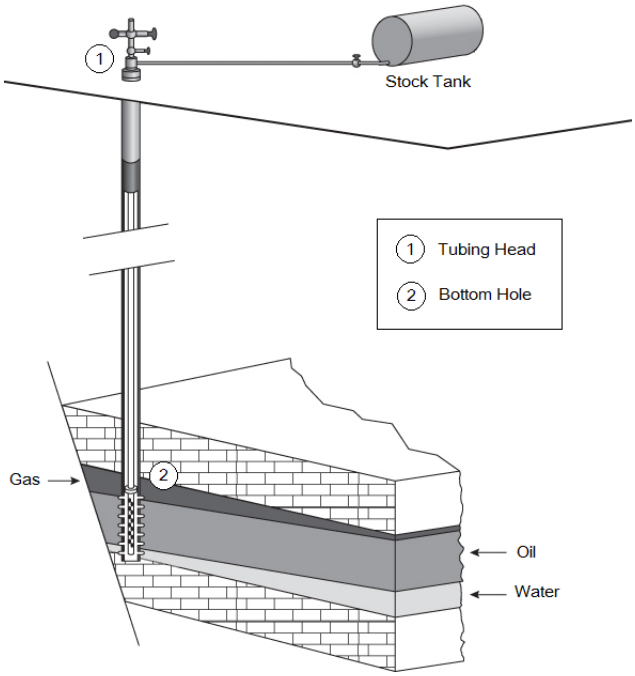

Figure 2.2: Simple production system (Boogaart, 2016).

The available pressure, or inflow node pressure for that system can be calculated as:

$$p_{res} - \Delta p_{res} - \Delta p_{tubing} = p_{th} \ , \tag{2-20}$$

and the required pressure, or outflow node pressure can be calculated as:

$$p_{out} + \Delta p_{surface} = p_{th} \ , \tag{2-21}$$

where p_{res} is the average reservoir pressure, p_{th} is the tubing head pressure, p_{out} is the stock tank pressure, $\Delta p_{surface}$ is the pressure drop through the surface facilities, Δp_{res} is the pressure drop in the reservoir, and Δp_{tubing} is the pressure drop in the tubing.

For the nodal analysis to be effective, the node must be properly defined, considering the flow rate into the node must equal the flow rate out of the node and only a single pressure can be assigned to the node. To find the system operating point, the IPR is plotted against the OPR (node pressure vs. flow rate) and the resulting intersection defines the operating node pressure and flow rate, as shown in Figure 2.3.

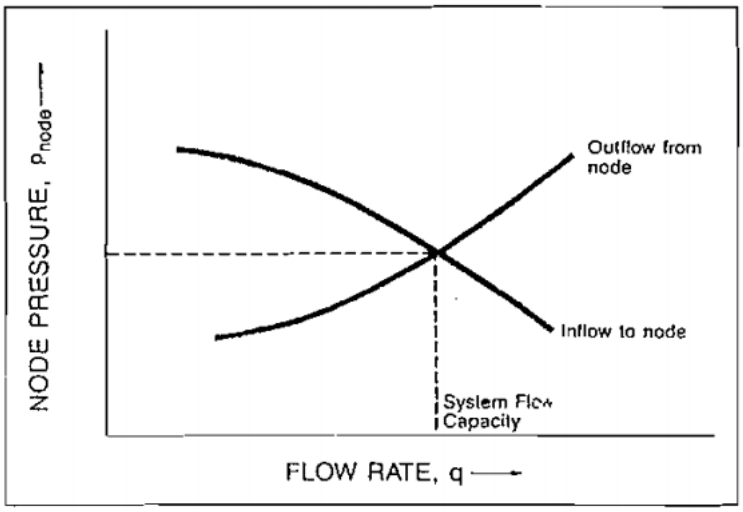

Figure 2.3: Determination of operating point (Beggs, 2003).

The OPR/TPR curve may have more than one intersection with the IPR, as shown in Figure 2.4. This can happen because of elevation pressure losses dominating low liquid rates, while friction losses dominating higher rates. An intersection to the right of the minimum pressure on the TPR curve is considered stable, because any small reduction or increase in the flow rate leads to a system response, either being the surface imposing pressure resistance or the well increasing pressure, that returns the well to the initial producing equilibrium. Intersections to the left of the minimum pressure on the TPR curve are considered unstable because any temporary displacement of the rate, leads to an increasing displacement, with the well producing smaller or higher rates (Gilbert, 1954).

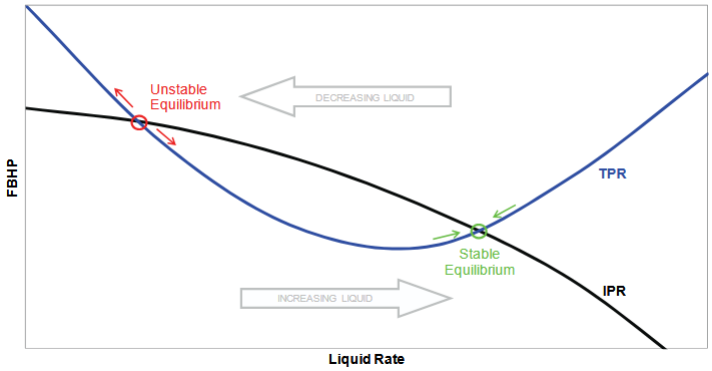

Figure 2.4: States of flow equilibrium (Lundberg, 2011). FBHP is the flowing bottomhole pressure.

2.3.5 Vertical lift performance tables

Commercial numerical reservoir simulators resort to interpolating BHP values from vertical lift performance (VLP) tables to avoid solving complex multiphase flow equations from correlations at each time step. These tables are representations of the pressure drop that occurs throughout the production system and are pre-generated using multiphase flow correlations on a third-party software specialized in wellbore and pipes modeling.

To create these tables, the engineers must first define depths, lengths, diameters, roughness and geometry of the pipes and wellbores. Temperature profiles of the surroundings and temperature exchange parameters are also required. Secondly, they must properly specify the range and discrete values of flow input parameters, which consist of wellhead pressure and rate (water or gas rate) for injector wells and wellhead pressure, gas relationships (gas-oil ratio, gas-liquid-ratio or oil-gas ratio), water relationships (water-oil ratio, water cut or water-gas ratio), artificial lift (mainly related to lift gas injection rate) and rate (oil, liquid or gas rate) for producer wells. Lastly, the correlations are chosen, and multiple steady-state flow simulations must be run resulting in tabulated bottomhole pressures, at a defined depth, for each combination of the input values.

Table 2.2 shows a simple example of a VLP table, using the input format of CMG simulators (CMG, 2022), for a producer well with a small number of discrete values for each input. These tables can easily have hundreds of lines when the proper range and discretizations of inputs are chosen. Each table used in a reservoir simulation must be numbered and contain a reference depth, which is accomplished by keywords **PTUBE1* and **DEPTH*, respectively. The discrete values of each input are presented in an array fashion represented by keywords. In this example, **OIL*, for well oil rate, **GOR*, for well gas-oil ratio, **WCUT*, for well water cut, **ALQ*, for artificial lift quantity and **WHP*, for wellhead pressure are specified. Each input value is numbered from left to right and the resulting bottomhole pressures are presented by the keyword **BHP*. The first four columns represent the combinations of the first four input values, while each remaining column represents the bottomhole pressures for each wellhead pressure.

For an injector well, the difference is that the table numbering keyword is *ITUBE1* and the only input keywords are **WAT*, for water injection rate or **GAS* for gas injection rate, and **WHP*, for wellhead pressure. The resulting VLP table is simpler since the first column of keyword **BHP* represents all the injection rate discrete values. The other columns represent the bottomhole

Table 2.2: Example of a producer VLP table (CMG, 2022).

```
*PTUBE1 1
*DEPTH 5000.0
*OIL  **rate(1) rate(2)  rate(3)   rate(4)
       0.0     4000.0   8000.0    16000.0
*GOR  **gfr(1) gfr(2)
       500.0   1000.0
*WCUT **wfr(1) wfr(2)
       0.00    0.50
*ALQ  **add(1)
       0.0
*WHP  **whp(1) whp(2)  whp(3)
       200.0   900.0   1600.0
*BHP
**irate igfr iwfr iadd bhp(1)  bhp(2)  bhp(3)
   1     1    1    1   2176.1  2873.7  3573.7
   1     1    2    1   2646.7  3344.7  4044.7
   1     2    1    1   1997.7  2670.9  3370.9
   1     2    2    1   2447.7  3124.7  3824.7
   2     1    1    1   2135.5  2876.6  3576.6
   2     1    2    1   2618.0  3351.2  4051.2
   2     2    1    1   1682.7  2674.6  3374.6
   2     2    2    1   2189.0  3132.3  3832.3
   3     1    1    1   2133.6  2884.2  3584.2
   3     1    2    1   2630.9  3368.4  4068.4
   3     2    1    1   1463.1  2684.5  3384.5
   3     2    2    1   2022.0  3152.8  3852.8
   4     1    1    1   2160.1  2912.5  3612.5
   4     1    2    1   2696.4  3433.4  4133.4
   4     2    1    1   1425.7  2721.3  3421.3
   4     2    2    1   2080.0  3231.0  3931.0
```

pressures for each wellhead pressure, as shown in Table 2.3.

Table 2.3: Example of an injector VLP table (CMG, 2022).

```
*ITUBE1 1
*DEPTH 1800.0
*WAT
** rate(1) rate(2) rate(3) rate(4) rate(5) rate(6)
   0.0     100.0   200.0   350.0   500.0   600.0
*WHP
**whp(1)   whp(2)   whp(3)   whp(4)   whp(5)
  101.325  10000.0  20000.0  30000.0  40000.0
*BHP
**irate bhp(1)   bhp(2)   bhp(3)   bhp(4)   bhp(5)
   1    17820.0  27794.0  37872.0  47949.0  58026.0
   2    17816.0  27791.0  37868.0  47945.0  58022.0
   3    17813.0  27788.0  37865.0  47942.0  58019.0
   4    17807.0  27782.0  37859.0  47936.0  58013.0
   5    17802.0  27777.0  37854.0  47931.0  58008.0
   6    17798.0  27773.0  37850.0  47927.0  58004.0
```

The table structure differs according to the commercial simulators. Nevertheless, they all work in a similar manner, with similar input and output, and represent a collection of OPR/TPR curves allowing the use of nodal analysis in the simulation for different combinations of inputs.

Figure 2.5 illustrates the representation of an example injector VLP table through a collection of TPR curves, each for a different WHP, while Figure 2.6 illustrates the same for a producer well with varying WHP and fixed gas-oil ratio (GOR), water cut (WCUT) and LGR (lift gas rate as the variable for artificial lift).

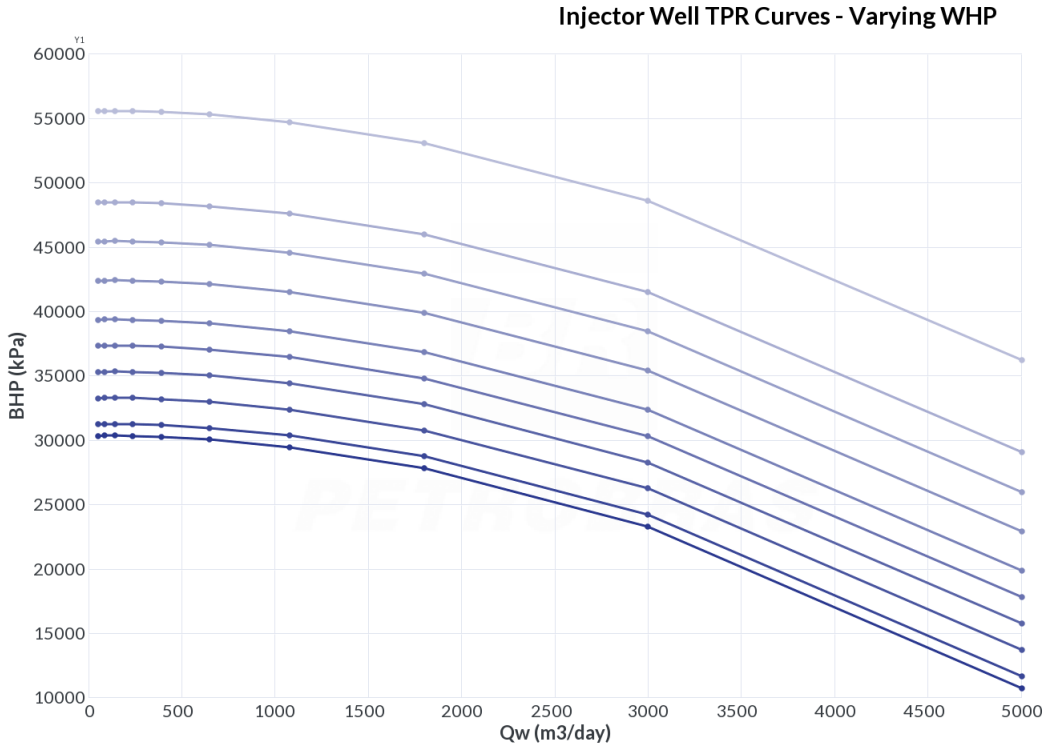

Figure 2.5: Example of an injector TPR curves represented by a VLP table.

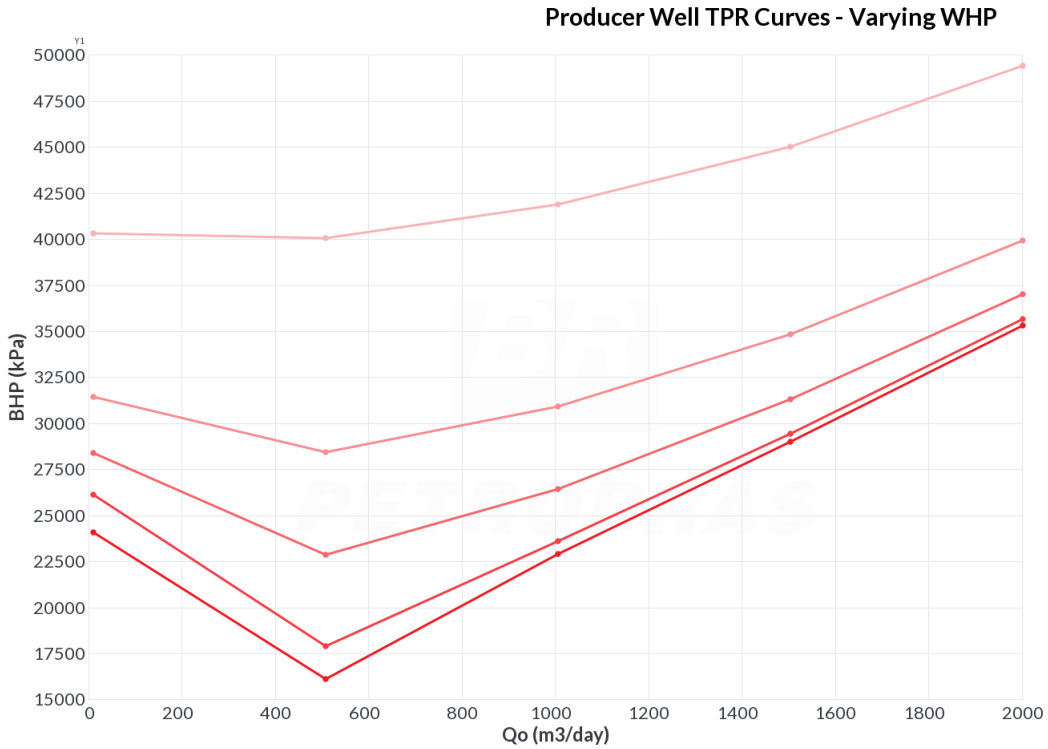

Figure 2.6: Example of a producer TPR curves represented by a VLP table.

3
Literature Review

3.1
GSIM development

The GSIM framework is a multipurpose reservoir simulator developed in a partnership between Petrobras and PUC-Rio. It was developed in C++ language and built upon TopSim (Duarte, 2016), a plugin-based architecture framework, which provides the modularity and flexibility to incorporate different formulations, solvers, and models. This architecture allows for new functionalities to be added quickly and reduces maintenance costs.

Initially, GSIM was developed with a focus on the implementation of a black oil model (Bastos, 2021), incorporating traditional and state-of-the-art techniques for multiphase flow simulation in porous media. Several plugin configurations were tested and compared against the commercial simulator IMEX (CMG, 2022), to evaluate their performance in solving multiphase flow problems. GSIM supports different numerical schemes, such as the fully implicit method (FIM) and the adaptive implicit method (AIM), as well as adaptive time-step control strategies.

Subsequently, GSIM was extended to incorporate compositional reservoir model simulation capabilities (Wang, 2024), representing an alternative to the black oil model. This evolution aims to enable the simulation of reservoirs with volatile oils or subject to enhanced oil recovery (EOR) processes where the migration of components between phases is significant. This version of GSIM also underwent validation processes, with results compared to those obtained by the commercial simulator GEM (CMG, 2022).

The modeling of petroleum flow in porous media involves the solution of nonlinear system of equations (Ertekin et al., 2001; Machado, 2023). The linearization process requires efficient solutions of linear system of equations. For this purpose, research has been conducted by Piazza (2019) to evaluate the performance of different linear solvers in the context of fully implicit reservoir simulation with GSIM. The objective was to identify the most robust and efficient solvers for the solution of the large-scale linear systems generated by the simulations.

Modenesi (2019) made efforts to extend GSIM to support unstructured grids. This capability aimed to optimize the geometric representation of complex reservoirs. The flexibility provided by unstructured meshes permits the use of small control volumes where sharp gradients occur, while coarser blocks can be applied elsewhere. Nevertheless, the establishment of sources or sinks may become more challenging.

No reservoir-surface coupling was available at the start of this work. Both black oil and compositional versions of GSIM only allowed specification of well bottomhole pressure and well flow rate. No study was found about the integration of wellbore pressure losses to the subsurface models.

3.2 Wellbore and production system coupling

The coupling of surface facilities to the subsurface simulator is necessary to allow specification of pressure and flow rates at the surface conditions. Dempsey et al. (1971) presented the idea that a reservoir simulation combined with wellbore and surface facilities calculations enhanced the deliverability prediction for a gas field. They used a model with calculations for each domain that would iterate until consistency through the whole system was achieved. Emanuel & Ranney (1981) expanded on this idea of iterative coupling by integrating a reservoir simulator to a piping network simulator. To minimize CPU time they replaced the rigorous well hydraulics calculations with pre-calculated flow tables correlating BHP against wellhead pressure, oil rate, water cut, GOR, and WCUT. This was one of the earliest mentions to the use of VLP tables. Breaux et al. (1985) made improvements to this integrated simulation and applied it to support the development plan for producing an oil reservoir at a specified rate.

Schiozer (1994) described three different methods for coupling reservoir and surface facilities. In order to reduce computation time, the explicit method solves the surface and reservoir at different time levels, requiring a balancing of the production system at the beginning of each time step to establish boundary conditions to the reservoir simulation. This can lead to large errors when rapid changes occur to production rates. The implicit method considers both the reservoir and the surface facilities as separate domains that can be solved separately using an iterative procedure until convergence in rates and bottomhole pressure is achieved. Lastly, in the fully-implicit method the surface facilities equations are integrated directly into the reservoir system. A single Jacobian matrix representing the entire system is utilized for the solution. This method demonstrates high accuracy but can be less efficient for large and

complex production systems.

Coats et al. (2004) presented the formulation for a black oil or compositional fully coupled surface and subsurface simulator. By solving the global system simultaneously, the model avoids inaccuracies and inefficiencies that arise from other coupling options.

Hiebert et al. (2011) and Hohendorff Filho (2021) categorized the integration methods in *ad hoc*, weak (explicit) coupling and strong (implicit) coupling. These are the definitions followed in this work. *Ad hoc* coupling integrates reservoir and surface facilities through the exchange of tabulated data containing pressure drop information. It is traditionally employed by commercial reservoir simulators for being less time consuming than the other forms of integration and for its simplicity, although it can have consistency problems and modeling limitations. The explicit solution may be obtained as part of an integrated computational code, which may not be as efficient as the implicit solution, when a subsurface model communicates with a well and surface model through an API (application programming interface) managed by an orchestrating module. This way the subsurface model runs to a specified time where hand-shaking occurs with the surface model. Such solution often occurs when the production system model is developed by a different development team without access to the code of the subsurface model. The frequency of handshaking depends on the changes in pressure, flow rates and composition. Hepguler et al. (1997), Trick (1998), and Ghorayeb et al. (2003) are examples of works on integrating reservoir simulation, through an interface, to a surface network simulation. In the implicit coupling, a single simulator is used to represent every domain of a field. The solution is made within a same framework, with no need to connect or transfer data to external simulators.

A nodal analysis (Beggs, 2003) is required for coupling the subsurface model with the wellbore and production system model. In essence, the available pressure from the reservoir must be in equilibrium with the required pressure to overcome the pressure losses along the production system to deliver the specified production. The available alternatives are to calculate the pressure losses in the production system during the nodal analysis or to use vertical lift performance (VLP) tables which involves various pressure losses under a range of wellhead pressures, total liquid, oil, gas or water rates, water cuts and gas-oil ratios.

When providing VLP tables, instead of the actual calculation of the pressure losses using the correlation, interpolation in the multidimensional tables is required. Bigdeli et al. (2020) states that formulations such as linear, bilinear or quadratic can be employed to interpolate the BHP from VLP tables,

but, based on the works of Emanuel & Ranney (1981) and Stackel & Brown (1981), focused on linear interpolation, investigating each input of the VLP tables as the independent variable, and comparing his implementation in the UTCOMPRS simulator (Chang, 1990) against CMG's GEM. He concluded that using the lower tabulated wellhead pressure as the parameter for linear interpolation achieved the best results, although observing differences that could be due to the formulation implemented.

Although the ultimate GSIM goal is to have a fully-fledged production system completely integrated with the subsurface model, the current work focuses exclusively on the coupling using VLP tables in the black oil formulation.

4
Reservoir-wellhead coupling implementation

4.1
VLP table interpolation

Vertical lift performance tables provide information related to pressure losses in the well tubing and pipes. Since these are generated for discrete values of flow rate, gas oil ratio, water cut, artificial lift, and WHP, interpolation is required for simulation calculations.

As discussed before, there is a difference in the number of dimensions between an injector VLP table and a producer VLP table. The former is three-dimensional, with two ordered input variables, injection rate and wellhead pressure, and one output, BHP, and the latter has six dimensions with five ordered input, production rate, gas relationship (e.g. GOR), water relationship (e.g. water cut), artificial lift (e.g. lift gas rate), and wellhead pressure, and one output, BHP.

4.1.1
Bilinear interpolation

For an injector hydraulics table, with two input variables, it seems natural to test the bilinear interpolation (Ascher & Greif, 2011). This method of interpolation consists of a linear interpolation in one direction followed by a linear interpolation in the other direction, resulting in a quadratic interpolation.

Figure 4.1 represents a scenario of interpolation of a given injection rate and a given wellhead pressure in an injector VLP table. Assuming that table extrapolation ought to be avoided, both the rate (Q) and WHP will fall between two sequenced tabulated values. For the sake of demonstration and simplicity we also assume that they are between their first and second respective tabulated values. Q_1, Q_2, WHP_1, WHP_2, $BHP_{1,1}$, $BHP_{1,2}$, $BHP_{2,1}$ and $BHP_{2,2}$ are all tabulated values.

Starting with a linear interpolation in the rate (Q) dimension, the weight of Q is defined as

$$W_Q = \frac{Q - Q_1}{Q_2 - Q_1} \,. \tag{4-1}$$

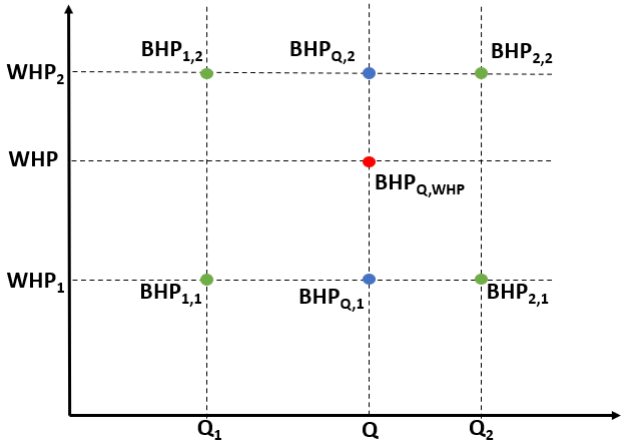

Figure 4.1: Example of a bilinear interpolation.

The BHP for Q and the first WHP is

$$BHP_{Q,1} = BHP_{1,1} + W_Q \left(BHP_{2,1} - BHP_{1,1}\right), \tag{4-2}$$

and for Q and the second WHP is

$$BHP_{Q,2} = BHP_{1,2} + W_Q(BHP_{2,2} - BHP_{1,2}). \tag{4-3}$$

Reorganizing Eqs. (4-2) and (4-3), another way of stating the BHP interpolations in the Q dimension is

$$BHP_{Q,1} = (1 - W_Q)BHP_{1,1} + W_Q BHP_{2,1}\,, \tag{4-4}$$

and

$$BHP_{Q,2} = (1 - W_Q)BHP_{1,2} + W_Q BHP_{2,2}\,. \tag{4-5}$$

To put these last two equations into words, the BHP interpolated value in the rate dimension, for a given WHP, is a weighting of the tabulated BHP values. When the rate index for the BHP is the lower value, the weighting factor assumes the value of $1 - W_Q$, and when the index is the upper value, the factor is W_Q. This way of thinking is important because it allows an easy generalization of the linear to bilinear and then to a multidimensional linear interpolation.

Following with a linear interpolation in the WHP dimension, the weight of WHP can be written as

$$W_{WHP} = \frac{WHP - WHP_1}{WHP_2 - WHP_1}\,, \tag{4-6}$$

and, using the generalization concept explained earlier, the interpolated BHP for Q and WHP as

$$BHP_{Q,WHP} = (1 - W_{WHP})BHP_{Q,1} + W_{WHP}BHP_{Q,2} \,. \tag{4-7}$$

Substituting Eq. (4-4) and Eq. (4-5) into Eq. (4-7), the expression representing the final interpolated BHP is expressed as

$$\begin{aligned} BHP_{Q,WHP} = (1 - W_Q)(1 - W_{WHP})BHP_{1,1} + \\ (1 - W_Q)W_{WHP}BHP_{1,2} + \\ W_Q(1 - W_{WHP})BHP_{2,1} + \\ W_Q W_{WHP}BHP_{2,2} \,. \end{aligned} \tag{4-8}$$

Note that the representation of the interpolated BHP in an injector VLP table is a weighting of the four corners that encompass the desired point. The weighting factor for each corner is the product of the weight of each dimension for that corner. As was shown in the interpolation equations, this dimension weight for a corner can assume two different values, depending on whether the corner has a lower or an upper index for that specific dimension.

A function to perform the bilinear interpolation for injector wells was implemented in GSIM and, as the equations indicate, every time a interpolation is required, four BHP values must be read from the table, two dimension weights and four corner weights must be computed.

4.1.2 Multidimensional linear interpolation

A typical producer VLP table has 5 sequential input variables :

1. Production rate (Q): oil phase, gas phase or liquid phase rate;
2. Gas fraction (GFR): gas-oil ratio (GOR), gas-liquid ratio (GLR) or oil-gas ratio (OGR);
3. Water fraction (WFR): water-oil ratio (WOR), water cut (WCUT) or water-gas ratio (WGR);
4. Artificial lift: Different representations are possible but only lift gas rate (LGR) was implemented in GSIM;
5. Wellhead pressure (WHP).

Bilinear interpolation must be extended to five dimensions to achieve a multi-linear interpolation (Ascher & Greif, 2011) in every dimension of the table. Using Eq. (4-8) as a starting point and the ideas discussed for the two dimensions interpolation, it becomes clear how to formulate the extension. First, the weight factor for each dimension must be computed. Second, since

there are five input dimensions and each dimension has a lower and an upper index, the generalization leads to 2^5 or 32 corners or tabulated BHP values to be consulted, instead of four.

Assuming, for simplicity, that the lower index for each dimension is 1 and the upper index is 2, the weighting factor for the Q dimension is

$$W_Q = \frac{Q - Q_1}{Q_2 - Q_1} \,, \tag{4-9}$$

for the gas fraction dimension is

$$W_{GFR} = \frac{GFR - GFR_1}{GFR_2 - GFR_1} \,, \tag{4-10}$$

for the water fraction is

$$W_{WFR} = \frac{WFR - WFR_1}{WFR_2 - WFR_1} \,, \tag{4-11}$$

for the lift gas rate is

$$W_{LGR} = \frac{LGR - LGR_1}{LGR_2 - LGR_1} \,, \tag{4-12}$$

and for WHP is

$$W_{WHP} = \frac{WHP - WHP_1}{WHP_2 - WHP_1} \,. \tag{4-13}$$

To serve as examples, the contribution of the first corner, the one with all the lower indexes, and the last corner, the one with all the upper indexes, can be represented as

$$BHP_1 = (1-W_Q)(1-W_{GFR})(1-W_{WFR})(1-W_{LGR})(1-W_{WHP})BHP_{1,1,1,1,1} \,, \tag{4-14}$$

and

$$BHP_{32} = W_Q W_{GFR} W_{WFR} W_{LGR} W_{WHP} BHP_{2,2,2,2,2} \,, \tag{4-15}$$

respectively. Any other corner will present a combination of lower and upper indexes of each dimension, and the correct adaptation must be made to the corner weighting factor. For example, assuming the second corner as the one where all inputs but the WHP have a lower index, the contribution of that corner is

$$BHP_2 = (1 - W_Q)(1 - W_{GFR})(1 - W_{WFR})(1 - W_{LGR}) W_{WHP} BHP_{1,1,1,1,2} \,. \tag{4-16}$$

To achieve the final BHP interpolation, all 32 corners contributions must be summed.

4.1.3 Interpolation validation

To validate the proposed interpolation functions, a simulation case study was elaborated with a 5-spot configuration and run on IMEX. A producer well is located at the center of the grid, while two water injectors are located at two opposing corners and two gas injectors at the other two corners. All wells have a VLP table assigned and are specified with wellhead pressure. The example tables were generated on the software Prosper (PETEX, 2024) from Petroleum Experts and can be found in Appendix A, in CMG format, along with all the tubing, pipes and correlations settings.

Figure 4.2 shows the three-dimensional view of phase saturations in the reservoir at the end of the simulation. Note that both injected water and gas breakthrough to the producer and that is very important for the validation because of different values of gas-oil ratio (GOR) and water cut impacting the pressure drop and interpolations.

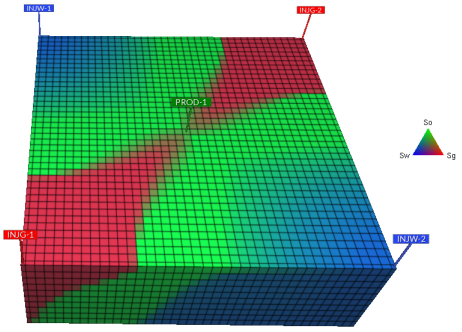

Figure 4.2: IMEX 3D model view at the end of simulation. PROD-1 (green) represents the producer well, INJW-1 and INJW-2 (blue) represent water injectors, and INJG-1 and INJG-2 (red) represent gas injectors.

Figure 4.3 presents the water rate, WHP and BHP of the water injector 1. Three time steps were chosen, each with a different combination of VLP table inputs (rate and WHP), and then the IMEX simulated BHP of the injector was compared against the bilinear interpolation algorithm, with results shown in Table 4.1.

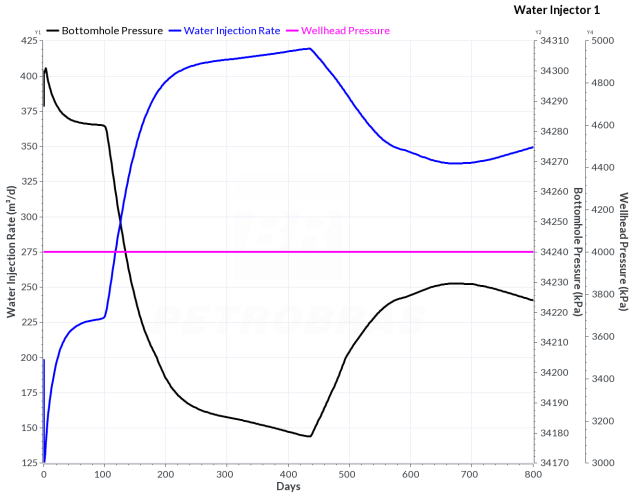

Figure 4.3: Water injector 1 curves.

Table 4.1: Water Injector VLP interpolation.

Time	Water Injection Rate	WHP	BHP	Interpol.
days	m^3/d	kPa	kPa	kPa
5	147.313	4000	34299.2	34299.2
481	395.962	4000	34198.1	34198.1
640	339.557	4000	34228.7	34228.7

Figure 4.4 shows the oil rate, GOR, WCUT, WHP, and BHP of the producer. A constant lift gas rate of 75000 m^3/d was also assigned to the producer. The multidimensional linear interpolation is compared to the IMEX simulated BHP in Table 4.2.

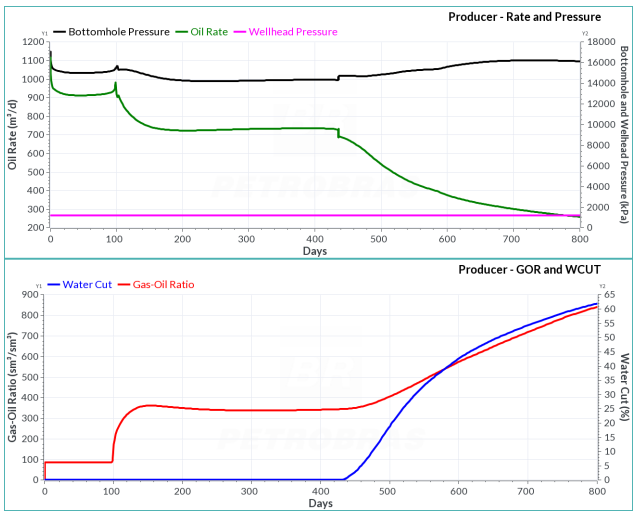

Figure 4.4: Producer curves.

Table 4.2: Producer VLP interpolation.

Time	Oil Rate	GOR	WCUT	LGR	WHP	BHP	Interpol.
days	m^3/d	sm^3/sm^3	%	m^3/d	kPa	kPa	kPa
5	947.4	84.4	0.05	75000	1200	15370.2	15370.2
481	596.5	378.7	12.12	75000	1200	14700.3	14700.3
640	337.6	632.6	48.07	75000	1200	15954.2	15954.2

Although this validation was not exhaustive, the proposed interpolation functions showed great promise and have now been implemented as GSIM's lookup tool for VLP tables. Other interpolation methods can be tested in the future but for the purposes of this work, bilinear and multidimensional linear interpolation seemed to suffice.

4.2 Newton's method implementation

To implement the reservoir coupling with the wellhead implicitly in GSIM, adaptations are necessary to the solution of the nonlinear equations already in use. GSIM uses finite differences for the discretization of the nonlinear partial differential equations and Newton's method for linearization

$$\mathbf{J}\delta\mathbf{X} = -\mathbf{R}\,, \tag{4-17}$$

where $\mathbf{R}$ is the vector of residuals, $\delta\mathbf{X}$ is a vector containing the increments of the primary variables and $\mathbf{J}$ is the Jacobian matrix with the derivatives of the residuals with respect to the primary variables.

The source and sink terms, which are impacted by the kind of well specification, appear on the residual vector and their derivatives appear on the Jacobian matrix. As this work focuses on a methodology to implement wellhead pressure specification using VLP tables for wells, there is a need to approach every term of Eq. (4-17) regarding only source and sink terms modifications. All other terms, accumulation and flux terms, that constitute the reservoir residuals are not affected by the specification of the wells.

Another important consideration is that grid blocks that contain wells completions are always treated implicitly by GSIM, even when using AIM solution method, so they will always have three reservoir primary variables, p_o, S_w and either p_b, if the block is undersaturated, or S_o, if saturated.

The generic structure of the Jacobian matrix in GSIM is shown in Figure 4.5, comprising of four submatrices:

– **RR**: containing the derivatives of reservoir equations with respect to reservoir primary variables;

- **RW**: containing the derivatives of reservoir equations with respect to well primary variables;
- **WR**: containing the derivatives of well equations with respect to reservoir primary variables;
- **WW**: containing the derivatives of well equations with respect to well primary variables;

Figure 4.5: Jacobian structure with sub matrices (Bastos, 2021).

For more detailed information about the structure and how it changes according to well specifications in GSIM, refer to the work of Bastos (2021). In summary, for bottomhole pressure specification GSIM works only with the **RR** submatrix, with no well equations and no well variables added to the Jacobian matrix. And for rate specification, all four submatrices are used and the well's reference layer bottomhole pressure, $p_{wf,ref}$, is considered a well primary variable.

For wellhead pressure specification, a decision was made to follow the structure of the bottomhole pressure specification, with only the **RR** submatrix and reservoir primary variables. The four submatrices solution is left to be investigated in the future and compared to the single submatrix one.

4.2.1 Residual term

The term of the reservoir residual equations concerning the coupling between reservoir and well is the source and sink term. For a given perforated grid block k, the water phase component is

$$q_{w,k} = -J_{w,k}(p_{w,k} - p_{wf,k}), \tag{4-18}$$

the oil phase component is

$$q_{o,k} = -J_{o,k}(p_{o,k} - p_{wf,k}), \tag{4-19}$$

and the gas component is

$$q_{g,k} = -J_{g,k}(p_{g,k} - p_{wf,k}) - R_{s,k}J_{o,k}(p_{o,k} - p_{wf,k}), \tag{4-20}$$

where $J_{w,k}$, $J_{o,k}$ and $J_{g,k}$ are the water, oil and gas productivity indexes for the perforated block, respectively. $p_{w,k}$, $p_{o,k}$ and $p_{g,k}$ are the block's phase pressure, that can differ from each other by the capillary effects. $R_{s,k}$ is the block's solution gas-oil ratio and $p_{wf,k}$ is the bottomhole pressure of the block. Although GSIM is designed to use capillary pressure in the calculations, in its well model plugin it is currently being neglected. For the remainder of this work, and only for well calculations, $p_{w,k}$, $p_{o,k}$ and $p_{g,k}$ are considered of the same magnitude.

The bottomhole pressure of a perforated grid block, in GSIM, can be written as

$$p_{wf,k} = p_{wf,ref} + \gamma_m \Delta Z_k \,, \tag{4-21}$$

where $p_{wf,ref}$ is the bottomhole pressure of the reference layer, γ_m is the mean well hydrostatic gradient and ΔZ_k is the height difference between the completion k and the reference layer.

Since the objective was to implement the specification of wellhead pressure, a way of bringing the information of the VLP tables to the source and sink term was required. Wellhead pressure is not a part of the well model but it can be used for the calculation of the bottomhole pressure of the reference layer. And the tool to estimate a well BHP, given a VLP table and a specified WHP is to use inflow performance relationship (IPR) and tubing performance relationship (TPR) for nodal analysis.

4.2.1.1 IPR calculation

The coupling between the production system and the reservoir in GSIM was implemented at the reference layer. So the first step in performing the nodal analysis is to determine the well's IPR at the reference layer depth.

From the well model, the relationship between a well's bottomhole pressure and rate for a single-layer well can be written as

$$p_{wf,ref} = \frac{q_w}{J_w} + p_w \,, \tag{4-22}$$

for the water phase,

$$p_{wf,ref} = \frac{q_o}{J_o} + p_o \,, \tag{4-23}$$

for the oil phase, and

$$p_{wf,ref} = \frac{q_g}{J_g + R_s J_o} + \frac{J_g p_g + R_s J_o p_o}{J_g + R_s J_o}\,, \tag{4-24}$$

for the gas phase.

It is important to highlight that the convention used in this work is that production rates carry a negative sign, while injection rates are positive. Eqs. (4-22) through (4-24) give the IPR for each phase. A liquid IPR and a total IPR can also be computed if desired. The line described by the IPR is considered the available pressure that can be delivered to the production system.

For a multilayer well, the IPR calculation is not so direct but can be derived. Using the oil phase as example and a well with n completions, the well oil rate is

$${Q_o}^{well} = \sum_{k=1}^{n} \left[-J_{o,k}\left(p_{o,k} - p_{wf,ref} - \gamma_m \Delta Z_k\right)\right]. \tag{4-25}$$

Rearrangement of Eq. (4-25) gives

$${Q_o}^{well} = \left(\sum_{k=1}^{n} -J_{o,k}\right)\left[\frac{\sum_{k=1}^{n} J_{o,k}\left(p_{o,k} - \gamma_m \Delta Z_k\right)}{\sum_{k=1}^{n} J_{o,k}} - p_{wf,ref}\right]. \tag{4-26}$$

Defining the well oil productivity index as

$$J_o^{well} = \sum_{k=1}^{n} -J_{o,k}\,, \tag{4-27}$$

and the average well oil pressure as

$$\overline{P_o} = \frac{\sum_{k=1}^{n} J_{o,k}(p_{o,k} - \gamma_m \Delta Z_k)}{\sum_{k=1}^{n} J_{o,k}}\,, \tag{4-28}$$

Eq. (4-26) can be rewritten as

$${Q_o}^{well} = -J_o^{well}(\overline{P_o} - p_{wf,ref})\,. \tag{4-29}$$

This representation is suggested by Ertekin et al. (2001) and similar relations can be derived for water, gas, liquid and total IPR. Note that $\overline{P_o}$ is a weighted pressure of the completions, hydrostatically corrected to the reference layer depth. The available pressure for a multilayer well is represented by

$$p_{wf,ref} = \frac{Q_o^{well}}{J_o^{well}} + \overline{P_o}\,. \tag{4-30}$$

4.2.1.2 Nodal Analysis

Now that the IPR at the reference layer's depth is calculated, the process of nodal analysis can begin. The objective is to find the intersection between

the IPR and the TPR. The TPR, for a combination of inputs, is given by a VLP table. The reference depth of the VLP table should be the same as the depth of the reference layer or else a hydrostatic correction to the output of the table must take place.

The algorithm implemented does the following :

- Identify the type of well (injector or producer);
- In the case of a producer well, estimates the gas and water fractions based on the phases productivity indexes at the beginning of the Newton iteration, and, if assigned, get the value of lift gas rate;
- WHP is given by the specification of the well;
- The correct phase IPR is selected corresponding to the phase rate informed in the VLP table;
- Iterates sequentially through all the tabulated rate values, calculating the available pressure, using the IPR, and the required pressure, interpolating the VLP table, for each rate.

This procedure allows the comparison between the available and required pressure for each rate and also between each rate and the next. This accomplishes two objectives:

- Identify all the intersections between the IPR and TPR;
- Identify if an intersection point is stable or unstable.

Assuming a linear behavior for the TPR between two sequenced rates, but with all other inputs fixed, with a stable intersection rate range identified, the exactly intersection point comes down to intersecting two line equations (IPR and TPR). With the intersected reference layer's BHP, the bottomhole pressure for all completions can be computed using the well's gradient and hence all completions rates can also be computed.

Figure 4.6 represents the nodal analysis for a producer well. The blue circles represent the available pressures and the red circles represent the required pressures for each rate informed in the VLP table. The derivative of the TPR at an intersection point defines the stability of the operating point. In other words, when a red circle is higher than a blue circle for a given tabulated rate and for the next rate the blue circle is higher, than there is an unstable intersection between the rates. On the other hand, if a blue circle is higher than a red circle for a given rate but for the next rate the red circle is higher, than there is a stable intersection point. Otherwise there are no intersections between the sequenced rates. If no intersection exists in any segment of rate, the well should be closed.

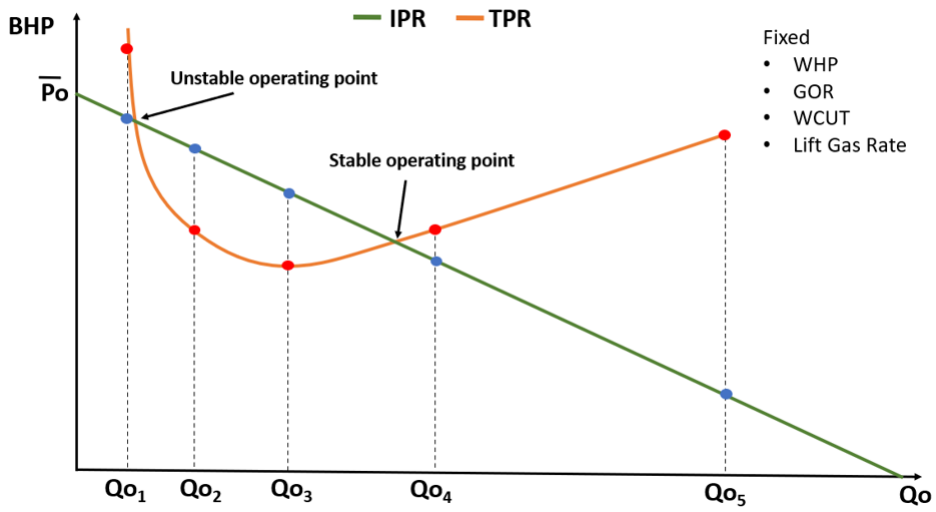

Figure 4.6: Nodal analysis implemented in GSIM.

4.2.2 Jacobian matrix term

The terms of interest are the partial derivatives of the source and sink terms with respect to the reservoir primary variables: $\partial q_\beta/\partial p_o$, $\partial q_\beta/\partial S_w$ and $\partial q_\beta/\partial p_b$ or $\partial q_\beta/\partial S_o$, with q representing the completion rate and β representing oil, gas or water phases. p_b is a primary variable when the grid block is undersaturated and S_o is the third primary variable when the block is saturated.

Let X_k represent the primary variables, $p_{o,k}$, $S_{w,k}$ and $p_{b,k}$ or $S_{o,k}$. For a rate specified well, its BHP, $p_{wf,ref}$, is also a primary variable. The derivatives for a given well completion k are

$$\frac{\partial q_{o,k}}{\partial X_k} = \frac{\partial[-J_{o,k}(p_{\beta,k} - p_{wf,ref} - \gamma_m \Delta Z_k)]}{\partial X_k} \tag{4-31}$$

for the oil phase,

$$\frac{\partial q_{w,k}}{\partial X_k} = \frac{\partial[-J_{w,k}(p_{w,k} - p_{wf,ref} - \gamma_m \Delta Z_k)]}{\partial X_k} \tag{4-32}$$

for the water phase, and

$$\frac{\partial q_{g,k}}{\partial X_k} = \frac{\partial\left[-J_{g,k}(p_{g,k} - p_{wf,ref} - \gamma_m \Delta Z_k) - R_{s,k} J_{o,k}(p_{o,k} - p_{wf,k})\right]}{\partial X_k} \tag{4-33}$$

for the gas phase.

In this research, a numerical derivative approach and a semi-analytical one were employed to estimate Eqs. (4-31) through (4-33), and are described next. An automatic differentiation (Aubert et al., 2001; Baydin et al., 2018)

solution is currently being implemented by the GSIM technical team, which avoids manually programming any derivatives present in the Jacobian matrix, but will not be addressed in this work.

4.2.2.1 Numerical approach

The numerical differentiation (Burden & Faires, 2010), for the sink and source terms, was the first implemented given its simplicity and generic application to all types of wells without change in complexity.

Given a small perturbation ϵ to the primary variable X_k, the idea is to approximate Eqs. (4-31) through (4-33) to

$$\frac{\partial q_{\beta,k}}{\partial X_k} \approx \frac{q_{\beta,k}(X_k+\epsilon) - q_{\beta,k}(X_k)}{\epsilon}. \tag{4-34}$$

While the terms $J_{\beta,k}(X_k+\epsilon)$, $p_{\beta,k}(X_k+\epsilon)$ and $\gamma_m(X_k+\epsilon)$ are straightforward because they depend only on perturbations of pressure, relative permeability and fluid properties, the term $p_{wf,ref}(X_k+\epsilon)$ demands some attention.

The proposed method for calculating $p_{wf,ref}(X_k+\epsilon)$ for a wellhead pressure specified well, assuming the production VLP table was generated with oil rate as one of the inputs, is to first estimate $J_o^{well}(X_k+\epsilon)$ and $\overline{P_o}(X_k+\epsilon)$ from Eqs. (4-27) and (4-28) and then redo the search for the operating point through the nodal analysis described earlier. If the table has liquid or gas rate as input, the appropriate well productivity index and pressure ($\overline{P}_\beta$) should be used.

In summary, the perturbation of a primary reservoir variable in a given well completion gives a new well IPR, which gives a new intersection point with the TPR. This process has to be done for every well completion but it is independent of the fluid phase β.

Note that for a bottomhole specified well, $p_{wf,ref}(X_k+\epsilon) = p_{wf,ref}(X_k)$, and for a flow rate specified well, because GSIM uses the coupled form for the Jacobian matrix with four submatrices, $p_{wf,ref}$ is a primary variable of the problem.

4.2.2.2 Semi-analytical approach

This approach relies on the expansion of Eqs. (4-31) through (4-33) (Ertekin et al., 2001), which can generally be rewritten as

$$\frac{\partial q_{\beta,k}}{\partial X_k} = -\left(p_{\beta,k} - p_{wf,ref} - \gamma_m \Delta Z_k\right)\frac{\partial J_{\beta,k}}{\partial X_k} - J_{\beta,k}\left(\frac{\partial p_{\beta,k}}{\partial X_k} - \Delta Z_k \frac{\partial \gamma_m}{\partial X_k}\right) + J_{\beta,k}\frac{\partial p_{wf,ref}}{\partial X_k}\,. \tag{4-35}$$

The expression for the derivatives of the gas rate of a producing well is slightly different, since an extra term containing the solution gas-oil ratio ($R_{s,k}$) is present, as shown in Eq. (4-33). For simplicity of demonstration that expression will be left aside, but it must be taken into account. It is semi-analytical because when further expanding the equations, some derivatives of tabulated values appear and numerical differentiation is employed. All terms are common to other forms of well specification and are well documented in the literature, with the exception of the term $\partial p_{wf,ref}/\partial X_k$ for a wellhead pressure specified well. For a bottomhole pressure specified well, $\partial p_{wf,ref}/\partial X_k = 0$, and for a flow rate specified well, $\partial p_{wf,ref}/\partial X_k = 0$, when differentiating with respect to reservoir primary variables, and $\partial p_{wf,ref}/\partial X_k = 1$, when differentiating with respect to well BHP primary variable.

Assuming the BHP of a well with WHP specification is a function of the parameters in its VLP table, for an injector well it can be written as

$$p_{wf,ref} = BHP(Q^{well}, WHP)\,, \tag{4-36}$$

and for a producer as

$$p_{wf,ref} = BHP(Q^{well}, GFR, WFR, LGR, WHP)\,, \tag{4-37}$$

with Q^{well} being a well phase rate, GFR the gas fraction, WFR the water fraction, LGR the lift gas rate and WHP the wellhead pressure. Applying the chain rule to Eqs. (4-36) and (4-37) when dealing with hydraulics flow tables for the coupling between reservoir and facilities as Yang et al. (2009), one can write for an injector well (with β being water or gas)

$$\frac{\partial p_{wf,ref}}{\partial X_k} = \frac{\partial p_{wf,ref}}{\partial Q_\beta^{well}}\frac{\partial Q_\beta^{well}}{\partial X_k} + \frac{\partial p_{wf,ref}}{\partial WHP}\frac{\partial WHP}{\partial X_k}\,, \tag{4-38}$$

and for a producer well, assuming oil rate, GOR, WCUT, LGR and WHP as inputs

$$\frac{\partial p_{wf,ref}}{\partial X_k} = \frac{\partial p_{wf,ref}}{\partial Q_o^{well}}\frac{\partial Q_o^{well}}{\partial X_k} + \frac{\partial p_{wf,ref}}{\partial GOR}\frac{\partial GOR}{\partial X_k} + \frac{\partial p_{wf,ref}}{\partial WCUT}\frac{\partial WCUT}{\partial X_k} + \frac{\partial p_{wf,ref}}{\partial LGR}\frac{\partial LGR}{\partial X_k} + \frac{\partial p_{wf,ref}}{\partial WHP}\frac{\partial WHP}{\partial X_k}\,. \tag{4-39}$$

The terms $\partial p_{wf,ref}/\partial Q_\beta^{well}$ and $\partial p_{wf,ref}/\partial WHP$ from Eq. (4-38) and

$\partial p_{wf,ref}/\partial Q_o^{well}$, $\partial p_{wf,ref}/\partial GOR$, $\partial p_{wf,ref}/\partial WCUT$, $\partial p_{wf,ref}/\partial LGR$ and $\partial p_{wf,ref}/\partial WHP$ from Eq. (4-39) can all be estimated numerically from the VLP tables. Assuming linear interpolation for a given input in the VLP table, these terms are the slopes of the lines between two sequenced tabulated values for each dimension. The term $\partial WHP/\partial X_k$ equals zero for wellhead pressure specification and, assuming a constant lift gas rate assignment, the term $\partial LGR/\partial X_k$ also equals zero. The terms $\partial Q_\beta^{well}/\partial X_k$ and $\partial Q_o^{well}/\partial X_k$ can be simplified to

$$\frac{\partial Q_\beta^{well}}{\partial X_k} = \frac{\partial q_{\beta,k}}{\partial X_k} \,, \tag{4-40}$$

and

$$\frac{\partial Q_o^{well}}{\partial X_k} = \frac{\partial q_{o,k}}{\partial X_k} \,, \tag{4-41}$$

given the fact that, for a well with n completions,

$$Q_\beta^{well} = \sum_{k=1}^{n} q_{\beta,k} \,, \tag{4-42}$$

and

$$Q_o^{well} = \sum_{k=1}^{n} q_{o,k} \,. \tag{4-43}$$

The only terms left to estimate are $\partial GOR/\partial X_k$ and $\partial WCUT/\partial X_k$. By definition,

$$GOR = \frac{Q_g^{well}}{Q_o^{well}} \,, \tag{4-44}$$

and

$$WCUT = \frac{Q_w^{well}}{Q_w^{well} + Q_o^{well}} \,. \tag{4-45}$$

The remaining terms can be written as (Yang et al., 2009)

$$\frac{\partial GOR}{\partial X_k} = \frac{1}{Q_o^{well}} \left(\frac{\partial Q_g^{well}}{\partial X_k} - GOR \frac{\partial Q_o^{well}}{\partial X_k} \right) \,, \tag{4-46}$$

and

$$\frac{\partial WCUT}{\partial X_k} = \frac{1}{Q_w^{well} + Q_o^{well}} \left[\frac{\partial Q_w^{well}}{\partial X_k} - WCUT \left(\frac{\partial Q_w^{well}}{\partial X_k} + \frac{\partial Q_o^{well}}{\partial X_k} \right) \right] \,. \tag{4-47}$$

Using Eq. (4-40) and Eq. (4-41), the above equations can be rewritten as

$$\frac{\partial GOR}{\partial X_k} = \frac{1}{Q_o^{well}} \left(\frac{\partial q_{g,k}}{\partial X_k} - GOR \frac{\partial q_{o,k}}{\partial X_k} \right) \,, \tag{4-48}$$

and

$$\frac{\partial WCUT}{\partial X_k} = \frac{1}{Q_w^{well} + Q_o^{well}} \left[\frac{\partial q_{w,k}}{\partial X_k} - WCUT \left(\frac{\partial q_{w,k}}{\partial X_k} + \frac{\partial q_{o,k}}{\partial X_k} \right) \right] \,. \tag{4-49}$$

Now it is possible to finally go back to Eq. (4-35) and substitute the term $\partial p_{wf,ref}/\partial X_k$. But first, for simplicity, let's define

$$A_{\beta,k} = -\left(p_{\beta,k} - p_{wf,ref} - \gamma_m \Delta Z_k\right) \frac{\partial J_{\beta,k}}{\partial X_k} - J_{\beta,k}\left(\frac{\partial p_{\beta,k}}{\partial X_k} - \Delta Z_k \frac{\partial \gamma_m}{\partial X_k}\right), \tag{4-50}$$

and rewrite Eq. (4-35) as

$$\frac{\partial q_{\beta,k}}{\partial X_k} = A_{\beta,k} + J_{\beta,k}\frac{\partial p_{wf,ref}}{\partial X_k}. \tag{4-51}$$

Using the fact that for wellhead pressure specification the WHP is constant and substituting Eq. (4-38) and Eq. (4-40) into Eq. (4-51), for an injector well, the derivative of the source and sink term can be written as

$$\frac{\partial q_{\beta,k}}{\partial X_k} = A_{\beta,k} + J_{\beta,k}\frac{\partial p_{wf,ref}}{\partial Q_\beta^{well}}\frac{\partial q_{\beta,k}}{\partial X_k}, \tag{4-52}$$

which can be further simplified to

$$\frac{\partial q_{\beta,k}}{\partial X_k} = \frac{A_{\beta,k}}{1 - J_{\beta,k}\dfrac{\partial p_{wf,ref}}{\partial Q_\beta^{well}}}. \tag{4-53}$$

Making use of Eq. (4-39) and Eq. (4-41) for a wellhead pressure specified producer well with a constant lift gas rate, Eq. (4-51) can be rewritten as

$$\frac{\partial q_{\beta,k}}{\partial X_k} = A_{\beta,k} + J_{\beta,k}\left(\frac{\partial p_{wf,ref}}{\partial Q_o^{well}}\frac{\partial Q_o^{well}}{\partial X_k} + \frac{\partial p_{wf,ref}}{\partial GOR}\frac{\partial GOR}{\partial X_k} + \frac{\partial p_{wf,ref}}{\partial WCUT}\frac{\partial WCUT}{\partial X_k}\right). \tag{4-54}$$

Substituting Eq. (4-48) and Eq. (4-49) into Eq. (4-54) gives the derivative of the source and sink term

$$\frac{\partial q_{\beta,k}}{\partial X_k} = A_{\beta,k} + J_{\beta,k}\left\{\frac{\partial p_{wf,ref}}{\partial Q_o^{well}}\frac{\partial q_{o,k}}{\partial X_k} + \frac{\partial p_{wf,ref}}{\partial GOR}\frac{1}{Q_o^{well}}\left(\frac{\partial q_{g,k}}{\partial X_k} - GOR\frac{\partial q_{o,k}}{\partial X_k}\right) + \frac{\partial p_{wf,ref}}{\partial WCUT}\frac{1}{Q_w^{well} + Q_o^{well}}\left[\frac{\partial q_{w,k}}{\partial X_k} - WCUT\left(\frac{\partial q_{w,k}}{\partial X_k} + \frac{\partial q_{o,k}}{\partial X_k}\right)\right]\right\}. \tag{4-55}$$

Note that this equation was derived for a producer VLP table with oil rate, GOR and WCUT as inputs. Any other choices of phase rate and gas and water fractions lead to a similar but different equation. Also, since β

represents three different phases and X_k represents three different reservoir primary variables, each well completion k has six derivative equations that should be part of the Jacobian matrix.

It is important to highlight that specifically for a producer well, Eq. (4-55) shows that regardless of the phase β, the derivatives of all three phases rates appear on the right hand side of the equation. This means that for each completion k and each primary variable X_k, there are three equations and three unknowns, which are the derivatives of the source and sink terms of each phase. So the drawback of the solution by the semi-analytical approach, for a producer well, is that it leads to solving different systems of linear equations. On the other hand, this solution, for the Jacobian term, doesn't require the search of a new intersection point between IPR and TPR through nodal analysis for every term of the matrix that represents a well completion.

4.3 Implementation challenges

GSIM has a plugin based architecture which means that each plugin has a specific responsibility towards the reservoir simulation. The ideal scenario is that the coding of one plugin doesn't require the knowledge of the coding of the other plugins, but only the knowledge of which interfaces to call upon. That being said, while studying GSIM's code and expanding the reservoir-well plugin, the focus of this work, it became clear that many well calculations were not centralized, but rather scattered in a few plugins. And the main reason is that GSIM black oil relies on the reservoir-well plugin for well calculations but also on the water, oil and gas plugins to mount the Jacobian matrix, including the source and sink derivative terms calculations. On top of that, as each phase plugin is called sequentially the semi-analytical approach to the Jacobian matrix terms of producer wells, proposed in this research, which requires a more centralized structure to deal with various systems of linear equations and with different phase rates derivatives as unknowns, had to be left for a future update.

Because of that, aiming at improving architecture, maintainability and future expansions, a lot of time and effort was given to organize and centralize all well calculations, including the derivatives for the Jacobian matrix, in the reservoir-well plugin, not only regarding wellhead pressure specification but all other previously implemented well specifications.

GSIM is also in continuous evolution, not only by researchers but also by a dedicated team in PUC-Rio, and that means, like any other software development, dealing with different versions, updates, code conflict, bugs and

performance issues. For most part of this research, any change of code would take several minutes to build and to be tested with a reservoir simulation in any version that was not the main, which made the process of coding and debugging very time consuming. This was later addressed by the dedicated team and now it requires a few seconds for any version, which all future researchers will benefit greatly.

One very important difficulty encountered was related to the calculation of the wellbore fluid gradient (γ_m). Ertekin et al. (2001) suggests two ways of estimating γ_m, with the first being a mean wellbore gradient for the entire well, using a mean bottomhole pressure, and the second using mean gravity of all fluids in the wellbore for each interval (distance between two completions) of the well. Firstly, GSIM was implemented using the mean wellbore gradient, but some improvements were found to be required in its calculations, which will have important impact in the structure of the reservoir-well plugin. Secondly, to guarantee we are only comparing the implementation of wellhead pressure specification, mainly for multilayer wells, it was relevant to know which method IMEX uses but it didn't become clear. For these reasons, when generating the case studies for result comparing, a constant value of γ_m was used.

4.4 Development considerations

The methodology for the implementation of wellhead pressure specification using vertical lift performance tables in GSIM was described along this chapter. However, some simplifications and assumptions were considered in the process as follows:

- Only the submatrix containing the derivatives of reservoir equations with respect to reservoir primary variables (RR) was used as the Jacobian matrix;
- Only constant lift gas rate was considered as the input associated to artificial lift in VLP tables from producers;
- BHP calculation is made at every Newton iteration;
- GOR and WCUT convergence check is not being performed at the end of the nodal analysis due to simulation convergence problems;
- Semi-analytical approach to the Jacobian matrix source and sink terms was implemented only for injector wells;
- Numerical approach to the Jacobian matrix source and sink terms is the default calculation and was implemented for producers and injectors;

– For the purpose of comparing results with the commercial simulator, constant values of mean wellbore fluid gradient (γ_m) were given for producers, water injectors and gas injectors with the objective to isolate WHP specification implementation effects.

5
Results

5.1
Models

To test and validate each step of the proposed implementation of reservoir-wellhead coupling on GSIM, a single-layer model and a multilayer model were created. Tables 5.1 and 5.2 show the dimensions of each grid.

Table 5.1: Single-layer grid.

Number of grid blocks in x, y and z	$10 \times 10 \times 1$
Grid block length in x and y (m)	50×50
Grid block thickness (m)	10
Grid top (m)	3000

Table 5.2: Multilayer grid.

Number of grid blocks in x, y and z	$10 \times 10 \times 5$
Grid block length in x and y (m)	50×50
Grid block thickness (m)	10
Grid top (m)	3000

For the physical properties that govern flow in porous media and fluid properties, a homogeneous approach was considered in order to isolate any kind of possible differences between GSIM and the reference simulator IMEX. The idea is to focus completely in the results of well pressures and rates when specifying wellhead pressure as boundary conditions, as to be able to validate the implementation. Table 5.3 presents the properties considered in the simulations.

Table 5.3: Physical properties.

Parameter	Value
Porosity	0.1
Permeability(m^2)	100
Rock compressibility (kPa^{-1})	5.1×10^{-7}
Initial reservoir pressure at 3005m (kPa)	30000
Bubble Pressure (kPa)	13000

A typical black oil fluid was considered, with the oil, gas and water properties used in the simulations represented in Tables 5.4, 5.5 and 5.6. Table 5.4 lists property values that would be obtained if unlimited gas were present (CMG, 2022), which means it allows a variable bubble pressure for the grid blocks depending on pressure and available gas. The reservoir is initialized with $13000\,kPa$ of bubble pressure and $30000\,kPa$ of initial pressure, the fluid starts approximately with a R_s of $84\,sm^3/sm^3$, a B_o of $1.2\,rm^3/sm^3$ and μ_o close to $2\,cp$. No fluid contacts were defined within the reservoir, so all grid blocks are saturated with oil and connate water.

Table 5.4: PVT properties.

P (kPa)	R_s (sm^3/sm^3)	B_o (rm^3/sm^3)	Eg (sm^3/rm^3)	μ_o (cp)	μ_g (cp)
101.32	0.00	1.0214	0.85942	3.8427	0.00962
1000.00	7.61	1.0475	8.72849	3.0517	0.01133
4000.00	29.37	1.1084	36.92436	2.5205	0.01249
7000.00	47.54	1.1525	67.60163	2.2083	0.01343
10000.00	65.67	1.1941	100.13027	1.9484	0.01468
13000.00	84.38	1.2355	133.54586	1.7247	0.01636
16000.00	103.96	1.2778	166.69395	1.5308	0.01849
19000.00	124.62	1.3216	198.46171	1.3617	0.02101
20340.43	134.26	1.3418	211.96577	1.2929	0.02223
23542.99	158.58	1.3924	242.13360	1.1435	0.02528
27189.85	188.87	1.4546	272.60379	0.9961	0.02886
31346.39	227.70	1.5336	302.40447	0.8516	0.03298
36070.96	279.31	1.6377	330.69715	0.7110	0.03782
41403.19	351.31	1.7822	356.66131	0.5751	0.04385
47333.86	458.85	1.9982	378.98218	0.4452	0.05227

Table 5.5: Additional oil and gas properties.

Parameter	Value
Oil Density(kg/m^3)	885.2414
Gas specific gravity	0.75
Oil compressibility (kPa^{-1})	1.810452×10^{-6}
Pressure dependence of μ_o (cp/kPa)	2.627705×10^{-5}

The production system for the case studies consider offshore wells, with a sea depth of $1000\,m$ and a tubing length of $2005\,m$. For simplicity, the surface facilities were considered to be on top of the wells, resulting in $1000\,m$ of vertical pipes connecting each well to the plant. To generate the vertical lift performance tables, the software Prosper from Petroleum Experts was used. All the parameters, correlations and the tables in CMG format can be found in Appendix A. Since the objective of this work is to implement the use of

Table 5.6: Water properties.

Parameter	Value
Reference pressure (kPa)	30000
Density(kg/m^3)	1024.4854
$B_w(rm^3/sm^3)$	1.0136
Compressibility (kPa^{-1})	5.763×10^{-7}
$\mu_w(cp)$	0.4823
Pressure dependence of μ_w (cp/kPa)	0.0

the VLP tables and not in the pressure drop calculation itself, any other third party software or correlations could had been used.

The last important simulation inputs are the relative permeability curves. A Corey correlation (Corey, 1954) was used to generate both the water-oil and gas-liquid tables used by IMEX and GSIM. Theses curves, in CMG format, can be found in Appendix B and are presented in Figure 5.1 and Figure 5.2.

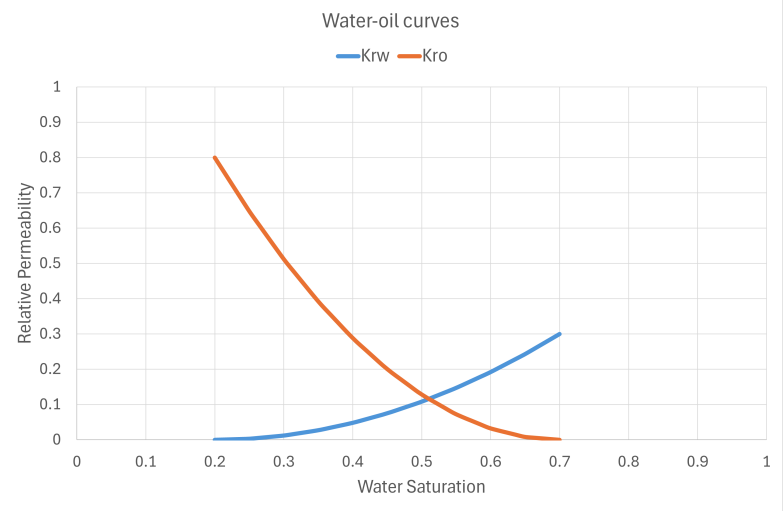

Figure 5.1: Water-oil relative permeability curves.

A configuration of two diagonally opposed producer and injector wells was used. Depending on the case study, the injector was defined as either injecting water or gas. The locations of the wells and their completions can be found in Table 5.7. The reference layer was set at the topmost layer $(k = 1)$ and, given the reservoir depth and grid block thickness presented in previous tables, the center of the reference layer, where the nodal analysis is performed, is at a depth of $3005\,m$. The VLP tables were generated to give bottomhole pressures at this reference depth.

Figure 5.3 shows a three-dimensional view of both the single-layer and multilayer models.

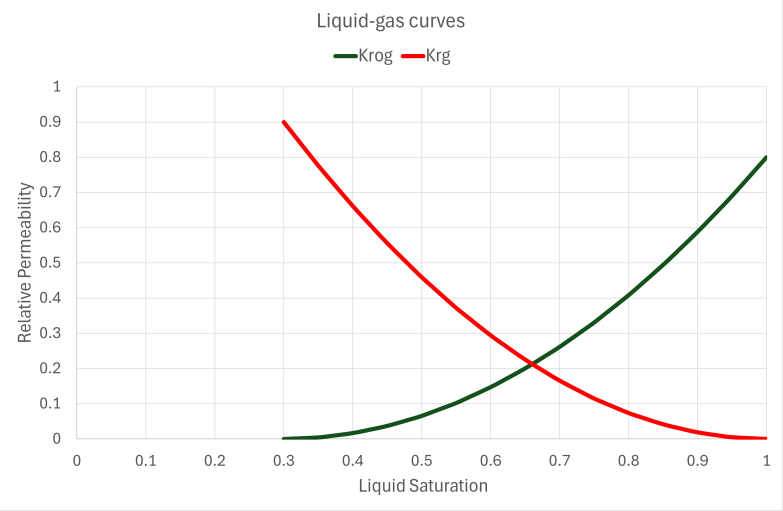

Figure 5.2: Liquid-gas relative permeability curves.

Table 5.7: Well locations.

Well	Single-layer model	Multilayer model
Injector $(i, j, k_1 : k_n)$	1 , 1 , 1:1	1, 1 , 1:5
Producer $(i, j, k_1 : k_n)$	10, 10, 1:1	10, 10, 1:5

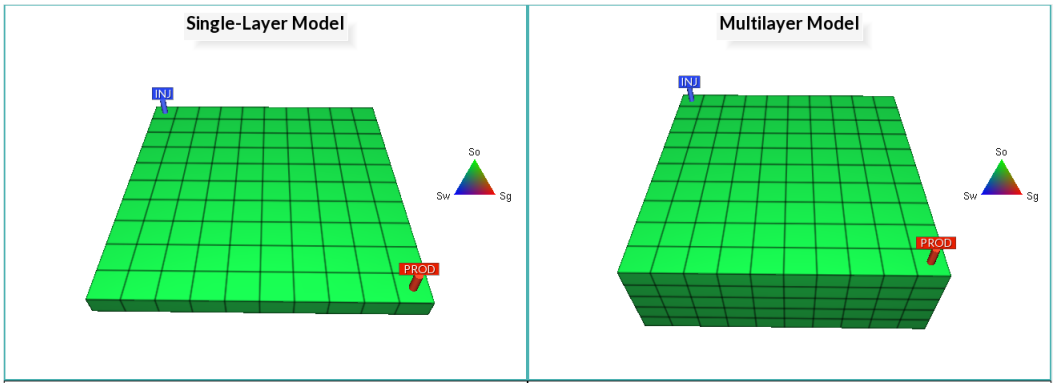

Figure 5.3: 2D and 3D models.

5.2
Case 1 - Water injector wells

The first case study consists of a water injector well constrained by wellhead pressure and a producer constrained by bottomhole pressure. The idea is to validate the reservoir-wellhead coupling implementation for injector well, while isolating possible impacts of the producer implementation.

The injector was specified with a WHP of $7000\,kPa$ and the producer was specified with a BHP of $15000\,kPa$. Only the injector had a VLP table assigned.

5.2.1
Single-layer

Figure 5.4 shows the producer well behavior along the simulation and indicates that GSIM and IMEX forecasts are consistent with each other, which was expected since BHP and rate specified wells were validated in previous GSIM works and is one of the assumptions. It is possible to note that around 400 days of elapsed time there is a water breakthrough, which suggests changes are expected on the injector behavior at around the same time. Since no relevant differences were found for the producer, there are no impact expected for the injector beyond the coupling implementation.

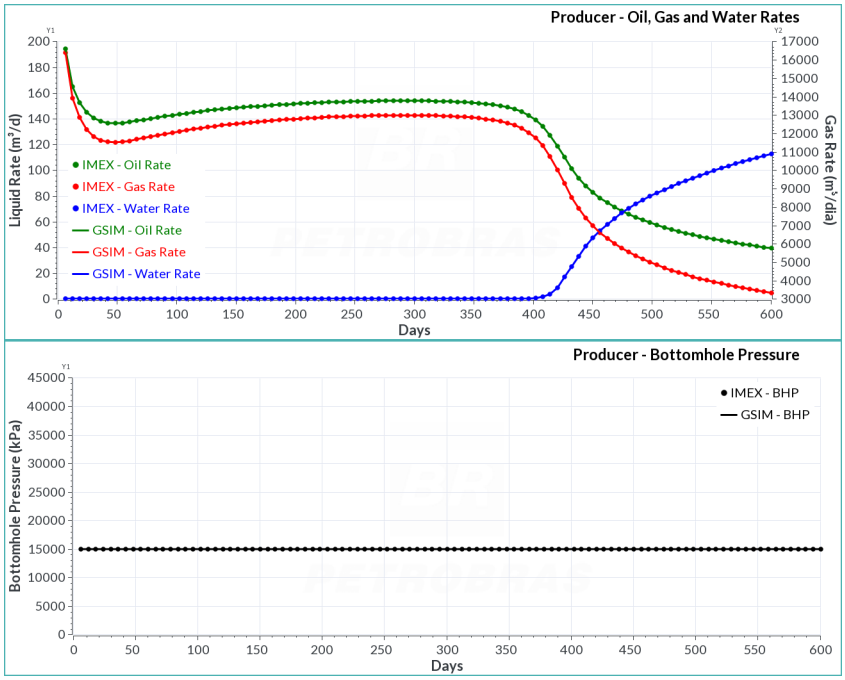

Figure 5.4: Case 1 Single-layer: Producer flow rates (top) and BHP (bottom).

Figure 5.5 shows that GSIM reservoir-wellhead coupling results for single-layer water injector well are comparable to IMEX. The dynamic behavior, with

rate and BHP increasing and decreasing during the simulation, was completely captured by GSIM, including the period of time after the water breakthrough on the producer. Not only the behavior but also the magnitude of the variables are similar to those in IMEX, with relative errors in BHP inferior to 4.2×10^{-7}.

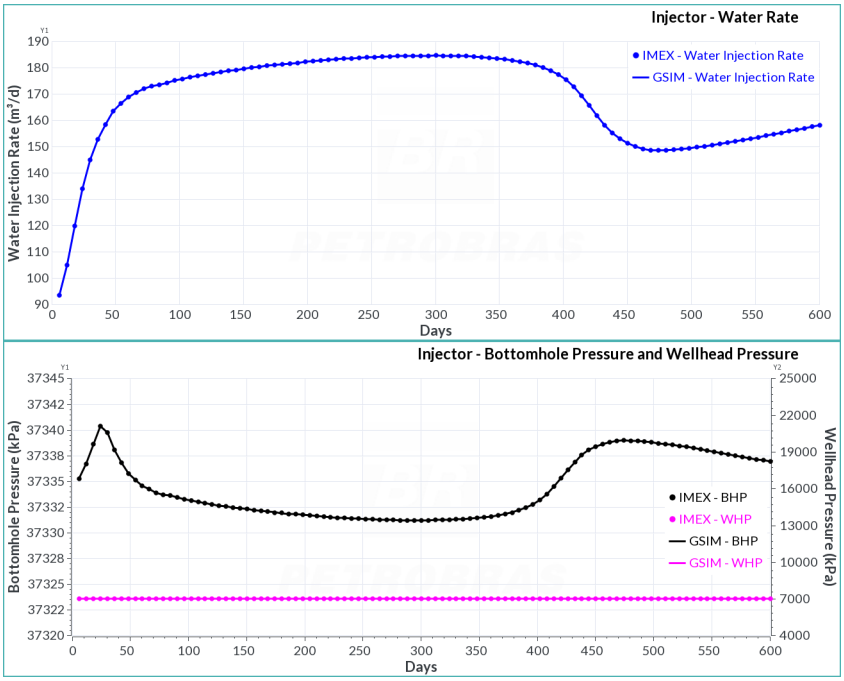

Figure 5.5: Case 1 Single-Layer: Injector flow rate (top), BHP and WHP (bottom).

5.2.2 Multilayer

Figure 5.6, similar to the single-layer model, illustrates that the BHP specified producer behavior in GSIM closely resembles that in IMEX, allowing to isolate the impact of the WHP specification implementation applied to the injector. The water breakthrough also happens near the 400 days of simulation.

Figure 5.7 shows that the multilayer injector WHP specification comes with small differences when compared to IMEX, especially in the initial time steps. The maximum relative error for the injector's BHP was 3.9×10^{-4}, while the average error was 3.9×10^{-5}. The overall behavior was once again captured by GSIM with results closely aligned with those of IMEX. It is also important to highlight the information that is brought to the simulation by using the VLP table. One can note that the difference between the injector WHP and BHP is the pressure drop along the production system pipes and well tubing all the way from the surface facilities to the reservoir sandface.

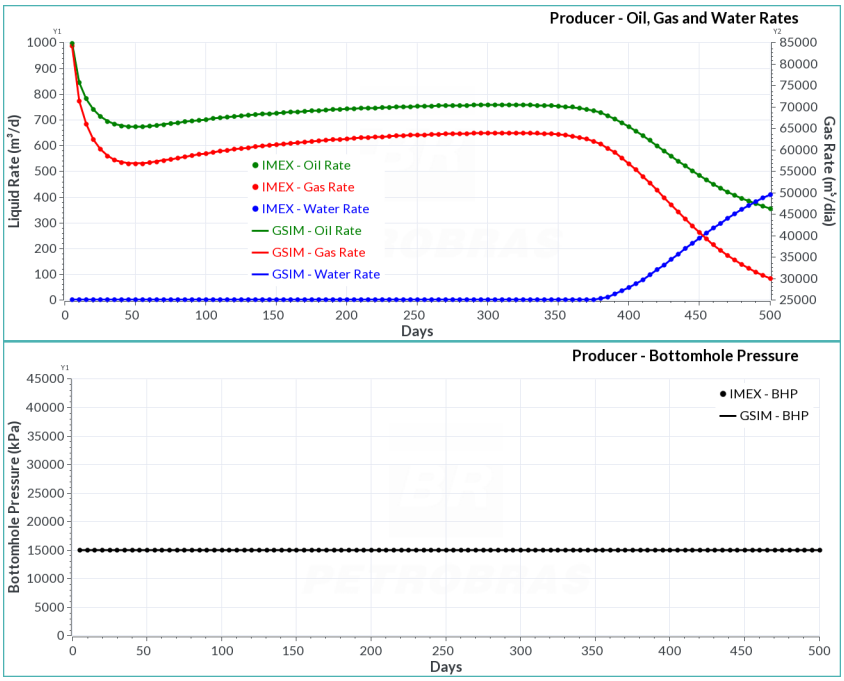

Figure 5.6: Case 1 Multilayer: Producer flow rates (top) and BHP (bottom).

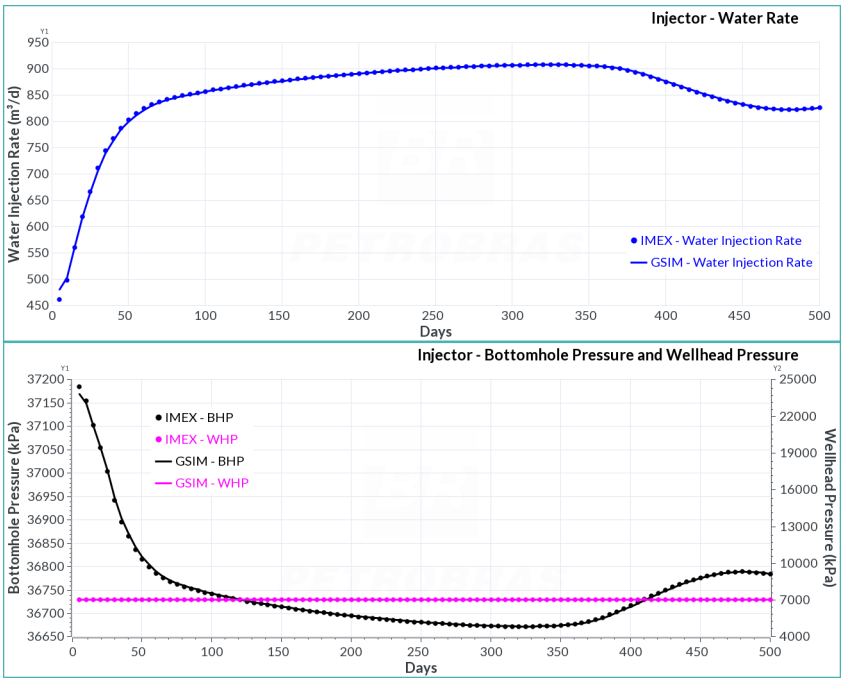

Figure 5.7: Case 1 Multilayer: Injector flow rate (top), BHP and WHP (bottom).

5.3 Case 2 - Gas injector wells

The second case study consisted of a gas injector well constrained by wellhead pressure, with a VLP table assigned, and a producer well constrained by bottomhole pressure. The objective was still to validate the implementation for injector well, including the specific differences to the previous case regarding the injection fluid type. The simulator has to be able to identify the fluid type given by the hydraulics table and to correctly calculate the associated IPR for the nodal analysis.

5.3.1 Single-layer

The injector was specified with a WHP of 25000 kPa and the producer was specified with a BHP of 13500 kPa.

Figure 5.8 shows that no significant differences exist between GSIM and IMEX results for the producer, as expected. Just like in the previous case, there is no expectation of deviation in the injector behavior due to the producer. Around 250 days into the simulation, a gas breakthrough can be observed, which will impact the injector response.

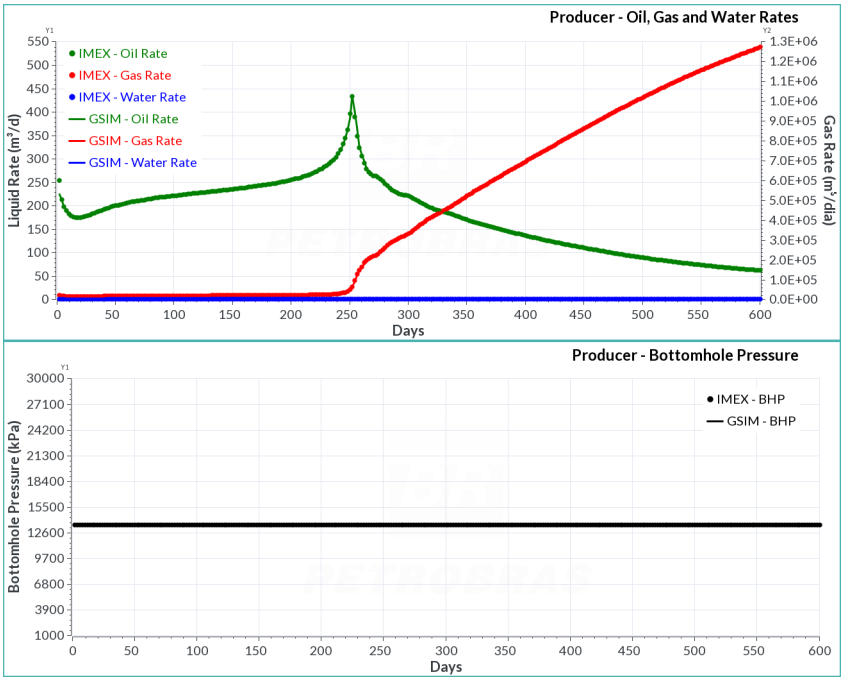

Figure 5.8: Case 2 Single-Layer: Producer flow rates (top) and BHP (bottom).

Figure 5.9 demonstrates once again that the coupling achieved in GSIM for single-layer injector wells is well suited when compared to IMEX. All BHP and gas injection rate behaviors provided in IMEX are replicated by GSIM.

The relative BHP errors in this case are inferior to 5.3×10^{-4}. It is worth noting that after the gas breakthrough on the producer, GSIM correctly estimates a continuous increase in the injection rate followed by a continuous decrease in BHP.

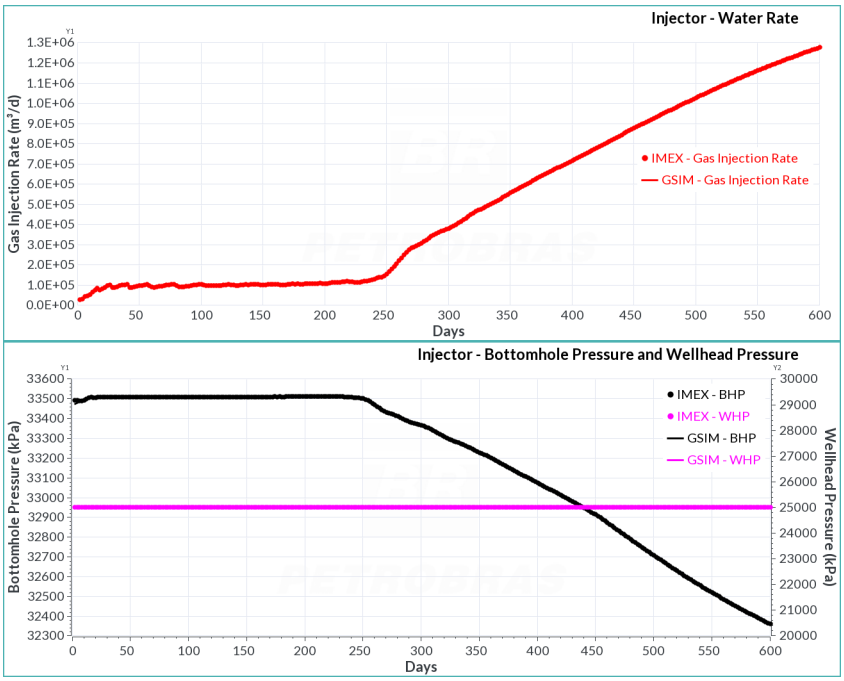

Figure 5.9: Case 2 Single-Layer: Injector flow rate (top), BHP and WHP (bottom).

5.3.2 Multilayer

The injector was specified with a WHP of 23000 kPa and the producer was specified with a BHP of 20000 kPa.

Figure 5.10 shows that already on the producer we encounter some differences between IMEX and GSIM. One reason identified for this to happen was a difference in the number of Newton iterations at each time step. For example, IMEX required two Newton iterations to converge the first time step, while GSIM required only one. Several other time steps were found to have different numbers of Newton iterations. A difference in treatment, between GSIM and IMEX, of the appearance and disappearance of the gas phase in the grid blocks may also be in play but is harder to assess. However, it is important to note that the overall GSIM behavior and magnitude of the oil, gas and water rates of the producer well are very similar to IMEX. Gas breakthrough happens between 150 and 200 days of simulation, so significant changes in the injector behavior are expected at the same time.

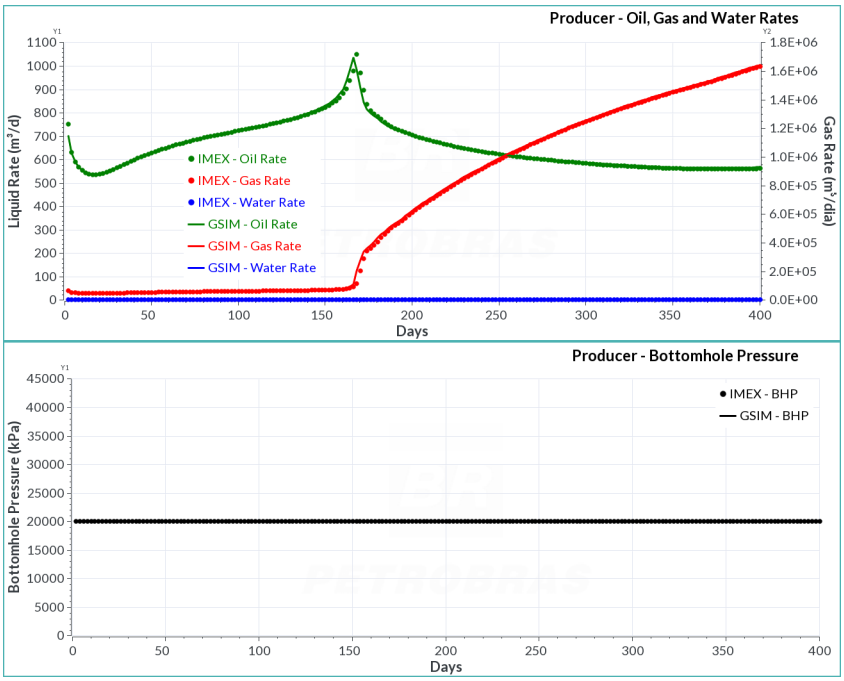

Figure 5.10: Case 2 Multilayer: Producer flow rates (top) and BHP (bottom).

Figure 5.11 shows that GSIM was able to capture IMEX's injector behavior very accurately, at least until gas breakthrough occurred, when GSIM started to slightly deviate from IMEX, as can be seen in the gas injection and BHP curves. Again, despite the differences encountered, the overall IMEX response was replicated by GSIM, with the average relative error in BHP being 9.9×10^{-4}, and the maximum relative error 2.6×10^{-3}. Given a fixed wellhead pressure, the prediction of increasing injection rate and declining BHP after the gas breakthrough on the producer is a great improvement to GSIM capabilities.

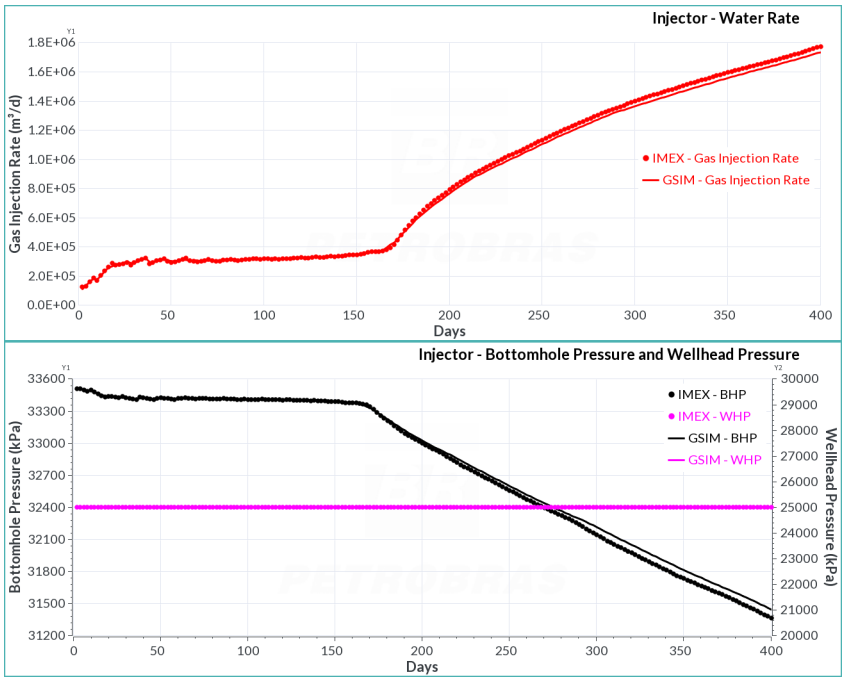

Figure 5.11: Case 2 Multilayer: Injector flow rates (top), BHP and WHP (bottom).

5.4 Case 3 - Producer wells

To validate the coupling implementation for producer wells isolated from possible impacts of the injector implementation, the third case study was generated with a water injector well specified with a bottomhole pressure of $34500\,kPa$ and the producer with a wellhead pressure of $2000\,kPa$. Artificial lift was also employed by assigning a constant lift gas rate of $50000\,m^3/d$. VLP table was only defined for the producer well.

5.4.1 Single-layer

Figure 5.12 shows a very good correspondence between IMEX and GSIM for the injector well rate, indicating that no differences in the injection are going to impact the results of the producer well. It is possible to note a initial transient with an increasing injection rate until around 50 days of simulation and also a change in behavior at around 450 days, indicating a possible water breakthrough on the producer.

Figure 5.13 presents the producer well behavior and shows a rather good matching between IMEX and GSIM. This result continues to demonstrate that the proposed implementation for reservoir to wellhead coupling for single-layer wells is completely compatible to the commercial simulator. Both the initial

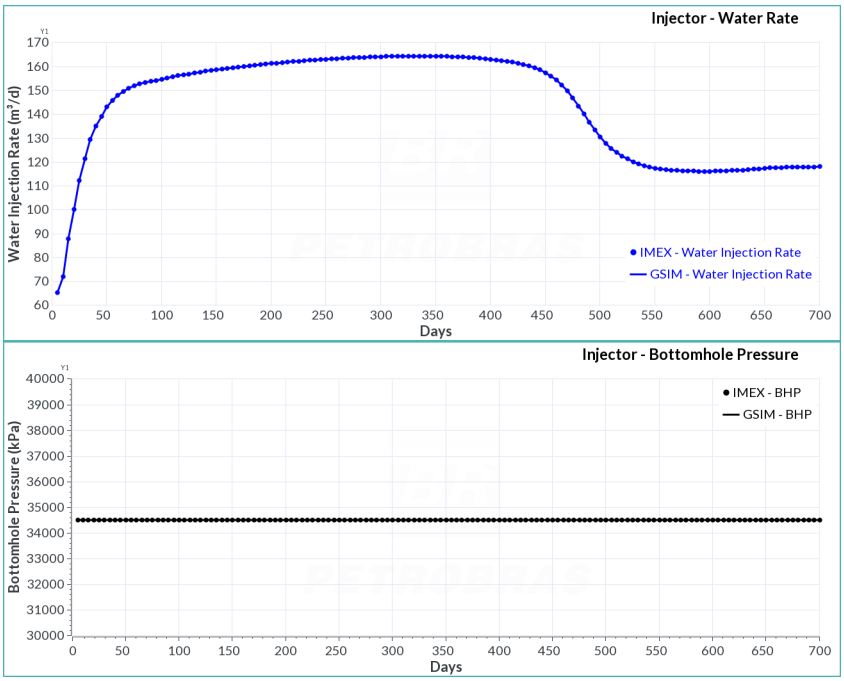

Figure 5.12: Case 3 Single-Layer: Injector flow rate (top) and BHP (bottom).

transient with declining oil and gas rates and the injection water breakthrough stage were captured by GSIM in the same way IMEX did, as shown by the matching rates and BHP, with relative errors in BHP inferior to 6.3×10^{-6}. An increased pressure drop in the production system is also evident when one compares the difference between BHP and WHP before and after the water breakthrough, which increases the well water cut and therefore the weight of the fluid column.

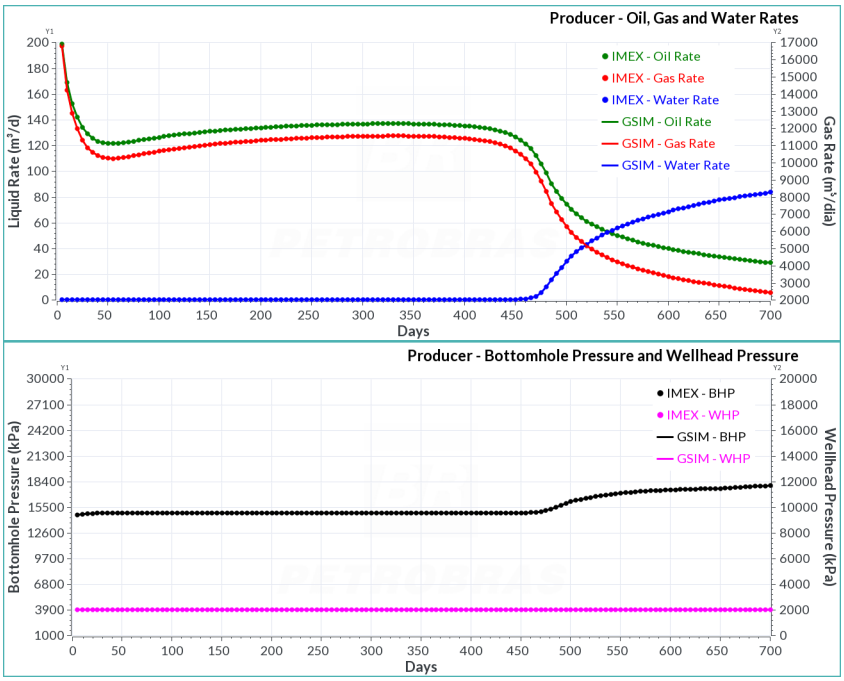

Figure 5.13: Case 3 Single-Layer: Producer flow rates (top), BHP and WHP (bottom).

5.4.2 Multilayer

Figure 5.14 shows that differences between IMEX and GSIM exist for multilayer wells. They are evident during the initial transient when the producer oil and gas rates are declining until around 50 days of simulation and also after 400 days when the injection water breakthrough happens and water cut starts to rise. It is worth noting that the differences do not seem to accumulate and tend do diminish over time, making the overall IMEX's producer rates and BHP behavior being captured by GSIM. The maximum relative error in the producer's BHP was 3.5%, while the average was 0.32%.

The injector well also presents some divergences when compared to IMEX, as shown in Figure 5.15, but it can be explained by the different producer response between the simulators. All the dynamic changes are captured by GSIM with differences in the initial transient and after 400 days, just like the producer.

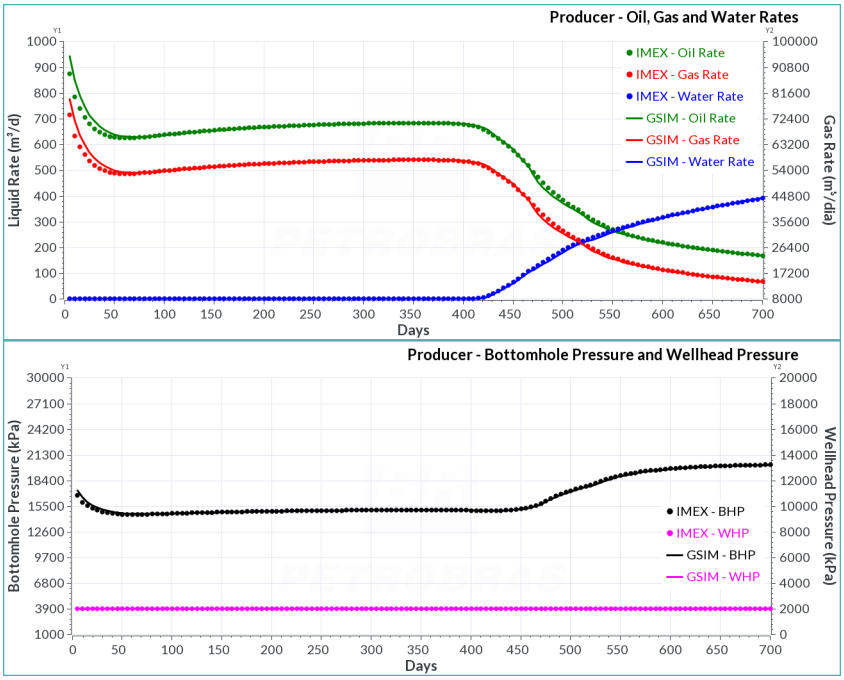

Figure 5.14: Case 3 Multilayer: Producer flow rates (top), BHP and WHP (bottom).

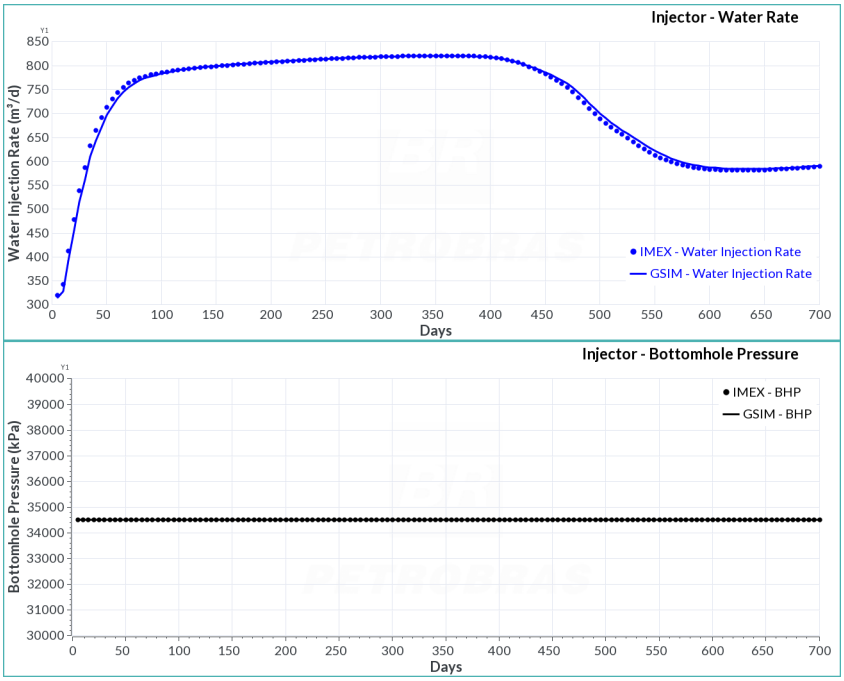

Figure 5.15: Case 3 Multilayer: Injector flow rate (top) and BHP (bottom).

5.5 Case 4 - Producers and Injectors

The fourth case study was elaborated to validate WHP specification on both the producer and the injector at the same time. The isolated validation was shown in previous sections but it is important to analyze how GSIM behaves when all the wells in the simulation are constrained by wellhead pressure and different VLP tables coexist. This case can also be linked to a usual production situation where the wells boundary conditions are imposed only by surface limitations, such as water injector pump pressure for injectors and separator pressure for producers.

The producer well was specified with a wellhead pressure of $2000\,kPa$ and the injector well with a wellhead pressure of $7000\,kPa$. Both wells have an assigned VLP table and the producer is operating with artificial lift in the form of a constant lift gas rate of $50000\,m^3/d$.

5.5.1 Single-layer

Figures 5.16 and 5.17 show great correspondence between IMEX and GSIM regarding single-layer producers and injector wells. The benefits of incorporating WHP specification into GSIM are very clear when considering what dynamically happens to the wells' bottomhole pressures and rates during the simulation. For a given fixed wellhead pressure, BHP and all the rates vary continuously, which cannot be captured by other forms of well specification. The initial transient and the water breakthrough stage observed in IMEX were replicated by GSIM in both wells. The maximum relative error in the producer's BHP was 5.1×10^{-6}, while in the injector's BHP it was 4.2×10^{-6}.

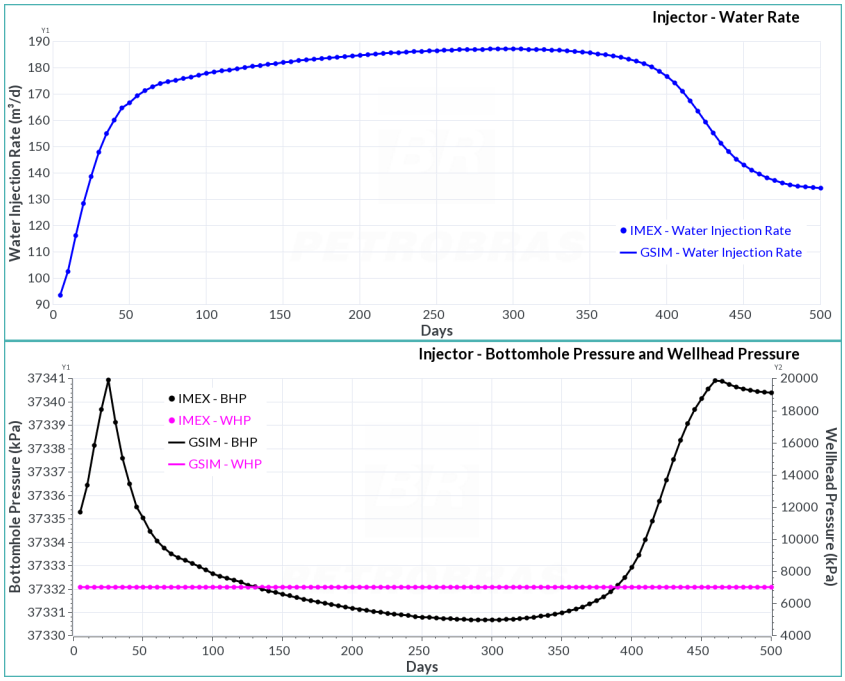

Figure 5.16: Case 4 Single-Layer: Injector flow rate (top), BHP and WHP (bottom).

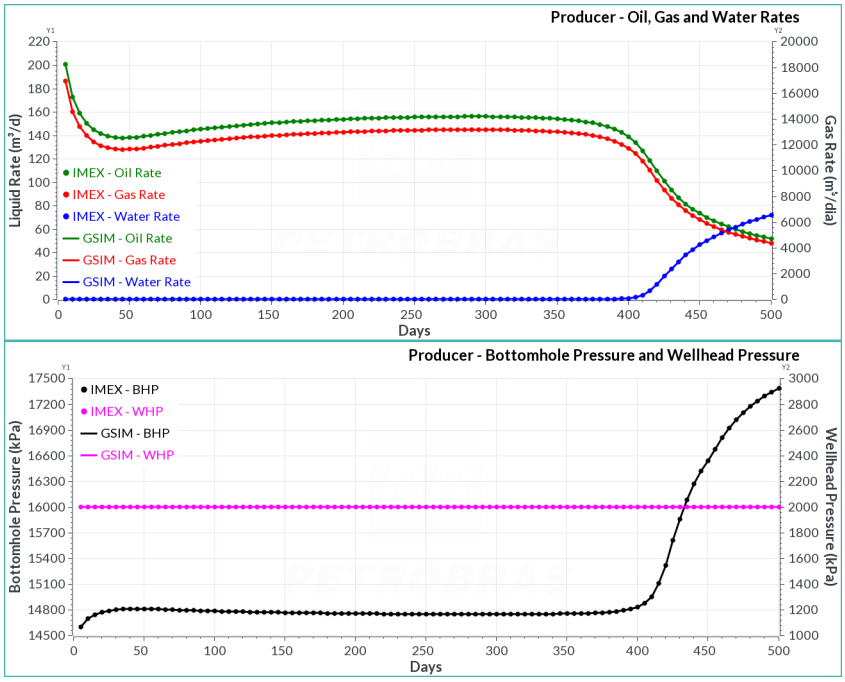

Figure 5.17: Case 4 Single-Layer: Producer flow rates (top), BHP and WHP (bottom).

5.5.2 Multilayer

The differences between IMEX and GSIM for multilayer wells continue to exist as can be seen in Figures 5.18 and 5.19. Again the divergences seem to happen on both wells during the initial transient and during the water breakthrough on production. Despite the differences, GSIM is able to capture the overall behavior of the well rates and BHP. The producer presented a maximum BHP relative error of 2.2%, and an average of 0.27%. The injector showed a maximum relative error of 0.07%, and an average of 0.01%.

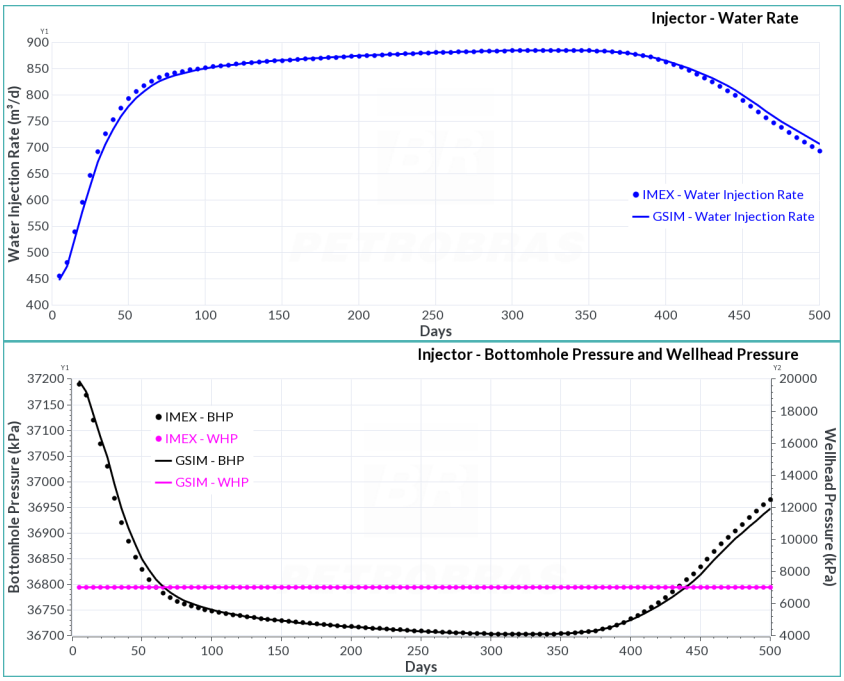

Figure 5.18: Case 4 Multilayer: Injector flow rate (top), BHP and WHP (bottom).

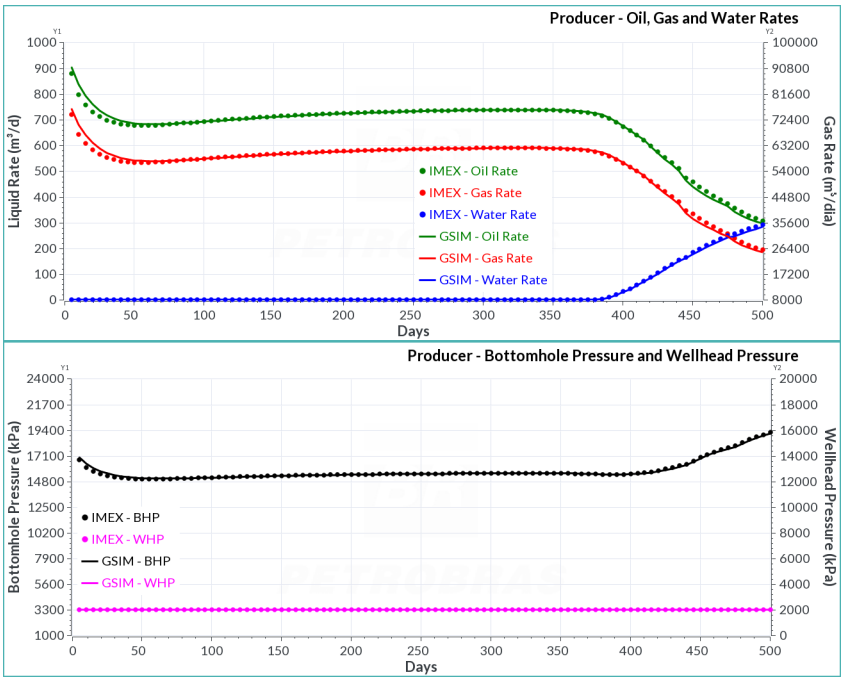

Figure 5.19: Case 4 Multilayer: Producer flow rates (top), BHP and WHP (bottom).

5.6 Case 5 - Constraint switch

The fifth case study was made to test the important simulator feature of switching between constraints, since a well can experience different kinds of restriction in its lifetime. Having surface plant limitations in mind, a usual production constraint begins as a maximum rate restriction, representing the plant's fluid treatment capacity, that over time switches to a minimum wellhead pressure when the well can no longer support the maximum rate and the minimum WHP at the same time. For the injector, a water rate specification was chosen to represent a typical demand for material balance in the reservoir and will also serve to test GSIM ability to predict the WHP using VLP table. For comparison purpose, both IMEX and GSIM were configured to repeat the time step when a switch in well constraint occurs.

5.6.1 Single-layer

The producer well was specified with a maximum oil rate of $175\,m^3/d$, a minimum wellhead pressure of $2200\,kPa$ and a constant lift gas rate of $50000\,m^3/d$ was also defined. The injector well was specified with a maximum water rate of $200\,m^3/d$. Both wells were given VLP tables.

Figure 5.20 shows the water injector operating with constant rate and the varying behavior of its WHP and BHP during the whole simulation. The implementation of WHP specification for single-layer injector wells continues to perform very well when compared to IMEX, since GSIM was able to capture both the magnitudes and every increase and decrease in BHP and WHP. It is also notable that GSIM was able to handle the interpolation and estimation of WHP, validating another improvement in GSIM's capabilities. This information can be very useful because it tells how much pressure is needed in the plant to deliver the desired injection rate in the well.

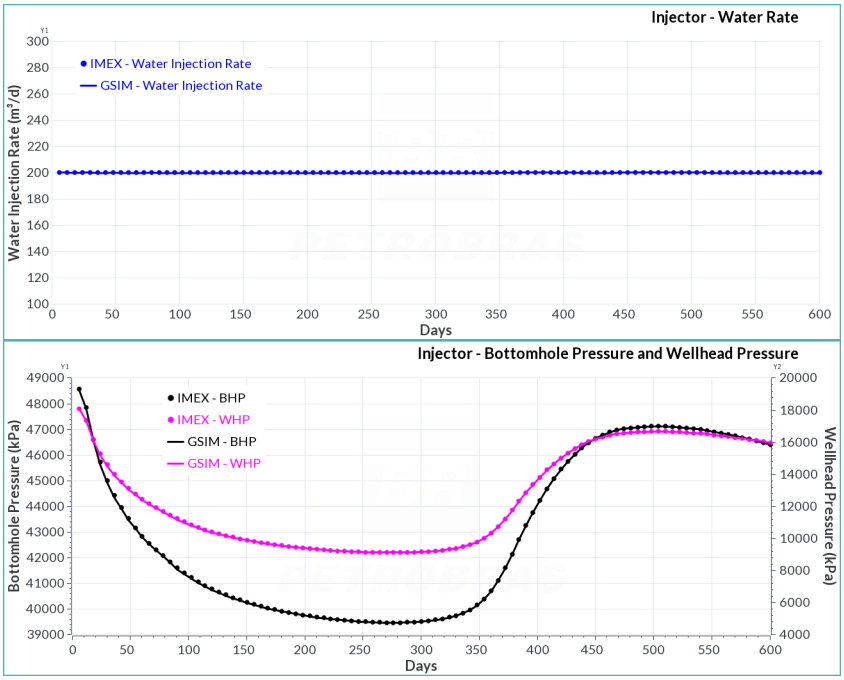

Figure 5.20: Case 5 Single-Layer - Injector flow rate (top), BHP and WHP (bottom).

As can be seen in Figure 5.21, the producer well opens up with the maximum rate of $175\,m^3/d$ and a WHP higher than the minimum specified, indicating that the well is being restricted at the surface to respect the rate constraint. As both BHP and WHP decline, a little before 100 days of simulation, the minimum wellhead pressure is reached and the constraint switch occurs. The well can no longer support the maximum oil rate, so the rate starts to decline and the WHP remains constant. All this behavior is shown in the commercial simulator and replicated by GSIM, including the final stage of the simulation when the water cut rises due to the injection water breakthrough. The proposed implementation of the single-layer producers wells achieved once again a very good matching to IMEX, with the maximum BHP relative error being 4.5×10^{-4}.

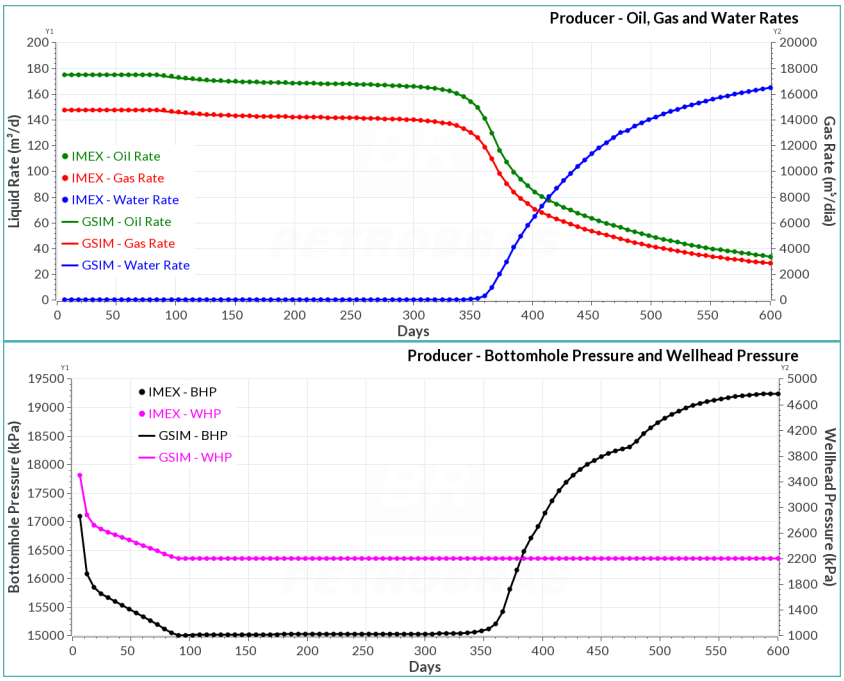

Figure 5.21: Case 5 Single-Layer - Producer flow rates (top), BHP and WHP(bottom).

5.6.2 Multilayer

The producer well was specified with a maximum oil rate of $700\,m^3/d$, a minimum wellhead pressure of $2200\,kPa$ and a constant lift gas rate of $50000\,m^3/d$ was also defined. The injector well was specified with a maximum water rate of $700\,m^3/d$. Both wells were given VLP tables.

Figure 5.22 shows no apparent deviation on the results of the injector well when compared to IMEX. Similar to what happened on the single-layer model, the injector BHP dynamically responds to what is going on in the reservoir and the WHP, based on the pressure drop information contained in the VLP table, also vary dynamically.

Figure 5.23 shows a very good agreement between IMEX and GSIM, although some differences can be spotted. They are apparent in the oil and gas rates as the water rate rises due to the injection breakthrough. Nevertheless, taking into account all that is happening, from rate constraint switch to WHP constraint and WHP interpolation to BHP interpolation, the curves show a very good matching. The average relative error in the producer's BHP was 0.3%, with a maximum of 1.08%.

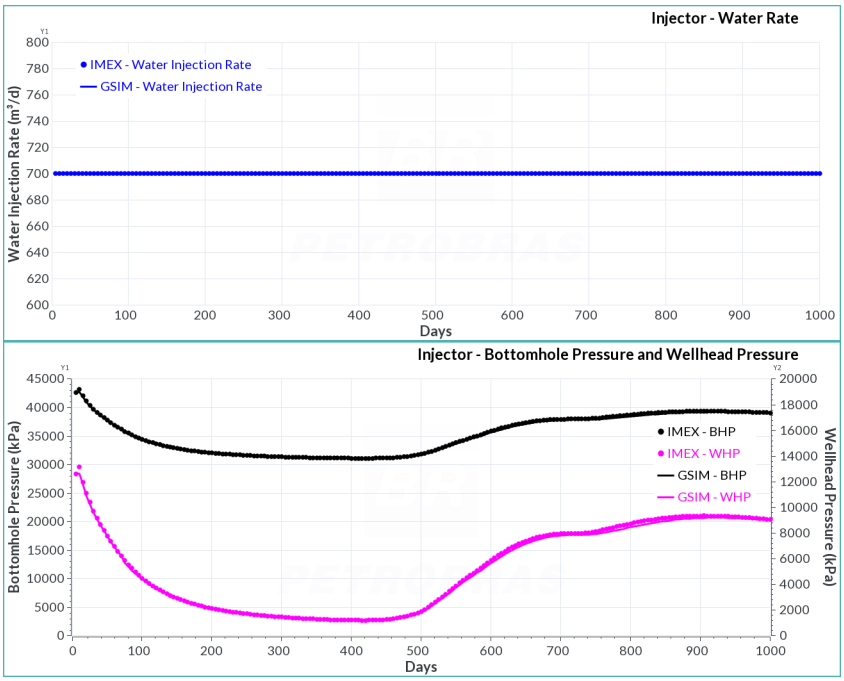

Figure 5.22: Case 5 Multilayer: Producer flow rates (top) and BHP (bottom).

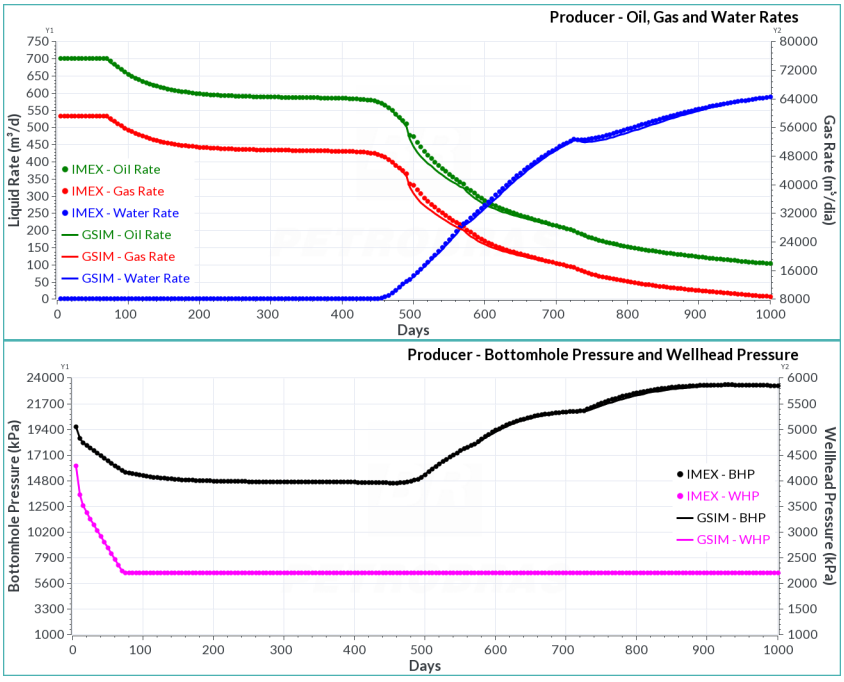

Figure 5.23: Case 5 Multilayer: Producer flow rates (top), BHP and WHP (bottom).

5.7 Comparing numerical and semi-analytical solution

As was discussed in the previous chapter, regarding the Jacobian matrix coupling implementation, not only a numerical approach to the derivatives of the sink/source terms was proposed but also a semi-analytical one. Given that it was shown that producers in the proposed semi-analytical solution lead to solving several different linear systems, the implementation and results validation were restricted to injector wells.

Revisiting the first case study, where a water injector was specified with a WHP of 7000 kPa and the producer was specified with a BHP of 15000 kPa, the two approaches are compared both in the single-layer model and multilayer model.

5.7.1 Single-layer

Figures 5.24 and 5.25 show that both solutions give approximately the same solution for the single-layer study. It is important to highlight that only the injector is operating under WHP specification. The transient behavior of the BHP and water rate were captured by both implementations in GSIM. No impact on the producer well was observed.

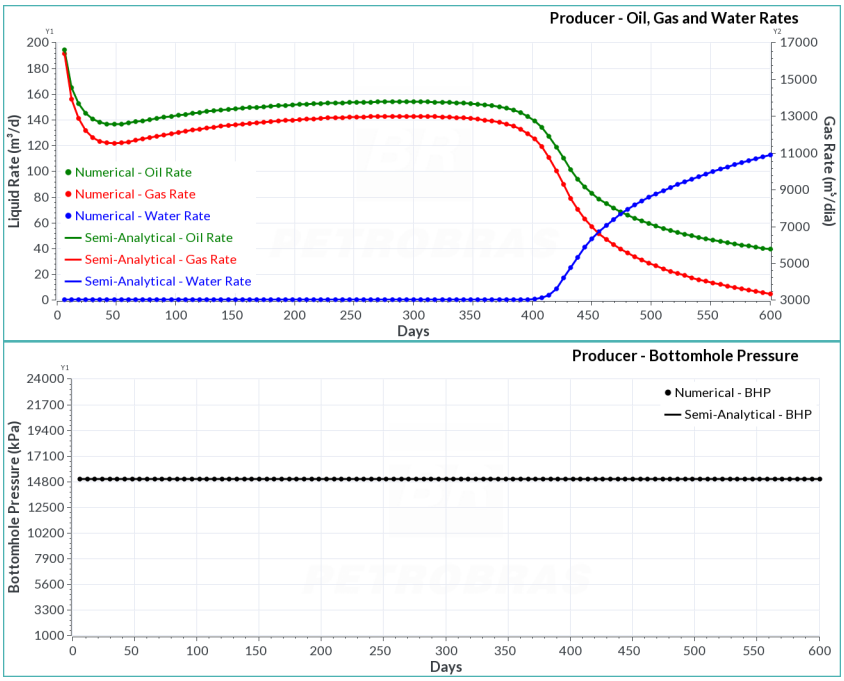

Figure 5.24: Case 1 Single-Layer numerical versus Semi-analytical: Producer flow rates (top) and BHP (bottom).

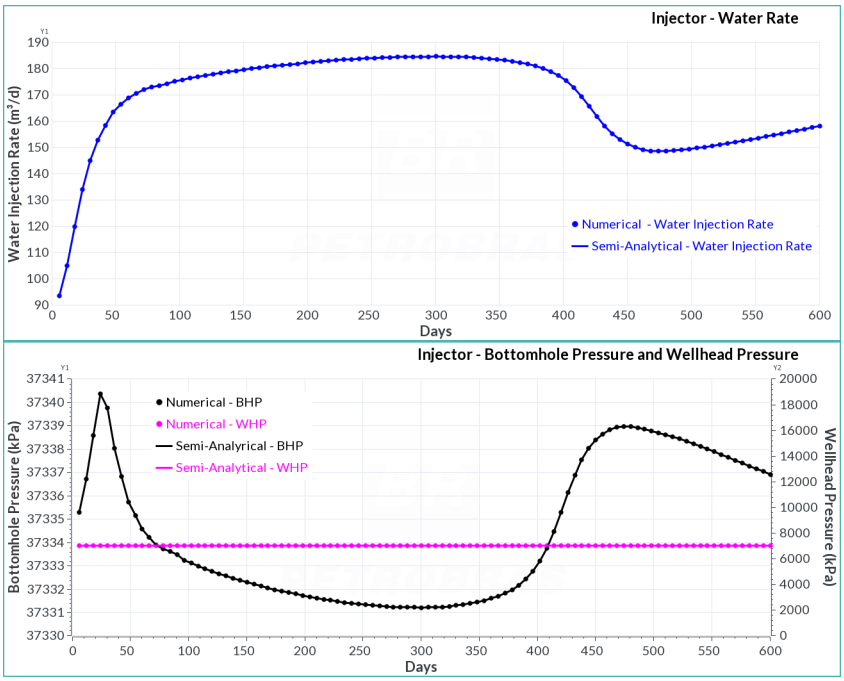

Figure 5.25: Case 1 Single-Layer numerical versus Semi-analytical: Injector flow rate (top) and BHP (bottom).

5.7.2 Multilayer

Figures 5.26 and 5.27 show that the solutions continue to agree even in the multilayer study. This is probably a hint that the differences between IMEX and GSIM encountered in the multilayer studies may not be due to the derivatives terms of the Jacobian matrix. Again, all the changes in water rate and BHP during the simulation were represented similarly by both implementations.

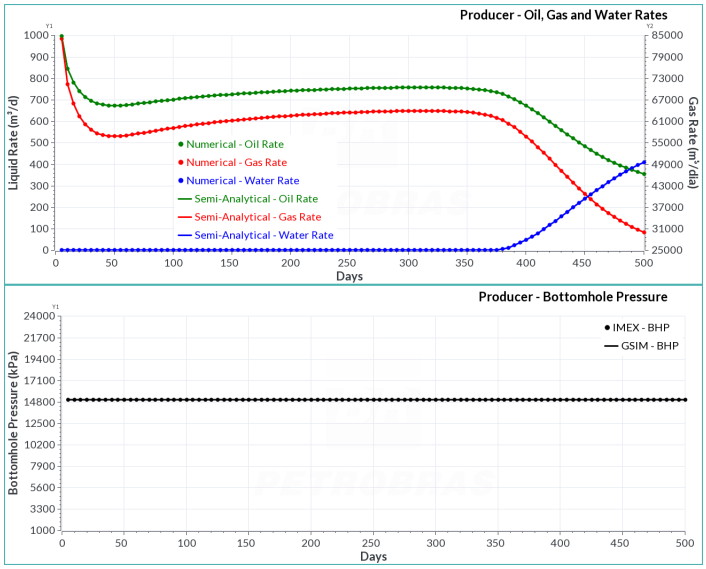

Figure 5.26: Case 1 Multilayer numerical versus Semi-analytical: Producer flow rates (top) and BHP (bottom).

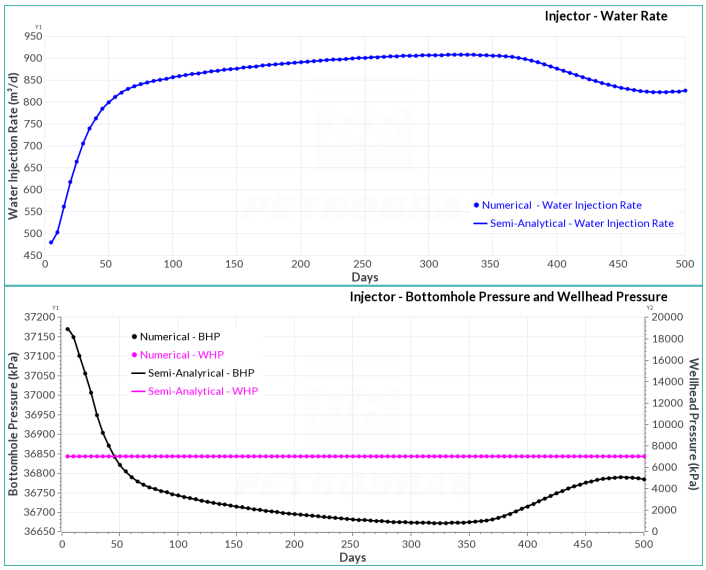

Figure 5.27: Case 1 Multilayer numerical versus Semi-analytical: Injector flow rates (top) and BHP (bottom).

6
Conclusions

This study focused on the development and validation of reservoir-wellhead coupling in the GSIM numerical simulator, using vertical lift performance tables to allow wellhead pressure well specification representing surface boundary conditions. This type of specification takes into account not only the reservoir behavior but also the production system and its associated pressure losses, increasing the predictive power of the simulator. Comparative studies were conducted against the commercial simulator IMEX and the main conclusions are discussed below.

The implemented methods for interpolating bottomhole pressure data from the VLP tables proved adequate for reproducing the results from IMEX. Injector tables, containing only two input variables, followed a bilinear interpolation function, while producer tables, with five input variables, required a multidimensional linear interpolation.

Single-layer wells performance under WHP specification demonstrated excellent agreement with IMEX. That remained true whether it was a water injector, gas injector or producer. The high correspondence reached for these scenarios allowed to further validate not only the interpolation functions but also the nodal analysis performed to estimate the bottomhole pressure and the numerical Jacobian matrix calculations.

Observed differences in WHP specified multilayer wells were more prominent in the short term and during transient or injected fluid breakthrough, but they tended to diminish and not accumulate over time. Despite the divergences, GSIM captured the overall behavior presented by IMEX simulations. One important consideration is that these transient differences are not exclusive of this research, as they can be observed in several other works, such as those of Bastos (2021), Bik Deli (2021), Wang (2024) and Farias (2025). Possible reasons include different formulations across the simulators, such as number of Newton iterations for convergence in some time steps, small differences in phase appearance and disappearance treatment when there is gas phase present, and different representation of wells, leading to slightly different productivity and injectivity indexes relating directly to perforated grid blocks domain and short term prediction.

Although the primary focus of the work was on WHP specification, the implementation also addressed the calculation of the WHP for rate specified wells and the ability to switch between constraints, such as transitioning from rate specified to WHP specified, provided a VLP table is assigned. These functionalities are valuable as they provide insight into the production system life cycle and the feasibility of operating conditions from a surface facility perspective.

In the pursuit of implementing the use of VLP tables for WHP specification implicitly, an alternative to the numerical derivatives for the Jacobian terms was proposed for both injectors and producers but implemented only for injector wells. The semi-analytical formulation was successfully tested against the numerical formulation and achieved the same results.

The presented results, supported by IMEX comparisons, indicate that the methodology implemented in GSIM for reservoir-wellhead coupling via VLP tables is robust and capable of representing the behavior of wells for integrated simulation studies.

6.1 Future work

In light of the studies developed for this work, the following suggestions for future work arise :

- Extend the implementation for GSIM compositional;
- Production and injection control of well groups;
- Reservoir pressure maintenance and voidage replacement control through well groups;
- Production and injection manifold control using vertical lift performance tables;
- Water and gas re-injection control from a subsea separator;
- Replacement of VLP tables with correlations to be dynamically computed throughout the simulation;
- Replacement of VLP tables with parametric equations representing response surfaces;
- Use VLP table representation for wellhead temperature control;
- Implement an explicit coupling between GSIM and a production system simulator.

Bibliography

AL-MUTAIRI, S.; HAYDER, E.; MUNOZ, A.; AL-SHAMMARI, A. ; AL-JAMA, N. **A study of coupling surface network to reservoir simulation model in a large middle east field**. In: SPE NORTH AFRICA TECHNICAL CONFERENCE AND EXHIBITION, SPE, 2010, p. 127976.

ASCHER, U. M.; GREIF, C. **A First Course in Numerical Methods**. Computational Science and Engineering Philadelphia: Society for Industrial and Applied Mathematics, 2011.

AUBERT, P.; DI CÉSARÉ, N. ; PIRONNEAU, O. **Automatic differentiation in c++ using expression templates and application to a flow control problem**. Computing and Visualization in Science, 3(4):197–208, 2001.

AZIZ, K.; SETTARI, A. **Petroleum reservoir simulation**. New York: Elsevier, 1979.

BARROUX, C. C.; DUCHET-SUCHAUX, P.; SAMIER, P. ; NABIL, R. **Linking reservoir and surface simulators: how to improve the coupled solutions**. In: SPE EUROPEC FEATURED AT EAGE CONFERENCE AND EXHIBITION, SPE, 2000, p. 65159.

BASTOS, T. S. **Development of a multipurpose reservoir simulator based on a plugin architecture**. Master's thesis, Pontifícia Universidade Católica do Rio de Janeiro, Rio de Janeiro, 2021.

BAYDIN, A. G.; PEARLMUTTER, B. A.; RADUL, A. A. ; SISKIND, J. M. **Automatic differentiation in machine learning: a survey**. Journal of machine learning research, 18(153):1–43, 2018.

BEGGS, H. D. **Production optimization using nodal (TM) analysis**. 2. ed. Tulsa: Ogci, 2003.

BIGDELI, A.; BARROSO, M. L.; LIMA, I. D. C. M.; MARCONDES, F. ; SEPEHRNOORI, K. **Investigation of different interpolation functions for a newly developed framework for sequential coupling of the**

reservoir, wells, and surface facilities. In: XLI IBERO-LATIN AMERICAN CONGRESS ON COMPUTATIONAL METHODS IN ENGINEERING, v. 2, n. 2, Foz do Iguaçu, 2020.

BIK DELI, A. **Sequential explicit and implicit coupling of 3D compositional reservoir, wells and surface facility**. PhD thesis, Universidade Federal do Ceará, Fortaleza, 2021.

BOOGAART, E. **Coupling between a reservoir and a surface facilities network**. Master's thesis, Delft University of Technology, Delft, 2016.

BREAUX, E. J.; MONROE, S. A.; BLANK, L. S.; YARBERRY, D. W. ; ALUMRAN, S. A. **Application of a reservoir simulator interfaced with a surface facility network: a case history**. Society of Petroleum Engineers Journal, 25(04):397–404, 1985.

BRILL, J. P.; MUKHERJEE, H. **Multiphase flow in wells**. Society of Petroleum Engineers of AIME, 1999.

BURDEN, R. L.; FAIRES, J. D. **Numerical Analysis**. 9. ed. United States: Cengage Learning, 2010.

CMG. **IMEX 2022.10 User Guide**. Computer Modelling Group, 2022.

CMG. **GEM 2022.10 User Guide**. Computer Modelling Group, 2022.

CHANG, Y. B. **Development and application of an equation of state compositional simulator**. PhD thesis, University of Texas, Austin, 1990.

CHAPPELEAR, J. E.; WILLIAMSON, A. S. **Representing wells in numerical reservoir simulation: Part 2–implementation**. Society of Petroleum Engineers Journal, 21(03):339–344, 1981.

CHEN, Z. **Reservoir simulation: mathematical techniques in oil recovery**. Philadelphia: Society for Industrial and Applied Mathematics, 2007.

COATS, B. K.; FLEMING, G. C.; WATTS, J. W.; RAMÉ, M. ; SHIRALKAR, G. S. **A generalized wellbore and surface facility model, fully coupled to a reservoir simulator**. SPE Reservoir Evaluation & Engineering, 7(02):132–142, 2004.

COLLINS, D. A.; NGHIEM, L. X.; LI, Y.-K. ; GRABONSTOTTER, J. **An efficient approach to adaptive-implicit compositional simulation with an equation of state**. SPE reservoir engineering, 7(02):259–264, 1992.

COREY, A. T. **The interrelation between gas and oil relative permeabilities**. Producers monthly, p. 38–41, 1954.

COREY, A. T.; RATHJENS, C. H.; HENDERSON, J. ; WYLLIE, M. **Three-phase relative permeability**. Journal of Petroleum Technology, 8(11):63–65, 1956.

CRAFT, B. C.; HAWKINS, M. ; TERRY, R. E. **Applied Petroleum Reservoir Engineering**. 2. ed. New Jersey: Prentice Hall PTR, 1991.

CRAIG, F. C. **The reservoir engineering aspects of waterflooding**. Monograph Series, Society of Petroleum Engineers of AIME, 1971.

DAKE, L. P. **Fundamentals of reservoir engineering**. Amsterdam: Elsevier, 1983.

DEMPSEY, J. R.; PATTERSON, J. K.; COATS, K. H. ; BRILL, J. P. **An efficient model for evaluating gas field gathering system design**. Journal of Petroleum Technology, 23(09):1067–1073, 1971.

DOBBS, W.; BROWNING, B.; KILLOUGH, J. ; KUMAR, A. **Coupled surface/subsurface simulation of an offshore k2 field**. In: SPE RESERVOIR CHARACTERISATION AND SIMULATION CONFERENCE AND EXHIBITION, SPE, 2011, p. 145070.

DUARTE, L. S. **TopSim: A plugin-based framework for large-scale numerical analysis**. PhD thesis, Pontifícia Universidade Católica do Rio de Janeiro, Rio de Janeiro, Sept. 2016.

EMANUEL, A. S.; RANNEY, J. C. **Studies of offshore reservoir with an interfaced reservoir/piping network simulator**. Journal of Petroleum Technology, 33(03):399–406, 1981.

ERTEKIN, T.; ABOU-KASSEM, J. H. ; KING, G. R. **Basic applied reservoir simulation**. Richardson: Henry L. Doherty Memorial Fund of AIME, 2001.

FARIAS, M. M. **Comparison of structured and unstructured formulations for compositional reservoir simulation**. PhD thesis, Universidade Federal do Ceará, Fortaleza, 2025.

FETKOVICH, M. J. **The isochronal testing of oil wells**. In: SPE ANNUAL TECHNICAL CONFERENCE AND EXHIBITION, SPE, 1973, p. SPE–4529.

FEVANG, Ø.; FOSSMARK, M. G.; NORDAAS KULKARNI, K.; LAURITSEN, H. T. ; SKJAEVELAND, S. M. **Vertical lift models substantiated by**

statfjord field data. In: SPE EUROPEC FEATURED AT EAGE CONFERENCE AND EXHIBITION, SPE, 2012, p. 154803.

FORSYTH JR, P. A.; SAMMON, P. H. **Practical considerations for adaptive implicit methods in reservoir simulation**. Journal of Computational Physics, 62(2):265–281, 1986.

GHORAYEB, K.; HOLMES, J.; TORRENS, R. ; GREWAL, B. **A general purpose controller for coupling multiple reservoir simulations and surface facility networks**. In: SPE RESERVOIR SIMULATION CONFERENCE, SPE, 2003, p. SPE–79702.

GILBERT, W. E. **Flowing and gas-lift well performance**. In: DRILLING AND PRODUCTION PRACTICE, API, 1954.

HEPGULER, G.; BARUA, S. ; BARD, W. **Integration of a field surface and production network with a reservoir simulator**. SPE Computer Applications, 9(03):88–92, 1997.

HIEBERT, A.; KHOSHKBARCHI, M.; SAMMON, P.; ALVES, I.; RODRIGUES, J. R.; BELIEN, A.; HOWELL, B.; SAAF, F. ; VALVATNE, P. **An advanced framework for simulating connected reservoirs, wells and production facilities**. In: SPE RESERVOIR SIMULATION CONFERENCE, SPE, 2011, p. 141012.

HOHENDORFF FILHO, J. C. V. **Desenvolvimento e gerenciamento de reservatórios de petróleo com foco na modelagem integrada com sistema de produção**. PhD thesis, Universidade Estadual de Campinas, Campinas, 2021.

HUBBERT, M. K. **Darcy's law and the field equations of the flow of underground fluids**. Transactions of the AIME, 207(01):222–239, 1956.

ISLAM, A. W.; SEPEHRNOORI, K. **A review on spe's comparative solution projects (csps)**. Journal of Petroleum Science Research, 2(4):167–180, 2013.

JIANG, Y. **Techniques for modeling complex reservoirs and advanced wells**. PhD thesis, Stanford University, Stanford, 2008.

LUNDBERG, B. **Well and reservoir behavior with varying associated gas/oil ratio**. In: SPE MIDDLE EAST OIL AND GAS SHOW AND CONFERENCE, SPE, 2011, p. SPE–142617.

MACHADO, M. V. B. **Modelagem numérica de reservatórios de petróleo: prática integrada de simulação**. 1. ed. Rio de Janeiro: PETROBRAS, 2023.

MODENESI, A. P. **Gridding and scaling strategies for unstructured reservoir simulation**. Master's thesis, Pontifícia Universidade Católica do Rio de Janeiro, Rio de Janeiro, 2019.

PETEX. **Prosper User Guide**. Petroleum Experts, 2024.

PEACEMAN, D. W. **Interpretation of well-block pressures in numerical reservoir simulation**. Society of Petroleum Engineers Journal, 18(03):183–194, 1978.

PEACEMAN, D. W. **Interpretation of well-block pressures in numerical reservoir simulation with nonsquare grid blocks and anisotropic permeability**. Society of Petroleum Engineers Journal, 23(03):531–543, 1983.

PIAZZA, R. E. **Performance assessment of linear solvers for fully implicit reservoir simulation**. Master's thesis, Pontifícia Universidade Católica do Rio de Janeiro, Rio de Janeiro, 2019.

ROSSI, R.; CASCIANO, C.; ELMUTARDI, M. M. ; TONDELLI, A. **Simplified network simulation vs. integrated asset modelling for management and development of offshore gas fields**. In: SPE RESERVOIR CHARACTERISATION AND SIMULATION CONFERENCE AND EXHIBITION, SPE, 2015, p. 175597.

SCHIOZER, D. **Simultaneous simulation of reservoir and surface facilities**. PhD thesis, Stanford University, Stanford, 1994.

STACKEL, A. W.; BROWN, H. M. **An example approach to predictive well management in reservoir simulation**. Journal of Petroleum Technology, 33(06):1087–1094, 1981.

STONE, H. L. **Probability model for estimating three-phase relative permeability**. Journal of Petroleum Technology, 22(02):214–218, 1970.

STONE, H. L. **Estimation of three-phase relative permeability and residual oil data**. Journal of Canadian Petroleum Technology, 12(04), 1973.

THOMAS, G. W.; THURNAU, D. H. **Reservoir simulation using an adaptive implicit method**. Society of Petroleum Engineers Journal, 23(05):759–768, 1983.

TRICK, M. D. **A different approach to coupling a reservoir simulator with a surface facilities model**. In: SPE UNCONVENTIONAL RESOURCES CONFERENCE/GAS TECHNOLOGY SYMPOSIUM, SPE, 1998, p. 40001.

VAN EVERDINGEN, A. F. **The skin effect and its influence on the productive capacity of a well**. Journal of petroleum technology, 5(06):171–176, 1953.

VOGEL, J. V. **Inflow performance relationships for solution-gas drive wells**. Journal of petroleum technology, 20(01):83–92, 1968.

WANG, A. **Development of a compositional reservoir simulator based on a plugin architecture**. Master's thesis, Pontifícia Universidade Católica do Rio de Janeiro, Rio de Janeiro, 2024.

WANG, Y. **Integrated production modeling to assess the effect of subsea water separation**. PhD thesis, Universidade Federal do Rio de Janeiro, Rio de Janeiro, 2019.

WILLIAMSON, A. S.; CHAPPELEAR, J. E. **Representing wells in numerical reservoir simulation: Part 1–theory**. Society of Petroleum Engineers Journal, 21(03):323–338, 1981.

YAHAYA, A. U.; AL GAHTANI, A. **A comparative study between empirical correlations & mechanistic models of vertical multiphase flow**. In: SPE KINGDOM OF SAUDI ARABIA ANNUAL TECHNICAL SYMPOSIUM AND EXHIBITION, SPE, 2010, p. 136931.

YANG, Y.; DAVIDSON, J. E.; FENTER, D. J.; OZEN, O. ; BOYETT, B. A. **Reservoir development modeling using full physics and proxy simulations**. In: INTERNATIONAL PETROLEUM TECHNOLOGY CONFERENCE, IPTC, 2009, p. 13536.

Appendix A

VLP tables

** Fluid : Oil
** PVT Method : Black Oil
** Equation Of State :
** Separator : Single-Stage
** Emulsions : No
** Hydrates : Disable Warning
** Water Viscosity : Use Default Correlation
** Water Vapour : No Calculations
** Viscosity Model : Newtonian Fluid
** Brine Properties Correlation : Default
** Brine Dissolved Gas Model : No Dissolved Gas
** Brine Thermal Properties : No Pressure Correction
** Steam Option : No Steam Calculations
** Flow Type : Tubing
** Well Type : Producer
** Artificial Lift : Gas Lift (Continuous)
** Lift Type : Fixed Depth of Injection
** Predicting : Pressure and Temperature (Surface Gradient)
** Temperature Model : Rough Approximation
** Range : Full System
** Completion : Cased Hole
** Sand Control : None
** Inflow Type : Single Branch
** Gas Coning : No
** Surface Equipment Correlation : Petroleum Experts 5
** Vertical Lift Correlation : Petroleum Experts 5
** Rate Method : User Selected
** Rate Type : Oil Rate
** Pressure Boundary Node : 1 Manifold 0 (m)
** Reporting Node : 8 Bottomhole 3005 (m)
** Sensitivity Variable 1 : Gas Oil Ratio

```
** Sensitivity Variable 2 : Water Cut
** Sensitivity Variable 3 : Gaslift Gas Injection Rate
** Sensitivity Variable 4 : Boundary Pressure
** EQUIPMENT SUMMARY START
** True Tubing Tubing
** Rate Measured Vertical Pipe Inside Inside
** Type Label Multiplier Depth Depth Length Diameter Roughness
** (m) (m) (m) (inches) (mm)
** Manifold 1 0 ** Pipe 1 1000.0 1000.0 4.00 0.185
** Xmas Tree 1 1000.0 1000.0
** Gaslift Valve 1 2905.0 2905.0 1905.0 3.90
** Tubing 1 3005.0 3005.0 100.0 3.90 0.185
** EQUIPMENT SUMMARY END
*PTUBE1
*DEPTH 3005
** 5 Oil Rate(s) (m3/day)
*OIL
** flo(1) flo(2) flo(3) flo(4) flo(5)
10.0 507.5 1005.0 1502.5 2000.0
** 5 GOR(s) (m3/m3)
*GOR
** gfr(1) gfr(2) gfr(3) gfr(4) gfr(5)
40 70 100 1000 50000
** 5 Water Cut(s) (fraction)
*WCUT
** wfr(1) wfr(2) wfr(3) wfr(4) wfr(5)
0 0.1 0.4 0.7 0.9
** 3 Injected Gas Rate value(s) (m3/day)
*LFG
** add(1) add(2) add(3)
0.0 100000.0 200000.0
** 5 WHP values (kPa)
*WHP
** whp(1) whp(2) whp(3) whp(4) whp(5)
101 1000 3000 6000 15000
*BHP
1 1 1 1 24577 25866 27986 31005 40030
1 1 1 2 2572 3346 6229 11974 27403
1 1 1 3 3874 4239 5913 9414 24131
```

1 1 2 1 24973 26258 28385 31406 40439
1 1 2 2 2591 3399 6285 12056 27543
1 1 2 3 3955 4181 5936 9736 24220
1 1 3 1 26182 27459 29605 32639 41696
1 1 3 2 2838 3686 6498 12322 27974
1 1 3 3 4222 4564 6152 10059 24513
1 1 4 1 27380 28652 30826 33878 42961
1 1 4 2 3418 4006 6875 12665 28459
1 1 4 3 4943 5252 6943 10860 24894
1 1 5 1 28058 29300 31485 34562 43668
1 1 5 2 4380 4845 7901 13820 29359
1 1 5 3 6529 6750 8058 11766 25756
1 2 1 1 23245 24910 27129 30138 39107
1 2 1 2 2517 3291 6214 11895 27062
1 2 1 3 3840 4148 5852 9515 23924
1 2 2 1 23685 25341 27567 30589 39572
1 2 2 2 2538 3347 6267 11962 27218
1 2 2 3 3919 4146 5916 9594 24026
1 2 3 1 25048 26680 28932 31997 41038
1 2 3 2 2785 3640 6470 12273 27718
1 2 3 3 4189 4695 6128 10173 24364
1 2 4 1 26434 28046 30337 33472 42585
1 2 4 2 3378 3971 6838 12679 28322
1 2 4 3 4917 5227 6909 10845 24804
1 2 5 1 27333 28865 31190 34360 43524
1 2 5 2 4356 4826 7872 13793 29307
1 2 5 3 6501 6723 8039 11755 25725
1 3 1 1 22329 24369 26518 29407 38105
1 3 1 2 2468 3247 6191 11883 26677
1 3 1 3 3809 4179 5871 9498 23695
1 3 2 1 22776 24803 26974 29888 38623
1 3 2 2 2513 3301 6243 11971 26856
1 3 2 3 3885 4118 5895 9576 23809
1 3 3 1 24086 26116 28403 31418 40299
1 3 3 2 2739 3597 6446 12271 27444
1 3 3 3 4160 4618 6108 10090 24195
1 3 4 1 25531 27535 29938 33086 42148
1 3 4 2 3347 3938 6812 12661 28159
1 3 4 3 4895 5206 6891 10831 24707

1 3 5 1 26583 28453 30899 34142 43356
1 3 5 2 4318 4802 7851 13768 29247
1 3 5 3 6489 6711 8028 11742 25689
1 4 1 1 705 13078 21261 26677 36747
1 4 1 2 2073 2750 5797 11374 26634
1 4 1 3 3506 3798 5568 9159 23743
1 4 2 1 767 13493 21595 27018 37143
1 4 2 2 2158 2785 5838 11453 26773
1 4 2 3 3571 3866 5586 9223 23834
1 4 3 1 1134 14757 22579 28048 38402
1 4 3 2 2345 3030 6009 11728 27202
1 4 3 3 3830 4155 5829 9650 24136
1 4 4 1 2764 15987 23490 29004 39699
1 4 4 2 3053 3531 6367 12121 27724
1 4 4 3 4601 4915 6591 10519 24541
1 4 5 1 8803 17848 24245 29418 40314
1 4 5 2 4092 4528 7422 13220 28673
1 4 5 3 6342 6564 7866 11500 25417
1 5 1 1 6886 7109 7940 10336 20728
1 5 1 2 8021 8266 8972 11096 21006
1 5 1 3 9126 9407 10012 11923 21356
1 5 2 1 6968 7200 8030 10412 20781
1 5 2 2 8121 8366 9068 11187 21063
1 5 2 3 9238 9510 10118 12018 21421
1 5 3 1 7369 7622 8435 10764 21029
1 5 3 2 8541 8823 9513 11584 21334
1 5 3 3 9691 10004 10606 12464 21725
1 5 4 1 8419 8653 9428 11638 21681
1 5 4 2 9686 9953 10614 12577 22027
1 5 4 3 10914 11220 11798 13555 22487
1 5 5 1 11312 11528 12231 14215 23594
1 5 5 2 12756 12980 13562 15340 24183
1 5 5 3 14221 14458 14971 16502 24870
2 1 1 1 17258 21013 26117 30589 39669
2 1 1 2 8990 9596 12858 18605 32003
2 1 1 3 10215 10370 12049 16100 29034
2 1 2 1 18295 21834 26605 31011 40097
2 1 2 2 9747 10404 13694 19418 32742
2 1 2 3 10830 11200 12760 16822 29676

2 1 3 1 22072 24592 28537 32510 41611
2 1 3 2 13832 14469 17741 23144 35751
2 1 3 3 14119 14461 16173 20247 32779
2 1 4 1 27742 29190 32014 35470 44577
2 1 4 2 23315 23879 26375 30628 41587
2 1 4 3 22974 23357 24965 28557 39685
2 1 5 1 48538 49312 51297 54251 63294
2 1 5 2 51144 51543 53038 55822 64777
2 1 5 3 53167 53451 54600 57086 65854
2 2 1 1 11564 14990 21509 27651 38653
2 2 1 2 8726 9219 12174 17817 31668
2 2 1 3 10236 10386 12059 15941 28831
2 2 2 1 13097 16271 22358 28227 39144
2 2 2 2 9495 9999 13002 18646 32403
2 2 2 3 10879 11164 12794 16659 29505
2 2 3 1 18633 20810 25491 30465 40900
2 2 3 2 13519 14094 17079 22416 35423
2 2 3 3 14258 14589 16182 20098 32610
2 2 4 1 26314 27593 30673 34518 44218
2 2 4 2 23136 23652 25996 30218 41367
2 2 4 3 23077 23457 24973 28455 39551
2 2 5 1 48823 49546 51438 54410 63340
2 2 5 2 51460 51803 53227 55992 64848
2 2 5 3 53439 53719 54826 57258 65983
2 3 1 1 9738 11707 17587 24513 37540
2 3 1 2 8754 9229 11750 16981 31248
2 3 1 3 10491 10627 11989 15664 28625
2 3 2 1 10916 12872 18706 25325 38090
2 3 2 2 9546 9986 12538 17790 31973
2 3 2 3 11190 11465 12731 16375 29303
2 3 3 1 16099 17914 22877 28416 40035
2 3 3 2 13352 13829 16406 21632 35009
2 3 3 3 14291 14610 16066 19878 32387
2 3 4 1 25233 26295 29466 33540 43770
2 3 4 2 22947 23409 25628 29753 41092
2 3 4 3 23136 23507 24938 28310 39390
2 3 5 1 49177 49767 51627 54571 63413
2 3 5 2 51669 51994 53356 56061 64904
2 3 5 3 53766 54045 55112 57451 66099

2 4 1 1 15122 15395 15928 17699 27119
2 4 1 2 16953 17256 17679 19130 27537
2 4 1 3 18754 19098 19448 20668 28224
2 4 2 1 15623 15909 16452 18242 27675
2 4 2 2 17438 17753 18182 19648 28075
2 4 2 3 19237 19584 19938 21169 28744
2 4 3 1 18141 18479 19058 20932 30418
2 4 3 2 19858 20224 20679 22204 30714
2 4 3 3 21587 21982 22354 23628 31279
2 4 4 1 25915 26365 26995 28932 38065
2 4 4 2 27378 27870 28373 29984 38378
2 4 4 3 28901 29431 29846 31211 38924
2 4 5 1 58372 58852 59476 61155 68560
2 4 5 2 60795 60896 61429 62941 69970
2 4 5 3 62931 62950 63418 64790 71468
2 5 1 1 1046576 1047230 1049703 1053834 1068268
2 5 1 2 1053142 1053803 1056274 1060424 1074991
2 5 1 3 1059756 1060411 1062896 1067031 1081765
2 5 2 1 1049768 1050625 1053563 1065096 1071180
2 5 2 2 1056377 1057214 1060157 1071756 1077920
2 5 2 3 1062982 1063841 1066782 1078446 1084714
2 5 3 1 1072582 1074370 1078421 1082749 1084807
2 5 3 2 1079290 1081071 1085146 1089459 1091602
2 5 3 3 1086038 1087813 1091867 1096190 1098415
2 5 4 1 1120392 1119998 1120518 1120809 1122622
2 5 4 2 1127375 1126955 1127469 1127770 1129591
2 5 4 3 1134381 1133962 1134469 1134773 1136606
2 5 5 1 1228156 1222146 1239572 1228833 1230306
2 5 5 2 1235582 1229612 1246927 1236264 1236158
2 5 5 3 1243026 1237106 1254341 1243715 1243635
3 1 1 1 20496 22383 26707 31119 40216
3 1 1 2 15250 15794 18718 23777 35773
3 1 1 3 15433 15790 17339 21259 33339
3 1 2 1 21770 23391 27371 31695 40795
3 1 2 2 16582 17221 19985 24897 36676
3 1 2 3 16636 16996 18595 22431 34340
3 1 3 1 25952 27215 30311 34145 43251
3 1 3 2 22532 23024 25385 29605 40500
3 1 3 3 22318 22696 24198 27704 38760

3 1 4 1 35837 36624 38854 42054 51143
3 1 4 2 36206 36587 38260 41419 50996
3 1 4 3 36903 37239 38451 41176 50584
3 1 5 1 107022 107690 109431 112122 120950
3 1 5 2 112643 112972 114457 116739 124890
3 1 5 3 117290 117594 118643 120869 128910
3 2 1 1 17002 18311 22703 28175 39241
3 2 1 2 14910 15346 17869 22756 35290
3 2 1 3 15741 16084 17470 21086 33093
3 2 2 1 18501 19732 23884 29056 39892
3 2 2 2 16291 16775 19202 23933 36207
3 2 2 3 16942 17294 18688 22253 34095
3 2 3 1 24127 25003 28163 32462 42631
3 2 3 2 22344 22768 24861 28927 40134
3 2 3 3 22574 22954 24290 27586 38552
3 2 4 1 35721 36300 38388 41661 50981
3 2 4 2 36475 36814 38334 41373 50940
3 2 4 3 37281 37617 38721 41318 50576
3 2 5 1 108475 109002 110434 113111 121538
3 2 5 2 113413 113781 115003 117384 125488
3 2 5 3 118216 118498 119668 121638 129515
3 3 1 1 15048 15872 19848 25608 38117
3 3 1 2 14715 15100 17151 21748 34709
3 3 1 3 15895 16218 17514 20838 32780
3 3 2 1 16491 17406 21210 26654 38841
3 3 2 2 16019 16426 18530 22985 35645
3 3 2 3 17140 17489 18709 22019 33783
3 3 3 1 22911 23598 26445 30897 41892
3 3 3 2 22158 22579 24403 28267 39694
3 3 3 3 22769 23141 24337 27428 38311
3 3 4 1 35748 36224 38108 41335 50822
3 3 4 2 36743 37065 38444 41353 50868
3 3 4 3 37628 37983 38993 41464 50586
3 3 5 1 109708 110081 111692 114264 122314
3 3 5 2 114464 114801 116015 118421 126176
3 3 5 3 119063 119334 120387 122477 130213
3 4 1 1 27240 27764 28010 28850 34667
3 4 1 2 36208 29460 29686 30433 35773
3 4 1 3 44309 31158 31376 32048 36973

3 4 2 1 28113 28656 28908 29761 35624
3 4 2 2 36123 30332 30565 31324 36711
3 4 2 3 42605 32014 32239 32920 37892
3 4 3 1 35669 33419 33698 34604 40636
3 4 3 2 38660 35039 35303 36112 41691
3 4 3 3 42411 36670 36929 37659 42837
3 4 4 1 50578 49487 49836 50820 56846
3 4 4 2 52907 51225 51577 52471 58184
3 4 4 3 55485 52977 53344 54160 59588
3 4 5 1 140355 140473 140933 142122 147808
3 4 5 2 143984 144074 144560 145686 151231
3 4 5 3 147665 147722 148217 149285 154691
3 5 1 1 3413093 3414275 3418457 3449252 3460940
3 5 1 2 3423167 3424380 3428572 3459443 3471064
3 5 1 3 3433555 3434766 3438973 3469941 3481575
3 5 2 1 3454628 3455938 3484810 3489465 3501134
3 5 2 2 3464824 3466120 3495084 3499728 3511468
3 5 2 3 3475446 3476787 3505738 3510364 3522130
3 5 3 1 3676605 3677843 3680946 3685170 3697097
3 5 3 2 3687392 3688574 3691731 3695918 3707896
3 5 3 3 3698460 3699783 3702835 3707014 3718966
3 5 4 1 4182954 4184357 4187380 4192017 4195057
3 5 4 2 4196940 4198242 4201352 4205990 4209235
3 5 4 3 4210384 4211732 4214746 4219408 4222896
3 5 5 1 5272182 5272450 5273334 5274482 5278241
3 5 5 2 5289012 5289352 5290070 5291346 5295060
3 5 5 3 5305506 5305880 5306662 5307780 5311576
4 1 1 1 23469 24469 27861 32106 41209
4 1 1 2 20252 20736 23073 27388 38412
4 1 1 3 20180 20551 22001 25500 36692
4 1 2 1 24734 25682 28922 32918 42023
4 1 2 2 21907 22354 24573 28722 39534
4 1 2 3 21805 22194 23597 27005 37969
4 1 3 1 30124 30891 33373 36898 46001
4 1 3 2 29067 29463 31268 34772 44835
4 1 3 3 29351 29705 30979 33943 43971
4 1 4 1 47555 48130 49957 52935 61993
4 1 4 2 50082 50450 51807 54507 63480
4 1 4 3 51946 52287 53304 55702 64542

4 1 5 1 200375 200960 202522 204928 213399
4 1 5 2 206686 207167 208700 210961 218698
4 1 5 3 213048 213416 214354 216448 224018
4 2 1 1 21168 21840 24924 29595 40326
4 2 1 2 20128 20513 22441 26488 37916
4 2 1 3 20650 21028 22232 25399 36430
4 2 2 1 22717 23417 26244 30731 41224
4 2 2 2 21816 22201 24015 27929 39075
4 2 2 3 22268 22643 23831 26931 37725
4 2 3 1 29345 29840 32053 35741 45543
4 2 3 2 29219 29577 31117 34434 44593
4 2 3 3 29815 30195 31286 34029 43848
4 2 4 1 48377 48790 50334 53232 62154
4 2 4 2 50932 51261 52453 54968 63710
4 2 4 3 52803 53113 54070 56278 64867
4 2 5 1 202256 202829 204685 206858 214868
4 2 5 2 208794 209212 210142 212410 220174
4 2 5 3 214474 214835 216123 218112 225503
4 3 1 1 19884 20421 22971 27589 39331
4 3 1 2 20046 20449 22007 25674 37351
4 3 1 3 21011 21398 22425 25285 36141
4 3 2 1 21676 22214 24557 28907 40319
4 3 2 2 21769 22139 23660 27212 38553
4 3 2 3 22636 23033 24038 26833 37458
4 3 3 1 29007 29438 31292 34836 45027
4 3 3 2 29411 29794 31097 34162 44323
4 3 3 3 30251 30654 31604 34118 43736
4 3 4 1 49227 49515 50896 53598 62421
4 3 4 2 51650 51955 53018 55396 63979
4 3 4 3 53653 53968 54859 56982 65270
4 3 5 1 204724 205211 206320 209042 216496
4 3 5 2 210623 211023 212352 214451 221809
4 3 5 3 216625 216721 217741 220128 227143
4 4 1 1 72836 39478 39760 40306 44509
4 4 1 2 83039 41125 41434 41942 45901
4 4 1 3 90967 42785 43130 43603 47346
4 4 2 1 67391 40932 41230 41788 46055
4 4 2 2 80914 42578 42907 43426 47448
4 4 2 3 90945 44239 44606 45090 48895

4 4 3 1 61066 48855 49240 49846 54373
4 4 3 2 68032 50552 50977 51545 55830
4 4 3 3 76747 52263 52740 53270 57339
4 4 4 1 81134 77239 77852 78581 83333
4 4 4 2 84639 79346 80025 80716 85334
4 4 4 3 88638 81494 82247 82902 87402
4 4 5 1 262050 262185 262713 263748 268881
4 4 5 2 266958 267075 267593 268652 273693
4 4 5 3 271938 272058 272549 273572 278528
4 5 1 1 7422640 7424442 7429288 7435917 7454831
4 5 1 2 7437643 7439382 7444221 7450862 7469820
4 5 1 3 7453042 7454762 7459574 7466190 7485092
4 5 2 1 7512858 7514605 7519292 7525874 7545126
4 5 2 2 7528394 7530075 7534790 7541334 7560692
4 5 2 3 7543722 7545440 7550116 7556686 7575958
4 5 3 1 7952787 7954666 7959462 7965510 7983808
4 5 3 2 7968437 7970160 7974913 7981487 7999682
4 5 3 3 7984262 7986155 7990903 7997834 8015978
4 5 4 1 9109857 9110672 9112419 9115281 9123484
4 5 4 2 9129523 9130422 9132205 9134973 9143231
4 5 4 3 9149825 9150620 9152484 9155284 9163452
4 5 5 1 11513238 11513624 11514669 11516117 11520787
4 5 5 2 11537989 11538440 11539449 11540939 11545473
4 5 5 3 11562834 11563306 11564278 11565742 11570381
5 1 1 1 26099 26839 29606 33501 42608
5 1 1 2 24393 24812 26706 30470 40860
5 1 1 3 24474 24845 26115 29258 39738
5 1 2 1 27628 28332 30849 34640 43746
5 1 2 2 26303 26709 28495 32099 42314
5 1 2 3 26462 26859 28087 31111 41356
5 1 3 1 34890 35403 37495 40739 49836
5 1 3 2 35368 35716 37209 40262 49809
5 1 3 3 36039 36411 37513 40116 49489
5 1 4 1 63138 63651 65277 68061 77078
5 1 4 2 66928 67325 68468 71037 79597
5 1 4 3 69998 70345 71247 73533 81948
5 1 5 1 323976 324575 325586 328248 336245
5 1 5 2 330734 331283 332798 335053 342482
5 1 5 3 337692 337895 339851 341798 348729

5 2 1 1 24737 25249 27477 31517 41860
5 2 1 2 24542 24909 26422 29843 40441
5 2 1 3 25117 25517 26550 29328 39534
5 2 2 1 26585 27080 29185 32990 43098
5 2 2 2 26496 26887 28314 31610 41968
5 2 2 3 27119 27520 28530 31232 41191
5 2 3 1 34931 35337 37029 40181 49607
5 2 3 2 35970 36307 37553 40344 49776
5 2 3 3 36817 37205 38132 40498 49545
5 2 4 1 64685 65053 66398 68965 77672
5 2 4 2 68388 68660 69700 72001 80242
5 2 4 3 71369 71720 72523 74557 82629
5 2 5 1 326735 327978 329298 331577 338988
5 2 5 2 333806 334317 335623 338341 345233
5 2 5 3 340713 341147 342294 345051 351493
5 3 1 1 24280 24654 26444 30171 41052
5 3 1 2 24763 25167 26368 29382 40013
5 3 1 3 25710 26136 26990 29438 39344
5 3 2 1 26252 26620 28321 31835 42401
5 3 2 2 26787 27188 28331 31278 41616
5 3 2 3 27725 28160 29003 31388 41048
5 3 3 1 35297 35638 37004 39917 49396
5 3 3 2 36608 36967 37997 40534 49776
5 3 3 3 37561 37997 38788 40943 49675
5 3 4 1 66330 66628 67771 70058 78511
5 3 4 2 69643 69910 70842 72956 81007
5 3 4 3 72776 73077 73922 75813 83566
5 3 5 1 330559 331092 332683 334817 341907
5 3 5 2 337500 337950 338753 341565 348162
5 3 5 3 344316 344731 345406 347379 354440
5 4 1 1 111395 51808 52367 52789 56196
5 4 1 2 118032 53539 54153 54554 57815
5 4 1 3 124334 55293 55961 56344 59471
5 4 2 1 111379 54027 54625 55057 58531
5 4 2 2 117973 55778 56431 56844 60170
5 4 2 3 124451 57551 58261 58655 61847
5 4 3 1 97319 66211 66987 67475 71252
5 4 3 2 104261 68101 68943 69412 73008
5 4 3 3 111318 70015 70927 71365 74800

5 4 4 1 119004 110994 112192 112792 116988
5 4 4 2 123210 113683 114967 115549 119659
5 4 4 3 127530 116391 117801 118371 122400
5 4 5 1 420950 421139 421699 422826 427737
5 4 5 2 427032 427214 427764 428817 433733
5 4 5 3 433138 433312 433854 434923 439760
5 5 1 1 12537141 12348048 12355187 12365897 12402542
5 5 1 2 12542456 12353262 12360417 12371105 12407668
5 5 1 3 12546761 12357588 12364815 12375431 12412055
5 5 2 1 12732465 12553309 12560784 12571808 12613012
5 5 2 2 12737569 12558020 12565302 12576473 12617570
5 5 2 3 12742699 12562615 12569911 12581042 12622174
5 5 3 1 13688139 13555063 13565141 13583759 13707370
5 5 3 2 13693203 13560293 13570291 13588895 13712407
5 5 3 3 13698919 13565946 13575917 13594561 13718125
5 5 4 1 15846636 15847758 15850114 15853693 15864202
5 5 4 2 15874659 15875678 15877984 15881568 15892098
5 5 4 3 15900644 15901742 15904040 15907747 15918221
5 5 5 1 20162916 20163862 20165914 20169048 20178178
5 5 5 2 20196306 20197308 20199360 20202400 20211694
5 5 5 3 20229174 20230240 20232166 20235252 20244600
** Fluid : Water
** PVT Method : Black Oil
** Equation Of State :
** Separator : Single-Stage
** Emulsions : No
** Hydrates : Disable Warning
** Water Viscosity : Use Default Correlation
** Water Vapour : No Calculations
** Viscosity Model : Newtonian Fluid
** Brine Properties Correlation : Default
** Brine Dissolved Gas Model : No Dissolved Gas
** Brine Thermal Properties : No Pressure Correction
**
** Steam Option : No Steam Calculations
** Flow Type : Tubing
** Well Type : Water Injector
** Artificial Lift : None
** Lift Type :

** Predicting : Pressure and Temperature (Surface Gradient)
** Temperature Model : Rough Approximation
** Range : Full System
** Completion : Cased Hole
** Sand Control : None
** Inflow Type : Single Branch
** Gas Coning : No
** Surface Equipment Correlation : Petroleum Experts 5
** Vertical Lift Correlation : Petroleum Experts 5
** Rate Method : User Selected
** Rate Type : Liquid Rate
** Pressure Boundary Node : 1 Manifold 0 (m)
** Reporting Node : 6 Bottomhole 3005 (m)
** Sensitivity Variable 1 : Boundary Pressure
** EQUIPMENT SUMMARY START
** True Tubing Tubing
** Rate Measured Vertical Pipe Inside Inside
** Type Label Multiplier Depth Depth Length Diameter Roughness
** (m) (m) (m) (inches) (mm)
** Manifold 1 0
** Pipe 1 1000.0 1000.0 4.00 0.185
** Xmas Tree 1 1000.0 1000.0
** Tubing 1 3005.0 3005.0 2005.0 3.90 0.185
** EQUIPMENT SUMMARY END
*ITUBE1 2
*DEPTH 3005
** 10 Water Rate(s) (m3/day)
*WAT
** flo(1) flo(2) flo(3) flo(4) flo(5) flo(6) flo(7) flo(8) flo(9) flo(10)
50.0 83.4 139.1 232.1 387.1 645.8 1077.2 1796.9 2997.4 5000.0
** 10 WHP values (kPa)
*WHP
** whp(1) whp(2) whp(3) whp(4) whp(5) whp(6) whp(7) whp(8) whp(9) whp(10)
101 1000 3000 5000 7000 9000 12000 15000 18000 25000
*BHP
1 30318 31229 33255 35282 37308 39335 42375 45414 48455 55549
2 30344 31254 33281 35307 37334 39360 42400 45440 48480 55574
3 30351 31262 33288 35314 37341 39368 42408 45448 48488 55582

4 30331 31241 33268 35294 37321 39348 42388 45428 48468 55562
5 30255 31166 33192 35219 37246 39272 42312 45353 48393 55488
6 30039 30950 32977 35004 37031 39057 42098 45138 48179 55274
7 29446 30357 32384 34411 36439 38466 41507 44549 47590 54687
8 27812 28723 30752 32781 34809 36838 39882 42925 45969 53071
9 23295 24208 26241 28273 30306 32339 35388 38437 41487 48602
10 10742 11660 13704 15747 17791 19834 22900 25965 29031 36184
** Fluid : Gas
** PVT Method : Black Oil
** Equation Of State :
** Separator : Single-Stage
** Emulsions : No
** Hydrates : Disable Warning
** Water Viscosity : Use Default Correlation
** Water Vapour : No Calculations
** Viscosity Model : Newtonian Fluid
** Brine Properties Correlation : Default
** Brine Dissolved Gas Model : No Dissolved Gas
** Brine Thermal Properties : No Pressure Correction
** Steam Option : No Steam Calculations
** Flow Type : Tubing
** Well Type : Injector
** Artificial Lift : None
** Lift Type :
** Predicting : Pressure and Temperature (Surface Gradient)
** Temperature Model : Rough Approximation
** Range : Full System
** Completion : Cased Hole
** Sand Control : None
** Inflow Type : Single Branch
** Gas Coning :
** Surface Equipment Correlation : Petroleum Experts 5
** Vertical Lift Correlation : Petroleum Experts 5
** Rate Method : User Selected
** Rate Type : Gas Rate
** Pressure Boundary Node : 1 Manifold 0 (m)
** Reporting Node : 6 Bottomhole 3005 (m)
** Sensitivity Variable 1 : Boundary Pressure
** EQUIPMENT SUMMARY START.

** True Tubing Tubing
** Rate Measured Vertical Pipe Inside Inside
** Type Label Multiplier Depth Depth Length Diameter Roughness
** (m) (m) (m) (inches) (mm)
** Manifold 1 0
** Pipe 1 1000.0 1000.0 6.00 0.185
** Xmas Tree 1 1000.0 1000.0
** Tubing 1 3005.0 3005.0 2005.0 4.90 0.185
** EQUIPMENT SUMMARY END
*ITUBE1 3
*DEPTH 3005
** 10 Gas Rate(s) (m3/day)
*GAS
** flo(1) flo(2) flo(3) flo(4) flo(5) flo(6) flo(7) flo(8) flo(9) flo(10)
50000.0 75331.5 113496.7 170997.6 257630.1 388153.3 584803.6 881082.6 1327465.8 1999999.9
** 10 WHP values (kPa)
*WHP
** whp(1) whp(2) whp(3) whp(4) whp(5) whp(6) whp(7) whp(8) whp(9) whp(10)
101 1000 5000 10000 15000 20000 30000 40000 50000 55000
*BHP
1 10.0 1250 6768 14419 21544 27792 39187 50015 60604 65845
2 9.0 1193 6761 14407 21543 27804 39206 50034 60621 65862
3 8.0 1049 6740 14383 21531 27805 39216 50045 60632 65873
4 7.0 598 6687 14335 21494 27783 39207 50040 60628 65869
5 6.0 7.0 6564 14248 21421 27727 39168 50008 60600 65843
6 5.0 6.0 6281 14091 21297 27626 39092 49943 60541 65786
7 4.0 5.0 5590 13790 21083 27453 38954 49822 60430 65678
8 3.0 4.0 3493 13147 20672 27124 38691 49587 60212 65466
9 2.0 3.0 4.0 11595 19788 26434 38138 49091 59749 65015
10 1.0 2.0 3.0 6516 17689 24876 36912 47993 58723 64016

Appendix B

Relative permeability tables

SWT SMOOTHEND OFF
**Sw Krw Krow
0.20000 0.00000 0.80000
0.21282 0.00077 0.76103
0.22564 0.00154 0.72205
0.23846 0.00231 0.68308
0.25128 0.00323 0.64451
0.26410 0.00554 0.60964
0.27692 0.00785 0.57477
0.28974 0.01015 0.53990
0.30256 0.01277 0.50585
0.31538 0.01662 0.47508
0.32821 0.02046 0.44431
0.34103 0.02431 0.41354
0.35385 0.02862 0.38400
0.36667 0.03400 0.35733
0.37949 0.03938 0.33067
0.39231 0.04477 0.30400
0.40513 0.05077 0.27897
0.41795 0.05769 0.25641
0.43077 0.06462 0.23385
0.44359 0.07154 0.21128
0.45641 0.07923 0.19077
0.46923 0.08769 0.17231
0.48205 0.09615 0.15385
0.49487 0.10462 0.13538
0.50769 0.11400 0.11938
0.52051 0.12400 0.10503
0.53333 0.13400 0.09067
0.54615 0.14400 0.07631
0.55897 0.15508 0.06482

0.57179 0.16662 0.05456
0.58462 0.17815 0.04431
0.59744 0.18969 0.03405
0.61026 0.20246 0.02708
0.62308 0.21554 0.02092
0.63590 0.22862 0.01477
0.64872 0.24169 0.00862
0.66154 0.25615 0.00615
0.67436 0.27077 0.00410
0.68718 0.28538 0.00205
0.70000 0.30000 0.00000
1.0 1.0 0.0
SLT SMOOTHEND OFF
**Sl Krg Krog
0.30000 0.90000 0.00000
0.31795 0.85549 0.00147
0.33590 0.81099 0.00293
0.35385 0.76719 0.00502
0.37179 0.72598 0.00942
0.38974 0.68477 0.01381
0.40769 0.64498 0.01947
0.42564 0.60706 0.02679
0.44359 0.56915 0.03412
0.46154 0.53336 0.04333
0.47949 0.49874 0.05358
0.49744 0.46413 0.06384
0.51538 0.43234 0.07661
0.53333 0.40102 0.08980
0.55128 0.36994 0.10319
0.56923 0.34192 0.11931
0.58718 0.31389 0.13543
0.60513 0.28681 0.15238
0.62308 0.26209 0.17143
0.64103 0.23736 0.19048
0.65897 0.21429 0.21099
0.67692 0.19286 0.23297
0.69487 0.17143 0.25495
0.71282 0.15235 0.27902
0.73077 0.13422 0.30392

0.74872 0.11609 0.32883
0.76667 0.10102 0.35646
0.78462 0.08619 0.38430
0.80256 0.07182 0.41256
0.82051 0.06028 0.44333
0.83846 0.04874 0.47410
0.85641 0.03838 0.50591
0.87436 0.03014 0.53961
0.89231 0.02190 0.57331
0.91026 0.01554 0.60869
0.92821 0.01060 0.64532
0.94615 0.00565 0.68195
0.96410 0.00330 0.72088
0.98205 0.00165 0.76044
1.00000 0.00000 0.80000
KROIL STONE2 SWSG